University of Stavanger

Faculty of Science and Technology

MASTER'S THESIS

Study program: Offshore technology Specialization: Marin and Subsea Technology	Spring semester, 2014 Open

Writer: Per Vabø Vatsvåg	………………………………………… (Writer's signature)

Faculty supervisor: Ove Tobias Gudmestad

External supervisor(s): Jan Vatsvåg (Global Maritime)

Thesis title:
Evaluation of Jack-up units in deeper water in the North Sea.

Credits (ECTS): 30

Key words: - Site-Specific Assessment - Parametric studies - Dynamic sensitive and drag dominated structures - Large extent of nonlinear effects - Non-Gaussian response - Two-stage deterministic quasi-static analysis procedure	Pages: ………………… + enclosure: ………… Stavanger, 16.06.2014 Date/year

Front page for master thesis
Faculty of Science and Technology
Decision made by the Dean October 30th 2009

EVALUATION OF JACK-UP UNITS IN DEEPER WATER IN THE NORTH SEA

Abstract

The aim of this thesis has been to investigate challenges and possible limitation associated with purpose-built jack-up units for weathering the ultra harsh environment of the North Sea. Two Site-Specific Assessments (SSAs) have been performed of a jack-up unit for all-year operations at the Johan Sverdrup field. The jack-up unit is a "similar" design as the MSC CJ-70 Class drilling unit, which is able to operate at water depths up to 150 meters and drill wells down to 10 000 meters. She is the largest built jack-up class unit in the world.

In addition to the Site-Specific Assessments (SSAs), a parameter study has been performed to investigate and quantify the sensitivities related to water depth, air gap, lightship weight, soil conditions and other effects related to uncertainties in stiffness, hydrodynamic loading, soil structure interaction, nonlinearities and statistical parameters.

Analysis methodology and procedures for assessing jack-up units have been much debated over the last 30 years. This is mainly caused by the large extent of nonlinearities associated with estimating the jack-up responses, due to a wide number of significant uncertainties. Nonlinearities arise because these units are drag dominated marine structures with nonlinear hydrodynamic loading, nonlinear stiffness characteristics due to the soil structure interaction and to P-δ effects in addition to be dynamic sensitive structure. The responses are therefore non-Gaussian implying assessment of various statistical methods to determine the extreme maximum responses in a seastate.

The nonlinear soil-structure interaction is one of the main uncertainties to overcome because of the complicated stiffness characteristics of the foundation, which is strongly nonlinear. The effects of foundation stiffnesses are significant when assessing a jack-up unit.

In this study, a two-stage deterministic procedure has been used to perform the analyses. This analysis procedure is considered acceptable by the industry because it produces satisfactory results and treats associated nonlinearities in an adequate manner. This analysis method together with the more stringent requirements in the Norwegian Annex in the ISO 19905-1 standard have been the basis for the assessment.

Results from the Site-Specific Assessments for the Johan Sverdrup field at 110 meter water depth show the purpose-built jack-up unit (MSC CJ-70 Class design) satisfies the regulatory requirements with respect to overturning stability, leg sliding, preload capacity, leg strength, leg holding system strength and foundation bearing capacity.

The parametric studies show that some parameters have significant effect on the extreme responses due to increasing water depth, foundation fixity and leg length. Several other parameters investigated did have only minor effects on the extreme responses.

Moving into much deeper water than 110 meter in the harsh environment of the North Sea is questionable due to the uncertainties inherent in the applied methods, the damping characteristics, nonlinear dynamic response estimations, the structural high yield strength capacities of the legs and the soil resistance capacities of the spudcans.

Background

To meet the world increasing demands for oil, exploration and exploitation have moved into deeper and deeper water and harsher environment. Today, oil companies are searching for oil in water depths up to 3000 meters and in any weather conditions ranging from typhoons to the arctic areas. Exploration has traditionally been carried out by two types of units; a floater (ship-shaped and semi-submersible units) and a jack-up (self-elevating unit) as this mission requires mobility. Together with the technological advances in drilling technology to meet the increasing water and increasing drilling depth, the equipment and the storage requirements for bulk and liquid have grown in size and weight. The units have therefore grown in similar manner.

The jack-up units are slender structures due to their layout. The platform deck is supported on either three or more independent moveable legs. By increasing the water depth, the structure becomes more and more susceptible to the dynamic responses as the natural periods move towards the peak of the wave energy spectrum. As a part of the development, the water depth limitations for jack-ups have increased by improving the structural robustness. The main objective of this work is to investigate the limitations of current jack-up units, purpose-built for the harsh environment in the North Sea, in relation to the water depths for operating in the North Sea and to assess the sensitivities to various parameters. It will also be evaluated what practical water depth limits are in the North Sea for such type of units.
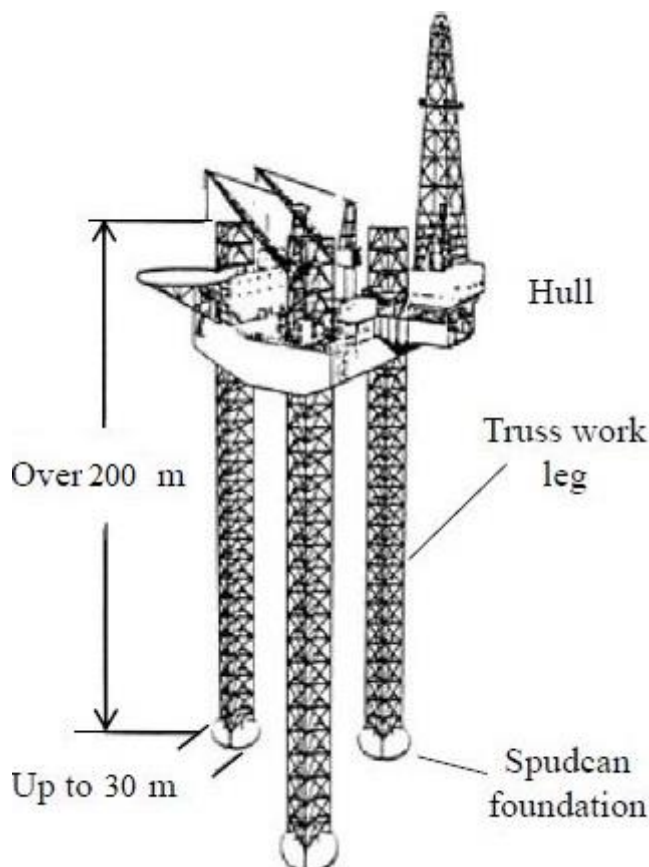

Figure i- A typical three-legged Jack-Up unit suitable for North Sea conditions (modified from Zhang, Bienen and Cassidy [32])

Acknowledgments

I would like to express my sincere gratitude towards my supervisor Prof. Ove Tobias Gudmestad, for his guidance, support and for providing me the subject of this thesis.

I am also very grateful to my father, Jan Vatsvåg for his help and guidance.

Finally, I would like to thank my fiancée and our son for their patience and encouragement throughout my academic endeavors.

Table of Content

Table of Figures

Table of Tables

Abbreviations

ALS	Accidental Limit State
BS	Base Shear
BSI	The British Standards Institution
CofG	Centre of Gravity
D/I	Drag-Inertia parameter
DAF	Dynamic Amplification Factor
DNV	Det Norske Veritas
DOF	Degrees Of Freedom
FEM	Finite Element Method
ISO	International Organization for Standardization
JONSWAP	Joint North Sea Wave Project
LAT	Lowest Astronomical Tide
LCG	Longitudinal Centre of Gravity
LSW	Light Ship Weight
MHWS	Mean High Water Spring
MODU	Mobile Offshore Drilling Unit
MPME	Most Probable Maximum Extreme
MSL	Mean Sea Level
NCS	Norwegian Continental Shelf
OTM	Overturning Moment
PDF	Probability Density Function
PSA	Petroleum Safety Authority
PVD	Principle of Virtual Displacements
RPD	Rack-Phase Differential
SDOF	Single Degree Of Freedom
SNAME	Society of Naval Architects and Marine Engineers
SSA	Site-Specific Assessment
TCG	Transverse Centre of Gravity
UC	Utilisation Check
ULS	Ultimate Limit State
W/J	Winterstein/Jensen method

Symbols

a	Depth embedment factor
A	Area of member
A_i	Harmonic amplitude of i
B	Effective spudcan diameter
BS_{QS}	Maximum deterministic base shear force from the extreme wave and current imposed on the quasi-static model
c	System damping
c_{cr}	Critical damping coefficient
C_D	Drag coefficient
C_{Dei}	Equivalent drag coefficient
C_M	Inertia coefficient
C_s	Shape coefficients
C_h	Depth factor
D	Diameter of member
D_s	Greatest depth of spudcan bearing area below the seafloor
d	Water depth
F	Unit load
F_{Amp}	Static amplitude of quasi-static base shear
F_{in}	Magnitude of the inertial loadset
F_h	Horizontal force applied to the spudcan
F_m	Bending moment applied to the spudcan
F_v	Vertical force applied to the spudcan
ΔF_{drag}	Drag force
$\Delta F_{inertia}$	Inertia force
F_w	Wind force
g	Acceleration of gravity
G	Shear modulus of the foundation soil
H	Wave height
H_s	Signficant wave height
k_i	Wave number
K_1	Vertical foundation stiffness
K_2	Horizontal foundation stiffness
K_3	Rotational foundation stiffness
K_v	Vertical leg-hull connection stiffness
K_r	Rotational leg-hull connection stiffness
$K_{d1,2,3}$	Stiffness depth factors
l_i	Reference length of member
m	Mass
M	Unit moment load
$\tilde{m}_n$	The n-th sample central moment
N	Number of samples in the simulated time series
OTM_{QS}	Maximum deterministic overturning moment at pinpoint from the extreme wave and current from the quasi-static analysis
p'_0	Effective overburden pressure of the maximum spudcan bearing area
P	Wind pressure
Q_h	Horizontal foundation capacity
Q_m	Moment foundation capacity

Q_v	Vertical bearing capacity
Q_{vo}	Vertical capacity achieved during preloading
Q_m	Moment foundation capacity
s	Height of bay
S_η	Power spectral density for the sea surface elevation
T	Time period
T_p	Peak period
T_{ass}	Associated H_{max} period
U	Fluid particle velocity
V	Current velocity
V_{zi}	Wind velocity
W	Average width of the rack
$\tilde{y}_1$	Skewness coefficient
$\tilde{y}_2$	Kurtosis coefficient
$\dot{z}$	Structural velocity vector

Greek letters

α_1	Angle between flow direction and member axis
α	Weibull scale parameter
β_1	Angle defining the member inclination from the horizontal plane
β	Weibull slope parameter
γ	Weibull threshold parameter
γ_s	Peak enhancement factor
Δ-Δ_c	Difference in vertical displacements between the detailed leg model and the detailed combined leg with the leg-hull connection
ζ	Damping ratio
η	Surface elevation process
θ	Angle between flow direction and plane of rack
θ-θ_c	Difference in rotations between the detailed leg model and the detailed combined leg with the leg-hull connection
κ	Gumbel scaling parameter
$\tilde{\mu}$	Sample mean
υ	Poisson's ratio of the foundation soil
ρ_{air}	Density of the air
ρ_R	Correlation coefficient of the static and dynamic responses
ρ_w	Mass density of water
$\tilde{\sigma}$	Standard deviation
ϕ_n	Series of coefficients
ϕ	Wave potential
ψ	Gumbel location parameter
φ_i	Independent random phases angles uniformly distributed 0 and 2π
ω_0	Natural frequency
ω	Wave circular frequency
ω_p	Spectral peak frequency
$\Delta\omega$	Spacing between discretized frequencies
Ω	Frequency ratio

1 INTRODUCTION

1.1 General

A jack-up is a self-elevating unit comprising a buoyant hull that can be raised over the sea surface by three or more steel legs supported on the seabed. The hull contains the facilities required to carry out the mission of the unit, such as drilling, production, construction support and as service platforms for offshore operations. The industry has also started using these units for installation and servicing offshore wind farms. The hull carries also all supporting functions such as accommodation, power generation, utilities etc. Most of these units are not self-propelled and therefore are dependent upon being towed by tugs or transported on heavy lift vessels between the different locations the units shall operate. These platforms are in general the most popular type of mobile units and there are about 540 jack-ups in operation in the world by end of 2013. They originated from drilling offshore in the Mississippi area in the early 1950s and the first one was designed by R. G. LeTourneau for Zapata Drilling.

1.2 Characteristics

A jack-up unit is composed of a hull, legs, footings, drilling package and other equipment. Hulls are mainly triangular, but other forms as rectangular, octagonal and shipshape are also present. The most common are three leg systems, whereof the legs are truss type structures with triangular or square trusses. For the shallow water, the legs may also be of tubular type. Tubular legs are less expensive than open-truss legs to fabricate, they are less stable and cannot adapt to stresses in the water as well as open-truss legs. For this reason, tubular-legged jack-ups are not used in waters exceeding a certain water depth (< 75m). At the bottom part of each leg, there is an independent/spudcan supported footing or a mat supported footing. Spudcans are fitted to support the legs on the seabed. These are typical cylindrically shaped steel shoes with pointed ends, similar to a cleat. A spike in the can is driven into the ocean floor, adding stability to the unit during operations. Jack-up units with cylindrical type legs typically have a mat supported footing. A mat supported footing is generally one common footing for all the legs. The shape is formed as a rectangular, "A" shape structure with a flat top and bottom, see the Figure 1-1 for an illustration.
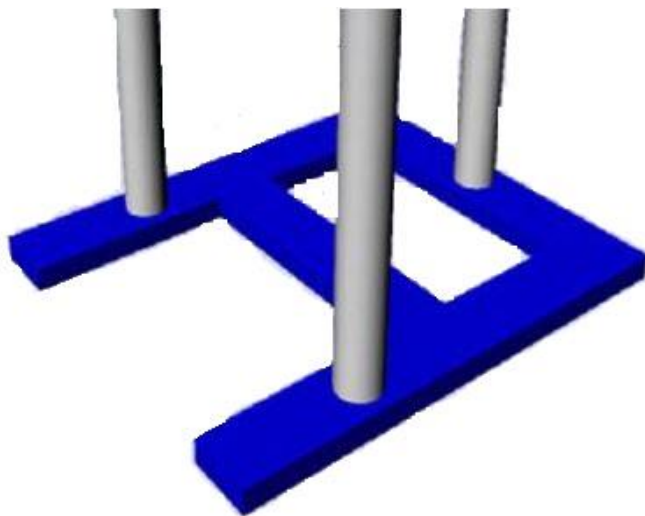
Figure 1-1- "A" shape structure with a flat top and bottom, extracted from Morandi [34]

Once a jack-up unit has been towed to site, the legs are jacked down to the seabed, where they continue to be jacked down into the seabed until there is adequate bearing capacity for the hull to climb out of the water. The foundations are then preloaded by filling up seawater into ballast tanks or by pre-driving the legs. The spudcan will penetrate through the soil until it has sufficient bearing capacity to carry the preload. The vertical bearing capacity will be equal to the applied preload. This preloading process will act as a proof test of the foundation by exposing it to a larger vertical load than would be expected during the design storm. After preloading, the ballast tanks are emptied and the hull is jacked clear to a predetermined distance above the still water level. This distance is called the "airgap" and is defined as the distance between the underside of the hull (keel) and still water level (MSL) [1] [2]. Figure 1-2 illustrates the operations of a jack-up unit from arriving at a site to be in full operation.
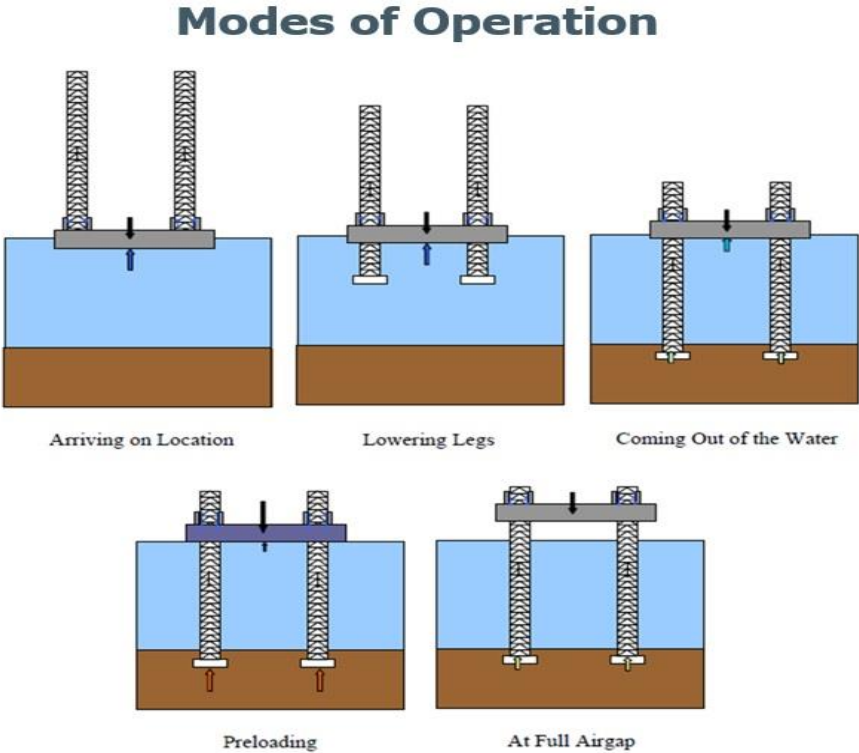
Figure 1-2 – Modes of operations when a jack-up is to operate at a location, extracted from Morandi [34]

Today jack-up units mainly consist of a rack and pinion system, with a floating or fixed jacking and an electric or hydraulic based power source. The rack and pinions are mounted on each chord element in the leg. The system works simply by applying a driving force in the gear box, which causes the pinions to rotate. The force created by the rotating pinion pushes the rack up or down, causing the leg to move. The pinions can either be opposed or radial, depending on the geometry of the leg.

Guides or "wear-plates" are always found on jack-up units with pinion system. One guide is located at the jackhouse (above the pinions) and one below. The guides protect the pinions by keeping the correct distance between the pinion and the rack.

The transfer of forces between the leg and hull depend on whether there is a fixation system or not. If the pinions are primarily used for jacking and not designed to transfer loads, then a fixation system is needed.

In jack-up units having a fixation system the transfer of axial loads and bending moment between the leg and hull is largely by means of a force couple due to vertical loads carried from the chord into the fixation or jacking system. The fixation system is equipped to resist large loads due to its high rigidity.

For systems without a fixation system the transfer of bending moment between the leg and hull is partly by means of a force couple due to horizontal loads carried from the chords through the upper and lower guides.
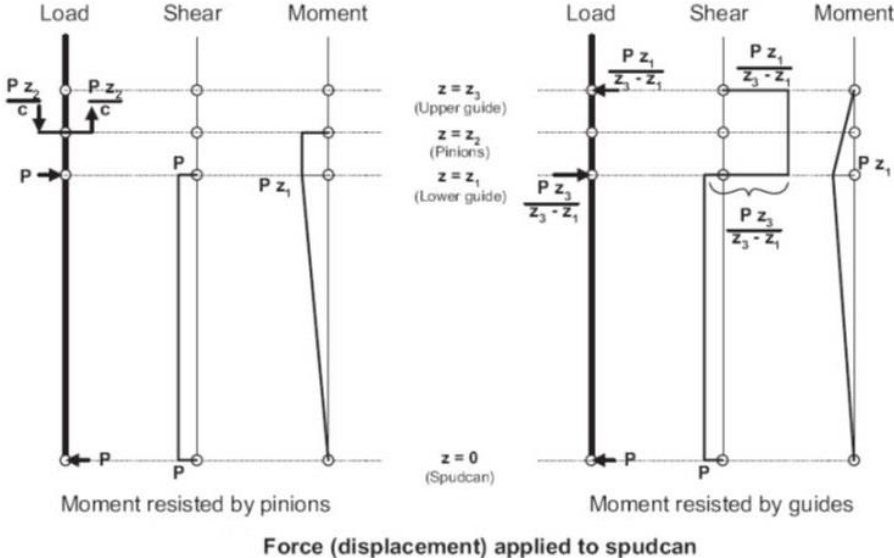
Figure 1-3 – Leg load distribution depending on system to transfer loads, extracted from the research report: Guidelines for jack-up units with particular reference to foundation integrity [33]

Jack-up units used for drilling activities have either a slot type drilling package, where the drilling takes place over an opening in the hull, or a cantilever drilling system, where the drilling occurs at a cantilever beam from the hull.

The slot type drilling is mainly for mat supported footing units, while the cantilever drilling is mainly for units with independent footings, illustrated in Figure 1-4. The cantilever drilling system is the far most popular drilling system due to great range of motion and high level of utilisation.
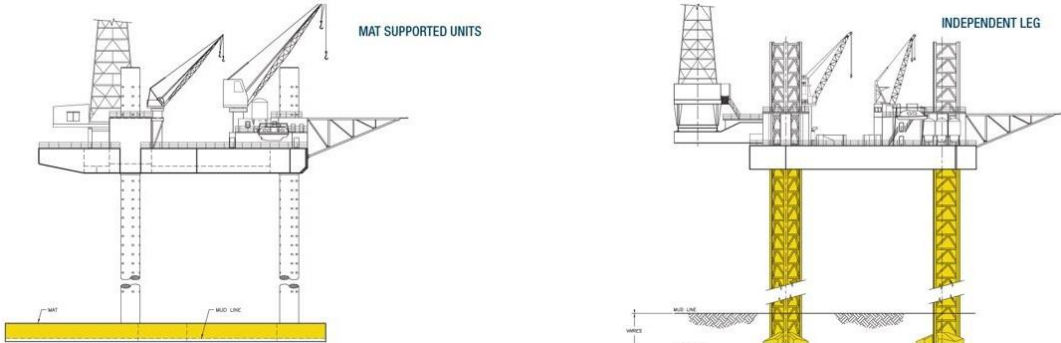
Figure 1-4 – Mat supported footing units versus independent leg footing units, extracted from Morandi [34]

1.3   Comparison of jack-up types

A comparison of unit types are listed in Table 1-1 to Table 1-3:

1.3.1   Number of legs

Table 1-1 - A comparison of number of legs

Four –legged arranged in a rectangular form		Three-legged arranged in a triangular form	
Advantages	Disadvantages	Advantages	Disadvantages
Little to no preload tanks required	Loss of deck load in the Afloat mode due to increased windage and additional weight of extra leg	Less weight, parts and power needed	Required preload tankage
The lack of tanks saves on money for piping and equipment, while adding more usable space within the hull			
More redundancy as the unit can stand on three legs	Adds more wind, wave and current loads	Allows for more deck load to be carried in the Afloat mode due to less windage and reduced leg weight	No leg redundancy
Units are stiffer in elevated mode			

1.3.2   Comparison of shape of legs

A truss leg is composed of 3 or 4 chords, horizontal and diagonal braces. The truss can be shaped as a revised K- or X-braces or a mix between them. The chords provide the axial and flexural stiffness. The horizontal braces provides the shear capacity of the leg.
A cylindrical leg is usually of hollow steel tube.

Table 1-2 - A comparison of shape of legs

Cylindrical legs (hollow steel tubes)		Truss legs, X or revised K-braces	
Advantages	Disadvantages	Advantages	Disadvantages
Small Gear Units	Limited to shallow water	Optimal steel utilisations	
Legs take up less deck area	Require more steel to achieve the same resistance to environmental loads and to provide the same elevated response as a truss leg	Lighter and stiffer legs	
Easier and cheaper to construct	Less stable and cannot adapt to stress in water like a truss structure	Reduced drag load	

1.3.3   Comparison of footings

Table 1-3 - A comparison of footings

Mat supported footing		Spudcan footing	
Advantages	Disadvantages	Advantages	Disadvantages
Minimising risks on soft or muddy soils (creates a lower bearing pressure by a distributed weight on a large area.) Small penetrations	Limited sea floors (not suitable for uneven seabed or seabed with larges slopes)	Better stability	Can cause deep impressions in softer soil, due to deep penetrations
Can carry more load. Afloat due to buoyancy chambers	Complicated flooding and emptying sequence	More versatile (A spudcan can be placed on uneven seabed and other difficult sea floors)	
Quicker installation and extraction			

1.4   Market

The jack-up unit was mainly designed for benign waters and with limited water depth capabilities. However, these units have become more popular for worldwide use including the Norwegian sector of the North Sea, due to their high mobility and economical gains. In the Southern part of the North Sea, they have been commonly used for years. Jack-ups designed to operate in the hostile environment of the Norwegian waters are limited to about 17 units, whereof 7 are under construction. Some of these are presently operating in the Southern part of the North Sea (in less than 100 meters water depth). Per today, the highest specification jack-up unit operating in the North Sea is based upon the MSC CJ70 design with a limiting operating depth of up to 150 meters water depth.
MSCs latest iteration of the CJ series is the CJ80 design. This unit is developed as a result of interest from the operators for a robust deep water jack-up for Norwegian and UK waters. The hull measures 100x110 m with 232 m long legs. This design will have a variable deck load capacity of up to 12000 tons. One of these units is currently under construction. F&G JU2000E is another popular jack-up design, suited for water depth up to 120 meters and moderate harsh environment areas. Seadrill currently has four of these units under construction.

All jack-up units designed for Norwegian waters are based upon a three legs design with open triangular shape.

1.5   Challenges

The most challenging areas for jack-up units are within transportation, setting the legs, extreme weather conditions and in the foundations.
A jack-up unit is dependent on the foundation as support for the legs and for determining the stiffness characteristics resulting in the weather conditions the jack-up can sustain.
The foundation must have sufficient strength so the spudcans at the base of the legs do not penetrate too far into the seabed when preload is applied and have enough resistance to avoid the spudcan to slide.
The research report by MSL Engineering Limited [33] has collected history of failure incidents of jack-ups from before 1980 and up to 2004.

They claim one third of jack-up accidents have been associated with foundation problems [33]. These problems are caused by various incidents such as punch-through, uneven seabed/scour/footprint, seafloor instability, sliding mat foundation, unexpected penetration and others.

It is evident from statistics, that punch-through during preloading is the most frequently encountered foundation problem for jack-up units [33].

The effect of an unexpected punch-through, which will occur at one leg, may be severe, resulting in the jack-up unit to rotate and the legs to bend/tilt, making the unit sway. Since the imposed tilt will cause additional out-of-balance moments, this will lead to an increased loading in the spudcan and hence further punch-through deformation.

Punch-through may typically arise in weak soil layer encountered beneath a strong surficial soil layer and the only way to avoid punch-through is to undertake a thorough soil survey at the site prior to installation of the jack-up unit.

Another fundamental issue with the foundation is that it can provide moment fixity to the spudcan. This will reduce the leg bending stiffness in the region of the leg-to-hull connection and increase the sway stiffness of the jack-up unit. Increased sway stiffness will reduce nonlinear large displacement effects and the dynamic effects on the unit [3].

Foundation fixity is one of the most important parameters related to a jack-up unit assessment because of its high influence on the natural periods. It is also one of the main uncertainties to overcome because of the complicated stiffness characteristics of the foundation.

A conservative approach is to assume the spudcan as a pinned support condition [4].

Jack-up units are designed with slender legs up to supporting a heavy topside. They are characterised by slender, drag-dominated and dynamically sensitive marine structures.

The biggest challenge and main concern for these units going into deeper water depths with harsh environmental conditions applied is related to their natural periods, which will be up to 10 seconds. This results in the natural periods near the maximum wave energy, yielding high dynamic amplifications and dynamic loading, causing extreme responses and high risks of foundation or structural collapse.

These deep-water units have also become so heavy, that there is limited number of heavy lift vessels being able to carry them for transportation. The steel used in the chord legs are also of very high quality limiting number of mills being able to manufacture the steel. The stability during transit is a constraint that has to be considered as a part of the design.

Rack-Phase differential (RPD) is another challenge, which may arise if there are high currents or uneven seabed. The effect of RPD can be quite extensive, causing buckling of braces between the chords and damage equipment.

The underwriters are therefore requiring an independent site assessment prior to relocate to new locations to minimize the risk of failure. Similar requirements are present for tow and transportation on heavy lift vessel, as many platforms have collapsed and sunk under transit.

1.6   Thesis outline

The aim of this thesis is to investigate the challenges and possible limitation associated with purpose-built jack-up units for weathering the ultra harsh environment of the North Sea.

A review of analysis methodologies and procedures applicable to a Site-Specific Assessment of a jack-up unit will be presented.
Two Site-Specific Assessments (SSAs) of a jack-up unit for all-year operations at the Johan Sverdrup field will be performed in accordance with the ISO 19905-1 [5] standard.

The jack-up unit studied is a "similar" design as the MSC CJ-70 Class drilling unit, which is able to operate at water depths up to 150 meters and drill wells down to 10 000 meters.

Finally, a parametric study will be addressed to investigate and quantify the sensitivities related to the assessment.

2   JACK-UP ASSESSMENT LEGISLATIVE REQUIREMENTS

2.1   General

Before a jack-up unit can operate at a given site, an assessment of its capacity to withstand a design storm must be performed for that particular location.
As jack-up units are regularly moved from location to location, with each location providing a unique set of conditions. Jack-up units are designed and classed for specific sets of conditions, but it is rare that the foundation parameters, environmental conditions, orientation, airgap requirements and required variable load will all be within the design assumptions. There are also regulatory and operator requirements that the unit has to satisfy prior to operation. Due to all the incidents that have occurred in the past, the underwriters require also analyses carried out at each location. This type of analyses are called a Site Specific Assessment (SSA).

In Norway, the Petroleum Safety Authority Norway (PSA) is the supreme legislative which enforces Rules and Regulations for offshore activities at the Norwegian Continental Shelf (NCS).
In accordance with PSA requirements, a Site-Specific Assessment for mobile self-elevating units shall be carried out using the requirements with specific reference to the ISO 19905-1 with the Norwegian Annex. It is also specified that an equivalent standard achieving the same level of safety can be applied. In Norway, it has been common to use the DNV-OS-C104 rules. It is also a regulatory (and underwriter) requirement that the unit shall be classed in a classification society and have the maritime certificates for operation.

In general, a Site-Specific Assessment (SSA) of a jack-up unit is based on the technical guidelines of SNAME 5-5A Practice [6] and the latest ISO19905-1 [5]. Using PSA requirements and the DNV-OS-C104, the analysis methods and procedures are the same as in SNAME 5-5A and ISO standard, but differ in regard to load and resistance factors. DNV-OS-C104 lacks also some specific guidance in certain instances (e.g. they do not provide any specific resistance factor for leg sliding).
The damping level is also different. PSA require a damping as 5% of critical, while ISO recommends 4 - 7% of critical, depending on whether relative velocities are included in the analysis.

2.2   Development and technological aspects

SNAME 5-5A Recommended Practice has been developed for over 20 years by a dedicated community of jack-up experts which included oil companies, drilling contractors, consultants and class societies. It was developed as an attempt to standardize jack-up assessment procedures to ensure an appropriate level of structural reliability.

Around 2008-2009, the process of evolving SNAME 5-5A into ISO 19905-1 begun, and as a part of the suite of ISO Offshore Standards. Additional and improved calculations methods have been introduced in the development of ISO 19905-1. Especially in regard to clay foundation, where findings by Templeton [8] is included in the ISO standard [5].

However, the overall methodology given in ISO standard is essentially the same as in SNAME 5-5A.

All checks that need to be made in a Site-Specific Assessment (SSA) according to SNAME 5-5A and ISO 19905-1 are listed below:

"Geometry: A check on leg length to ensure that the hull can be raised to the required elevation above the sea, taking account of the depth to which the legs will penetrate into the seabed. The elevation is determined by the more onerous of the need to clear wave crests and the interfacing demands of an offshore platform. The leg penetrations vary as a function of the foundation soil type and composition, and the applied bearing pressure.

"Punch-through" check: The leg penetration analysis should also identify the possibility of rapid leg penetration during positioning or pre-loading operations. If the rate of leg penetration exceeds the elevating speed of the jack-up, and if any hull-in-water buoyancy-generated is insufficient, the associated loss of hull trim/heel angle can result in damage to the jack-up and adjacent assets.

Overturning stability: A check is also made to ensure that the windward legs retain sufficient positive vertical reaction under the overturning effects of the assessment storm conditions. Structural and Foundation Strength Checks: Checks are made to ensure that, with the predicted final leg penetration and the vertical lateral & rotational support at bottom of legs, the unit has sufficient: pre-load/pre-drive capacity, leg uplift/sliding resistance, leg bearing failure resistance, leg strength, elevating system strength & fixation system strength [3]."

The Norwegian Annex in ISO 19905-1 has additional requirements for operations in Norwegian waters. The "Norwegian Annex" requires higher safety levels than the basic ISO 19905-1 criteria for survival (ULS) conditions.

- A load factor of 1.25 as opposed to 1.15
- 100-year wind and wave and 10-year current as opposed to 50-year wind, wave and current.

The analysis methods, described in the ISO standard together with the requirements in the Annex, have been employed as a basis for the analyses undertaken.

3 THEORETICAL BASIS FOR JACK-UP ANALYSES

3.1 Introduction

Performing a proper Site-Specific Assessment (SSA) for a jack-up unit require adequate modelling skills and a sufficient analysing method in order to treat all the difficulties attached to a jack-up analysis. These difficulties are mainly nonlinearities that lead to difficulties in both the modelling and the analysing parts.

In a Site-Specific Assessment (SSA), we normally include nonlinear hydrodynamic loading and nonlinear structural properties.

Hydrodynamic loading or the wave-current induced loading is nonlinear due to the nonlinear drag term and free surface effects, which makes the random excitation and the response for jack-up units non-Gaussian. This is being further compounded by nonlinearity in structural behaviour due to second order effects due to large structural motions, nonlinear soil-structure interaction, leg-hull connection and hydrodynamic damping caused by the relative velocity between the structure and water particles [10] [11] [12].

A dynamic short-term response analysis, using a time domain approach, is a recommended procedure to obtain the dynamic loading effects and the non-Gaussian response. Thus, the necessity of linearizing the nonlinear drag load and neglecting free surface effects are not needed.

The dynamic loading obtained from the short-term analysis is usually included in an inertial loadset into the global quasi-static analysis. This analysis method is called a two-stage deterministic analysis procedure and is presented in Chapter 5.

In the following Chapter, modelling procedures for performing a Site-Specific Assessment (SSA) following the ISO standard [5] is presented.

3.2 Modelling of the environmental loads

Environmental loading is generally estimated using a design seastate condition characterized by a stationary wave of short duration, usually to be of 3 or 6 hours. The loading within a seastate typically arise from waves, currents and wind. The design seastate is selected such that the expected largest wave amplitude within a storm duration equals the largest wave amplitude obtained from a long term analysis for a given return period (usually 100 years) [9]. Loading contributions within a seastate is illustrated in Figure 3-1.
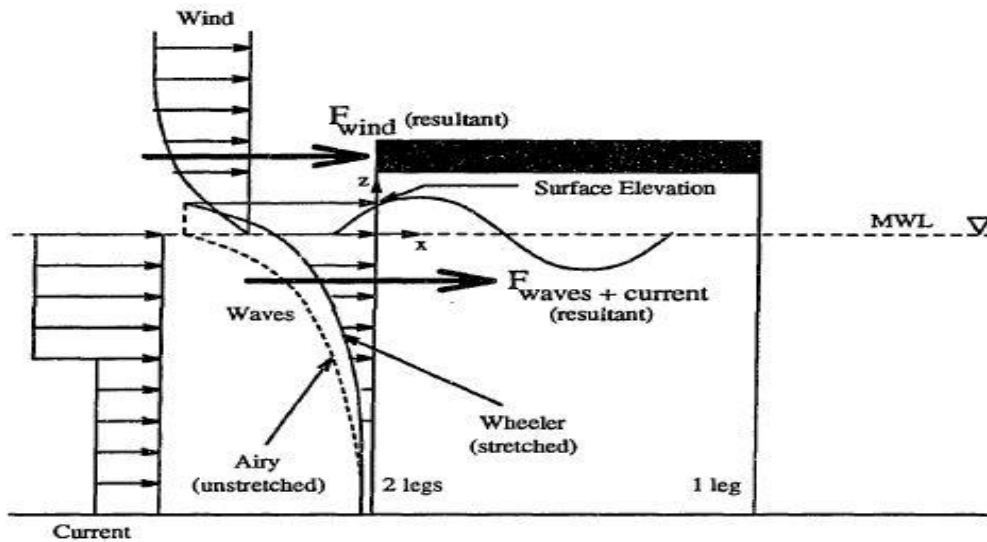
Figure 3-1 – Representation of wave, current and wind loads, extracted from Lancelot [13]

3.2.1   Wave and current loading

3.2.1.1   *Stochastic approach*

The wave loading in a seastate is determined by first obtaining a sea surface elevation history, using a wave spectrum, characterized by a significant wave height H_s, spectral peak period T_p and a possible spectral peakedness parameter γ.
The significant wave height and the spectral peak period provide information about the power spectral density of the sea surface elevation process.
A random Gaussian elevation process can be simulated using a wave spectrum together with random phases for each random wave component.
Water particle kinematics can be represented by utilising the linear Airy wave theory, or a modified linear theory (e.g. with linear stretching), along the elevation time history.

3.2.1.1.1   Simulation of water particle kinematics

The surface elevation process can be represented a sine series [13]:

$$\eta(x,t) = \sum_{i=1}^{n} A_i \sin(\omega_i t - k_i x - \varphi_i) \tag{3.1}$$

Where

η	- surface elevation process
A_i	- amplitudes for each harmonic component
ω_i	- wave circular frequency
t	- at any time
x	- the horizontal distance measured relative to the origin
φ_i	- independent random phases angles uniformly distributed 0 and 2π
k_i	- wave number corresponding to ω_i, given by:

$$\frac{\omega_i^2}{g} = k_i \tanh(k_i d) \tag{3.2}$$

Where

d   water depth
g   gravity

Amplitudes, a_i obtained from a wave spectrum can be given by:

$$a_i = \sqrt{2S_\eta(\omega_i)\Delta\omega}$$ (3.3)

Where

S_η - power spectral density for the sea surface elevation
$\Delta\omega$ - spacing between discretized frequencies

3.2.1.1.2   Sea surface elevation spectra

We employ a JONSWAP spectrum (Joint North Sea Wave Project) to represent the power spectral density of the surface elevation process. This wave spectrum is considered to represent North Sea conditions sufficiently. The formula for the JONSWAP spectrum may be given as follows [5]:

$$S_\eta(\omega) = \frac{5}{16}H_s^2\left(\frac{\omega_p^4}{\omega^5}\right)\exp\left[\frac{5}{4}\left(\frac{\omega}{\omega_p}\right)^{-4}\right](1-0.287\ln(\gamma))\gamma_s^b$$ (3.4)

Where

γ_s - peak enhancement factor
ω_p - spectral peak frequency, given by:

$$\omega_p = \frac{2\pi}{T_p}$$ (3.5)

b   - a parameter of the value of unity, given by:

$$b = \exp\left[-\frac{1}{2\sigma^2}\left(\frac{\omega-\omega_p}{\omega_p}\right)^2\right]$$ (3.6)

3.2.1.2   *Deterministic approach*

Wave loading using a deterministic approach, is obtained by stepping a single periodic extreme wave through the structure. Deterministic loading is characterized by that the loading is known at all instants of time. This is a popular approach in analysing slender fixed offshore structures, such as jack-up units. The water particle kinematics are usually represented by a higher order wave theory when using this approach.

The relations between the extreme deterministic wave height and the significant wave height in a three hour storm, may be given by:

$$H_{\max} \approx 1.86 H_s \qquad (3.7)$$

Where

$H_{\max}$ - maximum wave height (depending upon the number of cycles as this is representing a Rayleigh distribution of the peaks, i.e. wave average periods of 10 seconds in a three hour storm duration)

3.2.2   Wave kinematics

In this work, wave particles velocities and wave accelerations are obtained using the kinematics defined by Airy and Stokes 5th order wave theory.

The Airy wave theory is used in the first part of the dynamic analysis procedure, i.e. in determination of the dynamic amplification factors (DAFs), while Stokes 5th wave theory is used in the second part, i.e. in the deterministic analysis.

3.2.2.1   *Linear Airy wave theory*

The wave potential in linear Airy wave theory is given by:

$$\phi = \frac{A_i \omega_i}{k_i} \frac{\cosh\left(k_i\left(d+z\right)\right)}{\sinh\left(k_i d\right)} \cos\left(k_i x - \omega_i t\right) \qquad (3.8)$$

Since the Airy wave theory is based upon infinitesimal wave heights, the wave profile must be stretched or compressed to the actual wave surface. A linear stretching wave profile is adopted using the linear Wheeler stretching technique, which means that the Airy theory is stretched above mean sea water level and up to the top of the wave by substituting the vertical coordinate z with the scaled coordinate z' where the instantaneous surface elevation is

$$z_w = \frac{z - \eta}{1 + \eta / d} \qquad (3.9)$$

Where

z_w - modified coordinate for use in the particle velocity formulation

3.2.2.2   *Stokes 5th order wave theory*

The wave potential given in Stoke 5th order wave theory can be expressed by a series expansion with five terms:

$$\phi = \sum_{n=1}^{5} \phi_n \cosh\left(nk_j z\right) \cos\left(n\left(k_j x - \omega_j t\right)\right) \qquad (3.10)$$

Where

ϕ_n - series of coefficients

k_j - wave number corresponding to ω_j, given by

$$\frac{\omega_j^2}{g} = k_j \tanh\left(k_j d\right)\left[1 + \lambda^2 C_1 + \lambda^4 C_2\right] \tag{3.11}$$

Where λ, C_1 and C_2 are all coefficients, usually calculated using a method suggested by Skjelbreia and Hendrickson [14].

3.2.2.3   *Other wave theories*

Depending on range and validity, other wave theories may also be used. The applicability of wave theories can be illustrated graphically in accordance with SNAME 5-5A [7]:
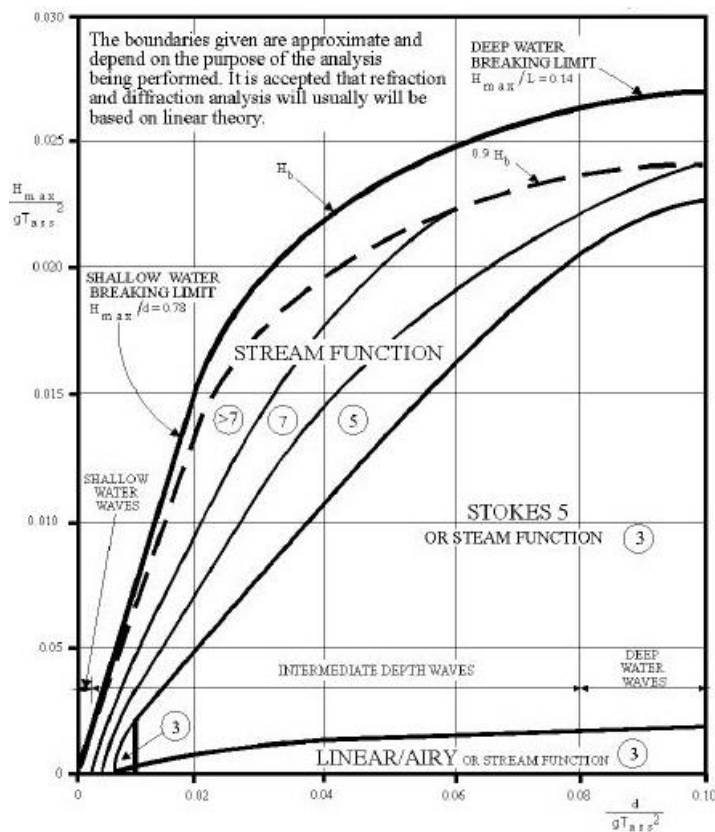
Figure 3-2- Applicability of wave theories, extracted from SNAME 5-5A Commentary Guidelines [7]

3.2.3   Kinematics reduction factor

A kinematic reduction factor is used when water particles are represented by a nonlinear wave theory. This kinematic reduction factor is calculated in accordance with ISO standard [5]. This factor reduces the wave force due to directional spreading or irregularity in wave profile, by factoring the horizontal velocity and acceleration. The reader is referred to ISO standard [5] for the formula expression.

14

3.2.4 Current

The current velocity comprise components due to tidal current, storm surge current and wind driven current and is included in the total fluid velocity by a vector sum of the velocity due to the wave particles and the current.

In a similar manner as for the Airy wave theory, a linear stretching current profile is adopted using the liner Wheeler stretching technique, in order to let the current profile be stretched or compressed to the actual wave surface.

The current at a distance above the mean water level is calculated from the following expression [15]:

$$V(z) = V_w(z) \frac{(z+d)}{(z_w+d)} \frac{d}{(d+\eta)} \tag{3.12}$$

Where

V_w - specified current at elevation z_w

3.2.5 Calculations of hydrodynamic forces

Hydrodynamic forces are computed using a modified version of the Morison's equation, composed of a nonlinear drag term plus an inertia force term.

The fluid force on a member, calculated using the Morison equation can be expressed as the vector sum of:

$$\Delta F = \Delta F_{drag} + \Delta F_{inertia} = \frac{1}{2} \rho_w D C_D (U - \dot{z}) |U - \dot{z}| + \rho_w C_M A \frac{\partial U}{\partial t} \tag{3.13}$$

Where

ΔF_{drag}	- drag force per unit length normal to the axis of member considered
ρ_w	- mass density of water
D	- effective diameter, equivalent diameter
C_D	- drag coefficient
U	- fluid particle velocity (wave particles + current) vector normal to the member
$\dot{z}$	- structural velocity vector normal to the member
$\Delta F_{inertia}$	- inertia force per unit length normal to the axis of member considered
C_M	- inertia coefficient
A	- area of member

The total force is obtained by integrating equation (3.13) along the member axis.

The quadratic drag term plus the integration of forces to the instantaneous wave surface makes the hydrodynamic force inherently nonlinear. Thus, the necessity of an iterative approach for calculation of the forces. The procedure for such an approach in SACS [15] is as follows:

"A wave is stepped through the structure such that one full cycle of the wave is completed. For each wave crest position the distributed member forces are computed using Morison's equation. Using static equilibrium, the equivalent joint forces are determined. The equivalent joint forces are multiplied by the modal eigenvectors to obtain the modal generalized forces for each wave crest position.

Considering each mode individually and assuming that the generalized force is a repeatable function, the generalized force may be decomposed into various Fourier components, each of which is a sinusoidal function with an associated phase angle. The modal response may then be calculated for each Fourier component of the generalized force. The total response of the mode is then determined by linearly combining the responses due to each component.

The motion of any point on the structure may be determined by summing the responses from all modes. Knowing this motion, the relative fluid velocity, U-ż, can be determined by subtracting the velocity of the structure from the water particle velocity. A new set of member forces are then calculated using Morison's equation.
The process is continued until the difference between the generalized forces for the current iteration and the generalized forces of the previous iteration are within the specified tolerance or the maximum number of iterations has been reached".
In this study the loads are calculated using the Morison equation at each step the wave is stepped through 5 degrees increments and at a total of 72 positions.

3.2.6 Wind loading

Components exposed to wind are divided into blocks, where the wind loading is obtained by multiplying the pressure by the projected block area. The total wind force can then be obtained by summing the wind loading over all blocks.
Wind forces are calculated using the following formula in ISO standard [5].

$$F_{Wi} = P_i A_{Wi} \tag{3.14}$$

Where

A_{Wi} - projected area of the surface or member normal to the force
P_i - wind pressure at the centre of block i, given by:

$$P_i = \frac{1}{2} \rho_{air} V_{Zi}^2 C_S \tag{3.15}$$

Where

ρ_{air} - density of the air
V_{Zi} - wind velocity at the centre of block *i*
C_s - shape coefficients

3.3 Structural modelling

3.3.1 General

There are different modelling techniques that can be used to depict jack-up units. These techniques have different applicability and limitations with respect to the units design and level of detailed checks. For a Site-Specific Assessment (SSA) it is rarely necessary to fully model the jack-up unit.
In this work, a jack-up unit is modelled as a so-called simplified 'barstool' model or an *equivalent* model, using an *equivalent* stiffness model of legs and spudcans, *equivalent* leg-hull connection springs and representative beam-element hull grillage.

This model is suitable for performing the global analyses, where global loads are assessed and checks of foundation, overturning stability and the global leg loads are covered.

After performing a global analysis of the barstool model, a more detailed analysis of a single leg model may be recommended to assess the strength of leg members and leg holding system. This detailed single leg model consists of a detailed leg and is used in conjunction with the reactions at the spudcan or the forces and moments in the vicinity of lower guide, obtained from the global barstool model.

Analysing a single detailed leg model is not considered in this study, because of insufficient design data and because a first pass estimate of leg and leg holding system from the global barstool analysis is considered sufficient.

The studied jack-up unit is triangular and symmetric shaped. The unit design basis is based upon the MSC-CJ70 Class drilling unit. Details about the design is given in Section 5.2. The structural modelling follow the requirements given in ISO standard [5].

The simplified barstool model representing the jack-up unit studied is given in Figure 3-3.
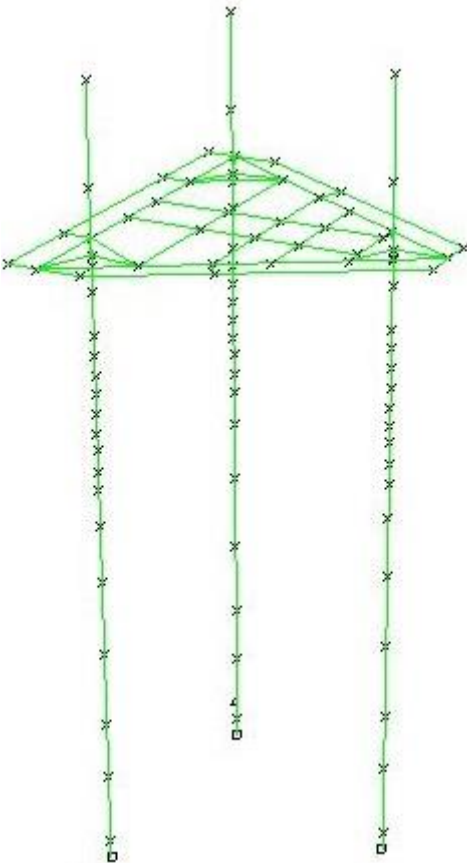
Figure 3-3- Jack-up unit represented as a simplified barstool model in SACS

3.3.2 Equivalent leg modelling

The equivalent leg model represents both the spudcan and legs.
The stiffness of a leg is characterized by the following equivalent cross sectional properties:

- Cross sectional area
- Moment of inertia
- Shear area
- Torsional moment of inertia

The most dominating factor affecting the leg stiffness is leg bending. The shear deflection of most members is small, but it can be significant in a lattice structure.
The legs in the barstool model is modelled by a series of collinear beams, where the cross sectional properties are derived by employing the formulas given in the ISO standard [5].
The determination of stiffness for the equivalent leg model is accomplished as outlined below.

3.3.2.1   Equations given in ISO standard

The equations given in the ISO standard [5] are shown in Figure 3-4 and Figure 3-5. Varying sizes of chords and braces along the leg can be accounted for by calculating the properties for each leg section and creating the equivalent leg model accordingly.

	Structure	Effective shear area
A		$A_{sl} = \dfrac{(1+v)sh^2}{\dfrac{d^3}{2A_D} + \dfrac{s^3}{6A_c}}$
B		$A_{sl} = \dfrac{(1+v)sh^2}{\dfrac{d^3}{A_D} + \dfrac{h^3}{SA_v} - \dfrac{s^3}{NA_c}\left(\dfrac{N^3}{3} - \sum_{i=1}^{N} i^2\right)}$
C		$A_{sl} = \dfrac{(1+v)sh^2}{\dfrac{d^3}{4A_D} - \dfrac{s^3}{12A_c}}$
D		$A_{sl} = \dfrac{(1+v)sh^2}{\dfrac{d^3}{2A_D} + \dfrac{h^3}{2A_v} + \dfrac{s^3}{6A_c}}$
E		$A_{sl} = \dfrac{48(1+v)I_G}{s^2\left(1 + \dfrac{d}{S}\dfrac{I_G}{I_B}\right)\dfrac{d}{h}}$

Figure 3-4- Equations for determining the effective shear area for two-dimensional structures, extracted from ISO19905-1 [5]

Leg type		Equivalent properties
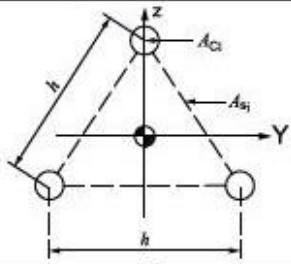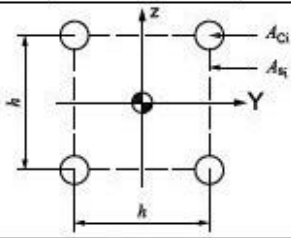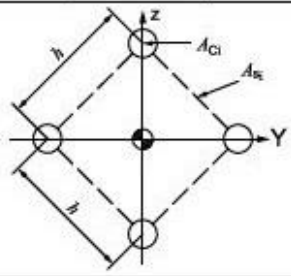
Figure 3-5 – Equations for determining the equivalent section properties of three-dimensional lattice legs, taken from ISO19905-1 [5]

3.3.3   Equivalent hydrodynamic coefficients

Hydrodynamic drag and mass coefficients are calculated using an equivalent drag coefficient C_{De}, and an equivalent mass coefficient C_{Me}, used on a lattice leg represented by an equivalent diameter D_e.
In accordance with the ISO standard [5], these are calculated using the following procedures.

3.3.3.1   Equivalent diameter

The equivalent diameter of the lattice leg can be given by:

$$D_e = \sqrt{\sum_{i=1}^{n}\left(D_i^2 l_i\right)/s} \qquad (3.16)$$

Where

D_i - reference diameter of member i
l_i - reference length of member i (node to node)
s   - height of one bay

3.3.3.2   *Equivalent drag coefficient*

The equivalent drag coefficient of the lattice leg is determined by:

$$C_{De} = \sum_{i=1}^{n} C_{Dei} \qquad (3.17)$$

Where

C_{Dei} - equivalent drag coefficient of each individual member i, given by:

$$C_{Dei} = \left[\sin^2 \beta_i + \cos^2 \beta_i \sin^2 \alpha_1 \right]^{3/2} C_{Di} \frac{D_i l_i}{D_e s} \qquad (3.18)$$

Where

C_{Di} - drag coefficient of each individual member i, related to the reference diameter
α_1 - angle between flow direction and member axis
β_1 - angle defining the member inclination from the horizontal plane

See Figure 3-6 for illustration of flow angles to a lattice leg structure within one bay height.
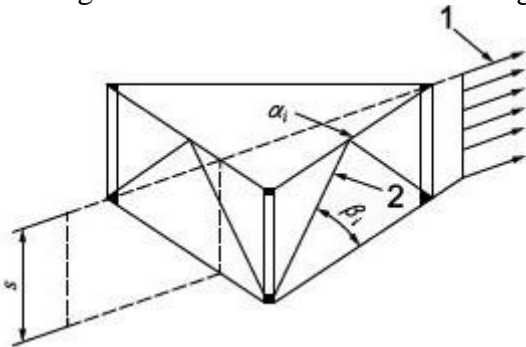
Figure 3-6 – Flow angles appropriate to a lattice leg, extracted from the ISO standard [5]

The drag coefficient of each individual member is calculated based on the geometry.
For plain tubular elements, such as internal, diagonals and horizontal elements, the individual drag coefficient is set to 1.05 (rough) and 0.65 (smooth).
In this study, the jack-up is assumed to have 3 split tube chords and X-bracing. This is used in large jack-up designs, such as the CJ70, CJ80 and JU2000E designs. A split tube chord is a chord combined with a rack. An illustration is shown in Figure 3-7.

CHORD SECTION DETAIL
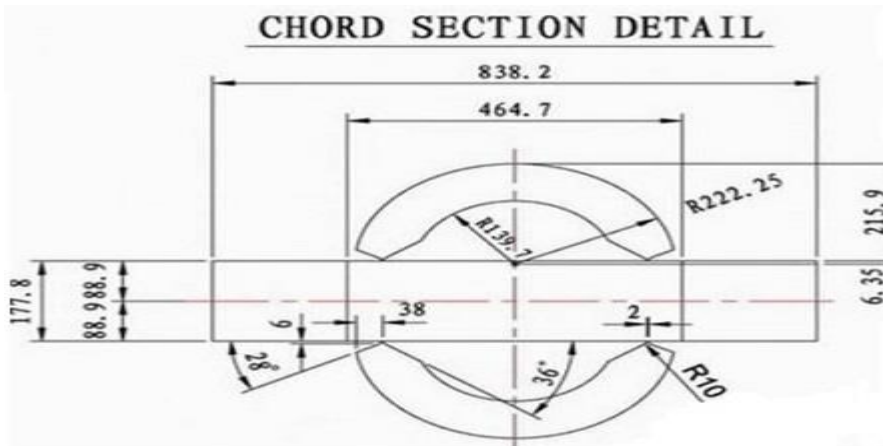
Figure 3-7- Chord Section details for JU2000E
(http://www.timeast.com.cn/dl/en/achievement_d.asp?id=154)

The drag coefficient for a split tube is calculated by:

$$C_{Di} = \begin{cases} C_{Do} & ;\ 0^{\circ} < \theta \le 20^{\circ} \\ C_{Do} + \left(C_{D1} \dfrac{W}{D_i} - C_{Do} \right) \sin^2 \left[\left(\theta - 20^{\circ} \right) 9/7 \right] & ;\ 20^{\circ} < \theta \le 90^{\circ} \end{cases} \tag{3.19}$$

Where

C_{Do}	- drag coefficient for a tubular with appropriate roughness
θ	- angle between flow direction and plane of rack
W	- average width of the rack
C_{D1}	- drag coefficient for flow normal to the rack, given by:

$$C_{D1} = \begin{cases} 1.8 & ; & W/D_i < 1.2 \\ 1.4 + 1/3 \left(W/D_i \right) & ; & 1.2 < W/D_i < 1.8 \\ 2.0 & ; & 1.8 < W/D_i \end{cases} \tag{3.20}$$
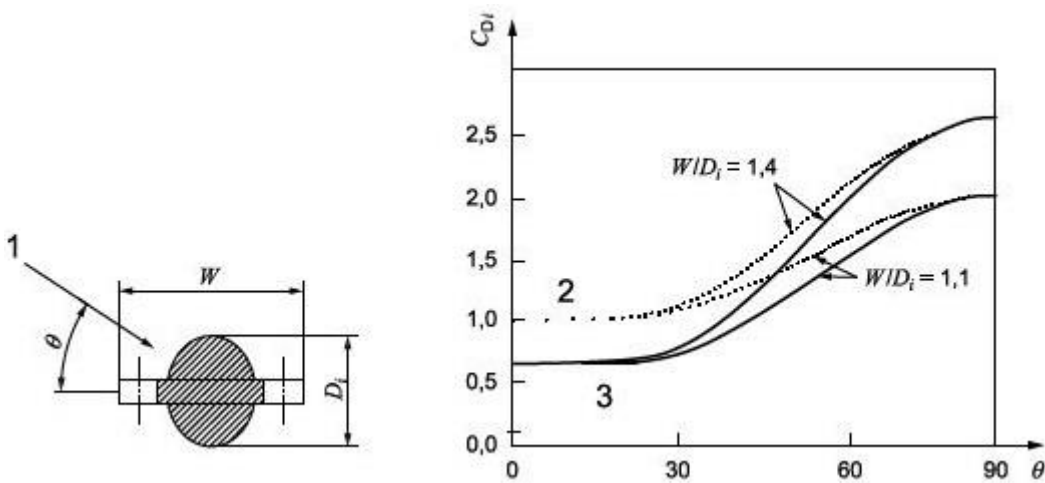
Figure 3-8- Split tube chord and graph showing typical values for individual drag coefficients, taken from the ISO standard [5]

3.3.3.3 *Equivalent mass coefficient*

The equivalent inertia coefficient C_{Me} of a lattice leg is recommended to fixed at 2.0 (smooth) and 1.80 (rough).
The added mass coefficient C_{Ae}, is defined as $(C_{Me}-1)$ and used in conjunction with the equivalent area of the leg, calculated by Section 3.3.2.1.

3.3.4 Equivalent hull modelling

The hull structure is modelled as a grillage of beam members. Cross-sectional properties of the beams are determined based on assumptions and previous reports. Normally, cross sectional parameters should be calculated based on original engineering drawings of the deck, i.e. based on information of bulkheads, side shell and the "effective width" of deck and bottom plating.

3.3.5 Modelling the leg-hull connection and stiffness

The leg-hull connection is of extreme importance to the analysis since it controls the distribution of leg bending moments and shears carried between the upper and lower guide structures and the jacking or fixation system. For new and large jack-up units it is common to have a floating or fixed fixation system [7]. For units with a fixation system it is common to transfer the leg bending moment and axial forces at the leg-hull connection by the fixation system because of its high stiffness. However, independent of system, it is very important that these systems are properly modelled in terms of stiffness, orientation and clearance.

In the barstool model, the leg-hull connection is accounted for by adding a rotational and vertical spring stiffness in order to account for rigidity of fixation or jacking system. The stiffnesses of the springs are derived by applying unit load/moment cases to two detailed leg model, one without a leg-hull connection and the other with leg-hull connection.

3.3.5.1 *Application of unit load approach*

The procedure to determine stiffness properties of the equivalent leg-hull connection using the unit load case approach is as follows.
Unit loads are applied to two detailed leg models, one model with and one without the leg hull connection. Difference in deflections and slopes between these two models, determines the stiffness properties of the equivalent leg-hull connection.
The detailed leg models acts a cantilever beam where the unit load is applied at the free end. The slope and rotation is calculated in accordance with elastic beam theory.

3.3.5.1.1 Axial unit load case

$$K_v = \frac{F}{\left(\Delta_C - \Delta\right)} \tag{3.21}$$

Where

K_v - vertical leg-hull connection stiffness
F   - unit load

Δ-Δ_c - difference in vertical displacements between the detailed leg model and the detailed combined leg with the leg-hull connection

3.3.5.1.2   Unit moment load case

$$K_r = \frac{M}{(\theta_C - \theta)}$$ (3.22)

Where

K_r - rotational leg-hull connection stiffness
M   - unit moment load
θ-θ_c - difference in rotations between the detailed leg model and the detailed combined leg with the leg-hull connection

The horizontal leg-hull connection stiffness is considered infinite.

3.3.6   P-δ effects

P-δ effect is a physical geometric nonlinearity, which cause large displacements. Since we deal with nonlinearity, the principle of superposition does not apply, which means a linear analysis will not account for these effects and thereby yield wrong results.
P-δ effects occur in a jack-up unit because is a relatively flexible structure and is subjected to lateral displacement of the hull during environmental actions. As a result of this hull translation, the vertical reaction of the spudcan does not pass through the centroid of the leg at the level of the hull.
This results in nonlinear large displacement effects:

   i)   Global P-δ effect, which will increase the global overturning moment (OTM).
   ii)   Local P-δ effect (Euler amplification), which will increase member stresses.

This phenomenon can be explained in a more general context:
The lateral stiffness of an element is a function of axial force such that axial compression reduces the lateral stiffness while axial tension increases the lateral stiffness. For typical linear static analysis, the effect of axial force on the lateral stiffness is negligible. For other structures, such as a large flexible jack-up unit, the axial force does have a significant effect on the lateral stiffness of the elements.

There are generally two available procedures to include the P-δ effects:

   i)   A nonlinear large displacement analysis
   ii)   A geometric stiffness method.

The procedure of the large displacement analysis may be performed by an implicit or explicit method. Normally an implicit (the full Newton-Raphson iterations) method is used, where the nonlinear solution is obtained by applying the load in increments and iteratively generating the stiffness matrix for next load increment from the deflected shape (nodal deflections) of the previous increment. For more information regarding nonlinear analysis, the reader is referred to Appendix A, A.1.4.

P-δ effects are automatically included in nonlinear large displacement analysis, because, in a large displacement analysis a new stiffness matrix is calculated for each load increment based on the displaced shape from the previous load increment, i.e. it automatically accounts for lateral stiffness in every load increment.

The alternative procedure is to use a linear geometric stiffness method. This method incorporates a linear correction term, a negative stiffness matrix into the global stiffness matrix prior to the linear analysis.
For further details on this procedure, the reader is referred to [7].

Figure 3-9 illustrate P-δ effects on a jack-up unit.
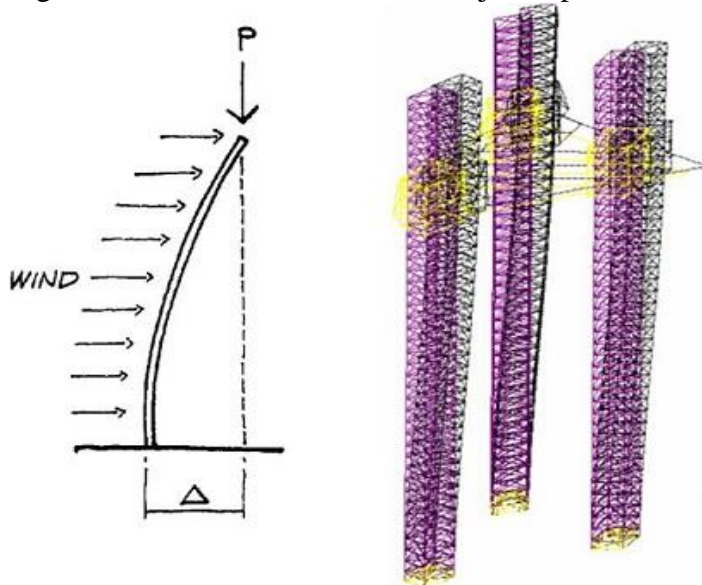
Figure 3-9- P-δ effects on a jack-up unit, extracted from Morandi [34]

3.4   Mass modelling

The mass elements included in this study are as follows:

- The elevated mass (arising from hull self-weight; mass of additional equipment, variable mass from drilling equipment and consumables and other supplies)
- Leg mass, added mass and any entrained and entrapped mass
- Spudcan mass and entrapped mass

The elevated mass (hull dead weight) is modelled at the hull, while the leg and spudcan mass are modelled as nodal masses along the leg.
The hull mass is modelled differently in the determining the DAFs (first phase) and in the global large displacement analysis (second phase).
In the first phase, hull mass is distributed in the grillage, while in the second phase, hull mass is partly (25 %) distributed in the grillage and the remainder as centre leg masses.

3.5 Damping modelling

Damping is expressed as a percentage of the critical damping, defined by:

$$\zeta = \frac{c}{c_{cr}} 100\% \tag{3.23}$$

Where

c   - system damping
c_{cr} - critical damping coefficient, defined by:

$$c_{cr} = 2m\omega_0 \tag{3.24}$$

Where

m   - system mass
ω_0 - natural frequencies of the system

There are mainly three media contributing to damping of a jack-up unit.
These are structural damping, due to internal friction in the structure itself and in the leg holding system.
Soil damping due to geometric and inner (hysteresis) damping.
Hydrodynamic damping consisting of small potential and drag damping mechanism. When relative velocity is used, the hydrodynamic damping is not accounted for, because the drag damping will implicitly be part of the hydrodynamic loads. The potential damping is considered negligible in jack-up structures.

A linear and viscous damping model is used to describe the damping mechanism in the jack-up structure. Where all contributing damping media are modelled by a proportional or Rayleigh damping model.
The total damping is set to 7 % of the critical damping, which is a recommendation by the ISO standard [5].

3.6 Soil modelling

A geotechnical assessment involving a site survey followed by a report including a FEA estimating the penetration and capacities are usually included in a Site-Specific Assessment (SSA) of a jack-up unit.
The penetration distance is determined by penetration analyses, expressed by a load-penetration curve. The maximum "allowable" penetration occurs at the jack-ups maximum preload capacity.
The governing factors establishing this curve is the soil conditions and the spudcan geometry.
An illustration of an example for two spudcan geometries following a different load-penetration curve in a soil condition of a thin top sand layer followed by a soft layer of clay is given in Figure 3-10.
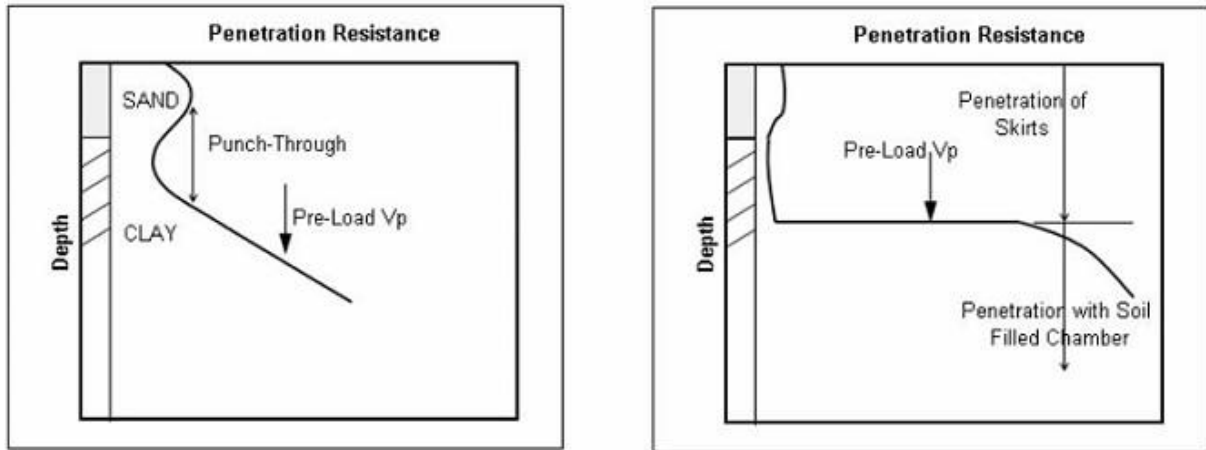
Figure 3-10- Punch-through profiles for a conventional spudcan (left) and a skirted spudcan (right), in the same soil conditions, taken from Guidelines for jack-up rigs with particular reference to foundation integrity [33]

Modern jackups, typically with skirted spudcans, will sit on a hard clay, with effective penetration levels between 2.0-3.5meters. The effective penetration, defined as the maximum penetration minus the spudcan tip, is also called seabed reaction points. At these points the foundation capacities are calculated, and modelled with or without nonlinear soil-structure interaction.

Foundation capacities and stiffnesses may be estimated by an FEA or calculated using semi-empirical formulas given in the ISO standard [5].

In this study, the nonlinear soil-structure interaction is represented by linear springs. The effective penetration level is assumed to be between 3.0-3.5meters and semi-empirical formulas given in the ISO standard [5] are used to determine foundation stiffnesses and capacities.

3.6.1 Foundation stiffnesses

Linear spring stiffnesses in vertical, horizontal and rotational are estimated based on elastic solutions for a rigid circular plate on an elastic half-space, using the following formulas given by the ISO standard [5]:

3.6.1.1 Vertical stiffness

$$K_1 = K_{d1} \frac{2GB}{(1-v)} \tag{3.25}$$

3.6.1.2 Horizontal stiffness

$$K_2 = K_{d2} \frac{16GB(1-v)}{(7-8v)} \tag{3.26}$$

3.6.1.3   *Rotational stiffness*

$$K_3 = K_{d3} \frac{GB^3}{3(1-v)}$$

(3.27)

Where

G	- shear modulus of the foundation soil
B	- effective spudcan diameter
υ	- poisson's ratio of the foundation soil
$K_{d1,2,3}$	- stiffness depth factors

3.6.2   Yield surface

The yield surface in the ISO standard [5] is developed based on ultimate vertical, horizontal and moment capacities using the following formula:

$$\left(\frac{F_h}{Q_h}\right)^2 + \left(\frac{F_m}{Q_m}\right)^2 - 16(1-a)\left(\frac{F_v}{Q_v}\right)^2\left(1-\frac{F_v}{Q_v}\right)^2 - 4a\left(\frac{F_v}{Q_v}\right)\left(1-\frac{F_v}{Q_v}\right) = 0$$

(3.28)

Where

F_h	- horizontal force applied to the spudcan
F_v	- vertical force applied to the spudcan
F_m	- bending moment applied to the spudcan
Q_h	- horizontal foundation capacity
Q_v	- vertical bearing capacity
Q_m	- moment foundation capacity
D_s	- greatest depth of spudcan bearing area below the sea floor
a	- depth embedment factor in clay, given by

$$a = \begin{cases} D_s / 2.5B & ; D < 2.5B \\ 1.0 & ; D \geq 2.5B \end{cases}$$

(3.29)

In sand the depth embedment factor is always zero.
The below chart shows a sample yield surface in sand based on $Q_h = 20000$kN, $Q_m = 250000$kNm, $Q_v = 160000$kN and a = 0.
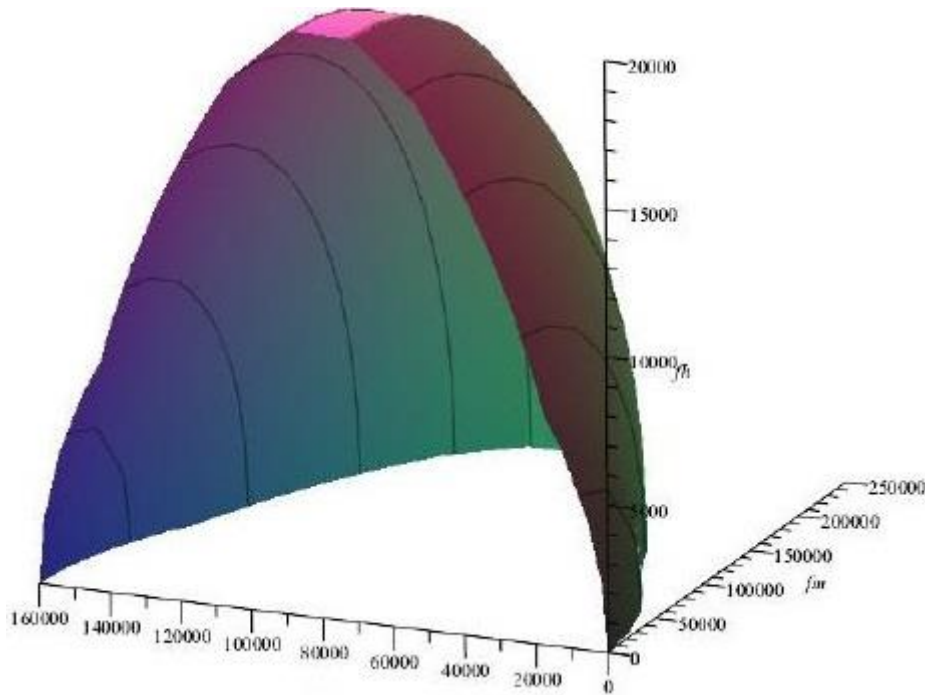
Figure 3-11- Example yield surface using Q_h=20000kN, Q_m=250000kNm, Q_v=160000KN and a=0

In this study, capacities are calculated using the following formula for clay formulation given in ISO standard [5]:

3.6.2.1 Vertical bearing capacity

$$Q_v = Q_{vo} \tag{3.30}$$

Where

Q_{vo} - vertical capacity achieved during preloading

3.6.2.2 Horizontal capacity

$$Q_h = C_h \left(Q_v - p'_0 \pi B^2 / 4\right) = C_h Q_{vnet} \tag{3.31}$$

Where

p'_0 - effective overburden pressure of the maximum spudcan bearing area
C_h - depth factor

3.6.2.3 Moment capacity

$$Q_m = \left[0.1 + 0.05a\left(1 + b / 2\right)\right] Q_{vnet} B \tag{3.32}$$

4 THEORETICAL BASIS FOR CALCULATING THE DYNAMIC RESPONSE

4.1 General

In accordance with the ISO standard [5], response of a jack up unit is determined by combining applied factored loading with a structural model to determine the internal forces in the members and the reactions at the foundations. These internal forces and reactions are compared with the factored resistances available to take up these loads to determine the safety of the unit. The loads consist of fixed loads (self-weight and non-varying loads) and variable loads, such as environmental and variable deck loads.

The ULS responses include assessment of overturning stability of the jack up, preload requirements, bearing capacity, leg strength, leg holding system strength, displacements at the spudcans and horizontal deflections of the hull.

4.2 Analyses techniques

The extreme ULS response can be determined by a two-stage deterministic storm analysis procedure using a quasi-static analysis that includes an inertial loadset, or by a more detailed fully integrated (random) dynamic procedure that uses a stochastic storm analysis.

The most common method is the two-stage deterministic storm analysis. This method assume that the extreme responses are uniquely linked to the occurrence of a single and periodic extreme wave. Deterministic responses are calculated by time stepping the single and periodic extreme wave through the structure.

4.2.1 Deterministic two-stage analysis

The first stage of this procedure is to estimate the dynamic response and determine the Dynamic Amplification Factors (DAFs) from a dynamic analysis, in order to develop an inertial loadset induced by the wave-current actions. The dynamic response is evaluated based on either a simple linear analysis (SDOF) or a complex (random dynamic) analysis.

The foundation and structural assessment is next performed using a quasi-static, iterative analysis technique, for which the dynamic actions have already been determined through the inertial loadset. The quasi-static analysis can be accomplished by means of either an elasto-plastic foundation model or by a simplified application of a full plasticity analysis. This full plasticity analysis is very commonly used, due to its simplicity and good results. The approach is basically just to apply moments on the spudcan by including a simple linear rotational spring. The moments applied are limited to the capacities, given in Chapter 3.6.2.3, which based on the yield interaction relationship between the gross vertical force (F_V), the horizontal force (F_H) and the moment (F_M) acting on the spudcan.

A flow chart describing the analysis procedure for a two-stage assessment is extracted from ISO standard [5] is given in Figure 4-1:
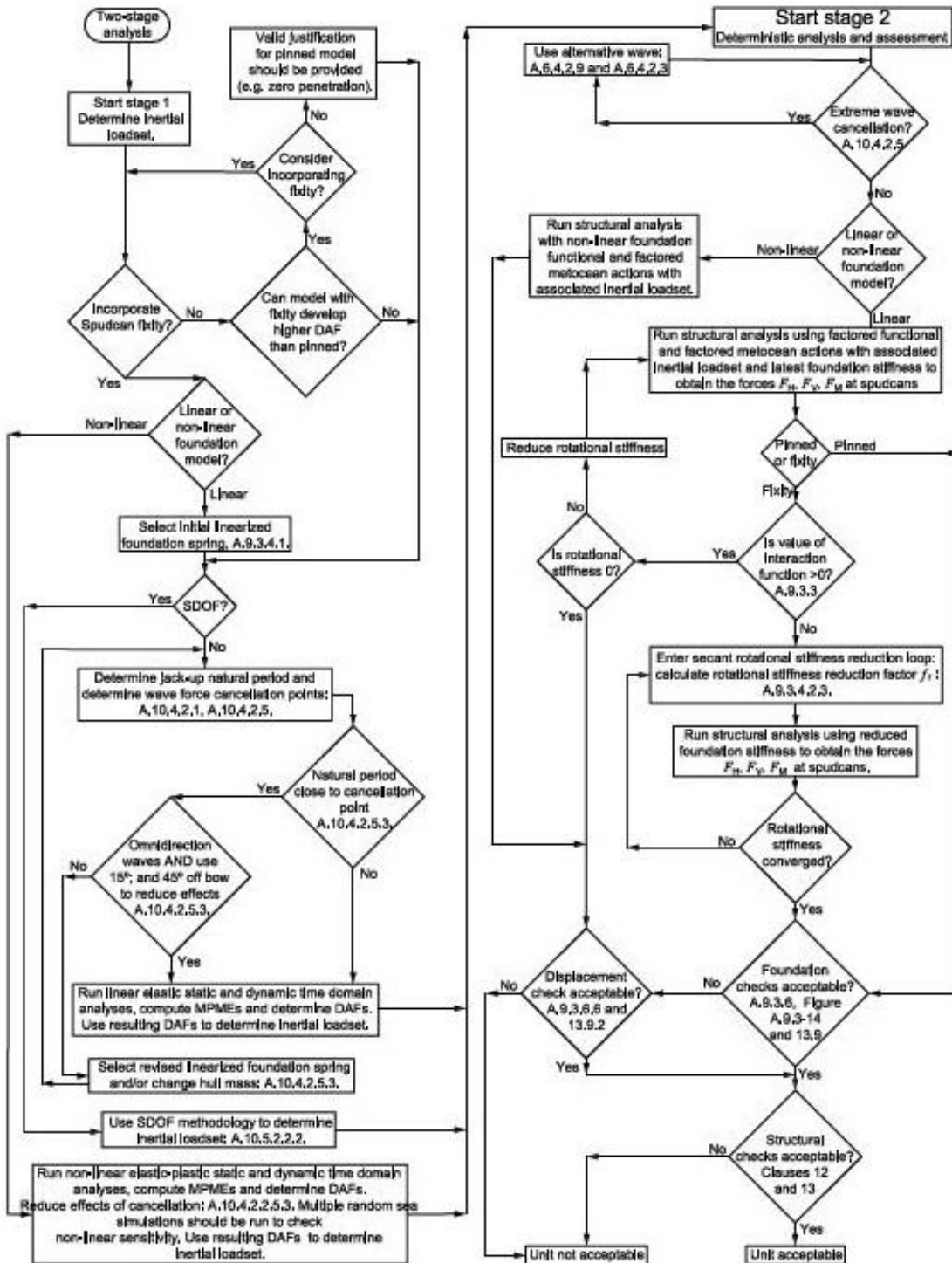
Figure 4-1- Analysis procedure for a two-stage deterministic assessment, extracted from ISO19905-1

4.2.2   Stochastic storm one-stage analysis

In this method, the dynamic structural analysis and assessment is performed using one model. This model must be fully detailed, and a nonlinear time domain analysis is performed taking into account the elasto-plastic behavior of the foundation.
This method often requires a complex incremental and an iterative calculation procedure. The outline procedure can be explained in the following steps: A random dynamic time domain analysis is first performed to determine the structural response and foundation forces at each time step. The next step is to capture the elastic and plastic portions of the foundation behavior at each time step using a nonlinear elasto-plastic model. The last and third step is to determine the extreme response from the non-Gaussian responses through a recommended stochastic method [5].

The alternative procedures can be summarized in Figure 4-2.

Parameter	Two-stage deterministic storm analysis			One-stage stochastic storm analysis
	Stage 1 Determine DAF		Stage 2 Single deterministic storm analysis	Multiple random time domain simulations
	$K_{DAF,SDOF}$	$K_{DAF,RANDOM}$		
Wave/current actions	not applicable	Random (superposition of linear components)	High order regular wave	Random (linear or higher order)
Dynamics	$K_{DAF,SDOF} = \dfrac{1}{\sqrt{(1-\Omega^2)^2+(2\zeta\Omega)^2}}$	Time domain simulations	Inertial loadset determined by means of $K_{DAF,SDOF}$ or $K_{DAF,RANDOM}$	Time domain simulations
Wind actions	not applicable	Ignore	Quasi-static	Quasi-static
Foundation	Linearized	Linearized	Non-linear	Non-linear
Structure	Stiffness from non-linear structure	Non-linear or calibrated to non-linear	Non-linear	Non-linear
Output	$K_{DAF,SDOF}$	$K_{DAF,RANDOM}$	(Global) responses	(Global) responses

Figure 4-2- Alternative procedures, extracted from ISO-19905-1

4.3   Dynamic analysing and determination of inertial loadset

4.3.1   Single Degree Of Freedom (SDOF) analysis

This method is very simple and typical used in a first pass assessment.
The jack-up is modeled as an equivalent mass-spring-damper mechanism. See illustration in Figure 4-3.
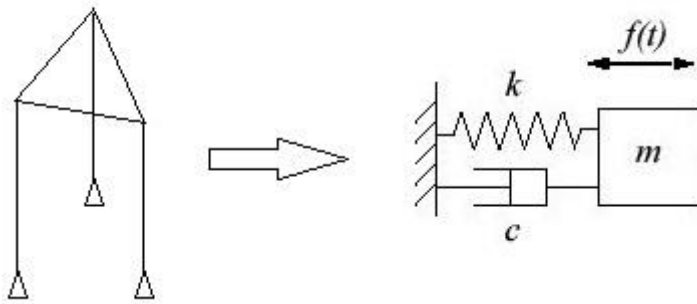
Figure 4-3 – A jack-up unit as an equivalent mass-spring-damper system

The method is fundamentally empirical because the wave and current loading does not occur at the mass centre (at the hull) and the loading is random and nonlinear.
The SDOF method has a limited range of applicability and can underestimate the DAF.
Examples of possible underestimates of DAFs are given below:
- Large current velocities compared to wave particle velocities.
- If natural period falls near a wave force peak.

The dynamic amplification factor (DAF) for a SDOF system, is defined as:

$$DAF_{SDOF} = \frac{1}{\sqrt{\left[\left(1-\Omega^2\right)^2 + \left(2\zeta\Omega\right)^2\right]}} \tag{4.1}$$

Where

ζ - damping ratio
Ω - frequency ratio, defined as:

$$\Omega = \frac{\omega}{\omega_0} \tag{4.2}$$

ω - wave circular frequency
ω_0 - natural frequency

The calculated DAFs from the SDOF analogy is used to calculate the inertial loadset which shall be applied at the mass (hull) centre in the direction of the wave propagation.

$$F_{in} = \left(DAF_{SDOF} - 1\right) F_{Amp} \tag{4.3}$$

Where

F_{in} - magnitude of the inertial loadset
F_{Amp} - static amplitude of quasi-static base shear $0.5(BS_{max} - BS_{min})$

4.3.2   Random dynamic analysis

A random dynamic analysis is based on considering a seastate as a random quantity, and is typical used to develop the dynamic response and determine the DAFs in a deterministic two-stage analysis. Random dynamic analysis may be performed in the time or frequency domain.

Frequency domain-spectral techniques are used to generate statistical measures of random structural response via the combination of structural transfer functions with an appropriate wave spectrum to produce response spectra.

The use of frequency domain spectral-analysis requires the response behavior to be linearized. This necessitates linearization of the wave-current Morison drag force term, exclusion of the free-surface inundation effects and the use of a linear representation of the structure and foundation [10]. The ISO standard [5] recommends a statistical linearization procedure formulated by Borgman [17].

In this study, a random dynamic time domain analysis is performed.

The methodology using a random dynamic time domain procedure is to determine the Most Probable Maximum Extreme (MPME) values of the dynamic and static responses from the time domain analysis with the created random wave surface history. DAF is defined as the ratio of these responses.

$$DAF_{random} = \frac{MPME_{dyn}}{MPME_{sta}} \tag{4.4}$$

Two DAFs are calculated, one for the base shear (BS) and one for the overturning moment (OTM).

The inertial loadset, which shall be imposed on the global quasi-static model, is calculated by:

$$F_{in} = (DAF_{BS} - 1) BS_{QS} \tag{4.5}$$

$$OTM = (DAF_{OTM} - 1) OTM_{QS} \tag{4.6}$$

where

BS_{QS} - maximum deterministic base shear force from the extreme wave and current imposed on the quasi-static model

OTM_{QS} - maximum deterministic overturning moment at the pinpoint from the extreme wave and current imposed on the quasi-static model

The random wave time domain analysis procedure can be described in simple steps:
A random wave train is simulated by superposition of a large number of Airy wave components with random phasing, the statistics of the water surface elevation checked against recommended tolerances, given in Section 4.3.4, this process being repeated until a validated sea surface elevation with acceptable statistics is obtained.
After a validated sea surface elevation with acceptable statistics obtained, the validated sea surface elevation, plus current, is passed through the structure in small intervals, and at each time step the total base shear (BS) and overturning moment (OTM) are calculated. The BS and OTM responses are calculated with mass (dynamic) and without mass (quasi-static).
The resulting DAFs is generated by determining the MPME of the non-Gaussian responses, i.e. post-processing the simulation data and using one of the stochastic methods described in the following section.

The random superposition model is able to incorporate nonlinearities from the hydrodynamic loads resulting in non-Gaussian responses.

The time domain analysis can be explained in simple steps:
The dynamic equation of motion (given in Appendix A, equation (A.1.17)) is solved in time domain using a stepwise method, Newmark β method, with a time step interval of 0.5 s. This analysis method is considered sufficient, since linear springs are representing the nonlinear effects of the soil-structure interaction and the leg-hull connection, damping is represented by percentage of critical, so the only nonlinearity comes from the environmental loads, i.e. drag force and integration of forces to the instantaneous wave surface. These load nonlinearities are isolated in the external load vector F_t located on the right hand side of equation (A.1.17) and the solution can efficiently be carried out without any need for updating the system matrices. A linear numerical procedure of the time domain analysis is therefore considered sufficient.

4.3.3 Statistical properties

In order to properly model the sea surface elevation in a correct manner, and to be able to estimate non-Gaussian responses using statistical random time series analysis, three statistical properties are essential. Namely the standard deviation, skewness and kurtosis.
The standard deviation can be given by:

$$\tilde{\sigma} = \sqrt{\tilde{m}_2} \qquad (4.7)$$

Karunakaran [9] define the skewness and the kurtosis coefficients as:

Skewness coefficient

$$\tilde{\gamma}_1 = \left(\frac{\tilde{m}_3}{\tilde{m}_2^{\frac{3}{2}}} \right) \qquad (4.8)$$

Kurtosis coefficient

$$\tilde{\gamma}_2 = \left(\frac{\tilde{m}_4}{\tilde{m}_2^2} \right) \qquad (4.9)$$

Where

$\tilde{y}_1$ - skewness coefficient
$\tilde{y}_2$ - kurtosis coefficient

$\tilde{m}_n$ denotes the n-th sample central moment calculated as:

$$\tilde{m}_n = \frac{1}{N} \sum_{i=1}^{N} \left(x_i - \tilde{\mu} \right)^n \qquad (4.10)$$

Where

x_i	- sample values
$\tilde{\mu}$	- sample mean
N	- number of samples in the simulated time series

The skewness coefficient describes the symmetry properties of the distribution. An increase of the coefficient indicates that the extremes of the process are increased. The distribution is symmetric if the skewness is zero. Positive values indicate a skew distributed to higher values, and negative values indicate as skewed distributions to lower values. Karunakaran [9] have illustrated the skewness coefficient, given in Figure 4-4.

The kurtosis coefficient indicate the relative amount of large values and thus the extremes of the underlying process are increased if this coefficient is increased.

The kurtosis coefficient describes the relation between small and large values in a time period. An increase in the kurtosis coefficient indicates that the number of large values in the time period is increasing. For a Gaussian process the kurtosis coefficient is 3.0. According to Haver, an increase in the kurtosis from 3.0 to 3.1 in a wave measurement in one seastate, increase the largest waves with 0.3-0.4m [18].
Karunakaran [9] have illustrated the kurtosis coefficient, given in Figure 4-5.
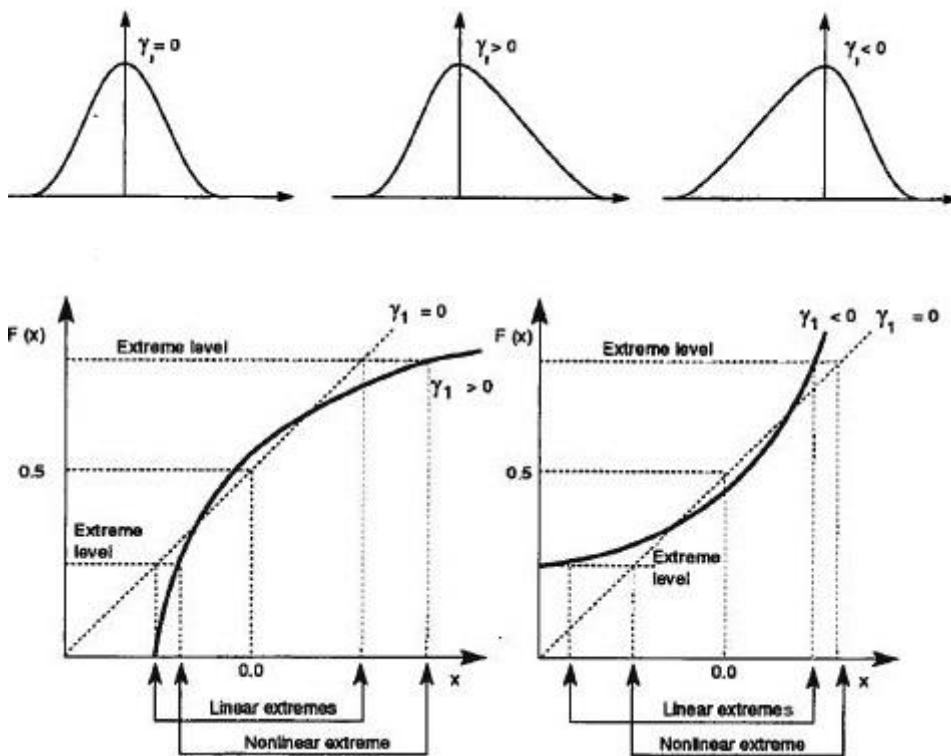
Figure 4-4- An illustration of the skewness coefficient, extracted from Karunakaran [9]

35
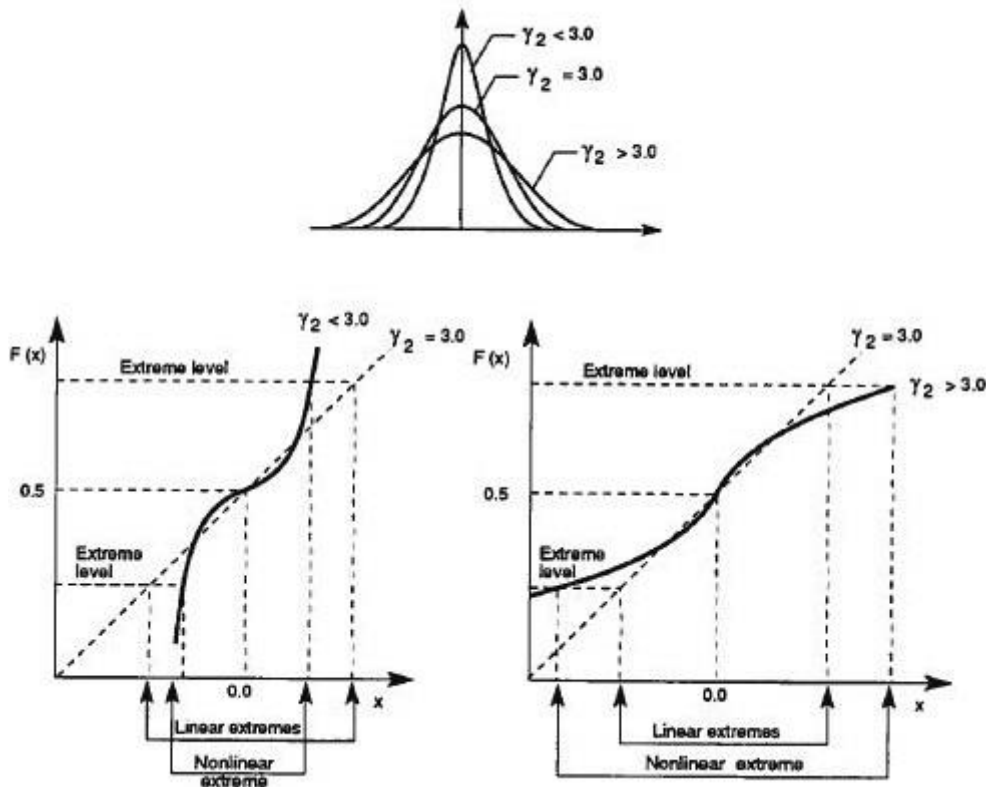
Figure 4-5 - An illustration of the kurtosis coefficient, taken from Karunakaran [9]

4.3.4   Acceptance and recommendation criteria

The acceptance and recommendation criteria for a random wave time simulation given in ISO-19905-1[5] is shown below:
For application of a time domain analysis:
Generate random sea from at least 200 components and use division of generally equal energy.
The sea surface must obey the following criteria;

- Correct mean wave elevation
- Standard deviation= $(H_s/4)\pm1\%$
- $-0.03 <$ skewness < 0.03
- $2.9 <$ kurtosis < 3.1
- Max crest elevation= $\{(H_s/4)\sqrt{2\ln(N)}\}$ -5% to +7.5%
  Where N is the number of cycles in the time series being qualified, $N \approx$ Duration / T_z
- Integration time-step less than the smaller of: $T_z/20$ or $T_n/20$

The duration of simulations must be sufficient with the method being used to determine the MPME responses.

4.4   Determination of MPME response

The structural response subjected to random seastates (from the random analysis), is predicted from stochastic methods, where the intent is to determine the Most Probable Maximum Extreme (MPME) of the BS and OTM responses using statistical methods.
As described earlier, wave-current induced loading is nonlinear due to the nonlinear drag term and free surface effects, which makes the response non-Gaussian. The statistics of this type of

processes are generally not known theoretically, but the extremes are generally larger than the extremes of a corresponding Gaussian random process.

The extreme response that should be checked in a jack-up site assessment (ULS) is the MPME response, which has a 63 % of exceedance in a three-hour storm.

The MPME is defined as the mode value or highest point on the probability density function (PDF) for extreme values of a random variable. This is approximately equivalent to the 1/1000 highest peak level in a three-hour storm and the extreme with approximately a 63 % chance of exceedance [5].

4.4.1   Stochastic methods

The ISO standard [5] recommends four prevalent methods for determining the MPME.

- Drag-inertia parameter
- Fit Weibull distribution
- Fit Gumbel distribution
- Apply Winterstein's Hermite polynomial method

4.4.1.1   Drag-inertia parameter (D/I method)

The drag-inertia method is a popular time domain method for estimating the contribution of dynamic to the response of a jack-up unit. The method was developed by Shell International Petroleum and is often referred to as the "Shell" or "SIPM" method [10].

The method is based on the assumption that the extreme value of a standardised process can be calculated by splitting the process into two parts, evaluating the extreme values of each and the correlation coefficient between the two and then combining them:

$$\left(MPM_{dyn}\right)^2 = \left(MPM_{sta}\right)^2 + \left(MPM_{ine}\right)^2 + 2\rho_R\left(MPM_{sta}\right)\left(MPM_{ine}\right) \qquad (4.11)$$

where

ρ_R - correlation coefficient of the static and dynamic responses

The extreme values of the dynamic response can therefore be estimated from the extreme values of the quasi-static response and the "inertial" response, which is the difference between the dynamic response and quasi-static response. The means and standard deviations of the response are extracted from the time domain responses.

The key procedure to this method is to determine the MPM factor for quasi-static response. Three methods are described below.

i)   Static extreme can be estimated by combining the extreme of quasi-static response to the drag term to the extreme quasi-static response of the inertia term using the Morison wave formula, by using the formula for the correlation coefficient of the quasi-static and "inertia" responses, given in Appendix A.

ii)   Or, as the structural responses are nonlinear and non-Gussian, the static extreme can be estimated using a non-Gaussian measure. By introducing a parameter K, defined as the ratio of the drag force to the inertia force acting on a structural member. The purpose of this function K, depending on the member hydrodynamic properties and seastate, shall measure the degree of nonlinearity and the deviation from a Gaussian process. As an engineering postulate, the probability density function of force per unit length, may be

used to predict other structural responses by obtaining an appropriate value of K from time domain simulations. The K can either be estimated from the standard deviation of the response, due to the drag and inertia load separately.

iii)   Or, the K can be estimated from the kurtosis of the structural response and further used to calculate the MPM factor for the quasi-static response.

The latter approach is the most common. See Lu et al. [9] for more details and a comparison between the approaches.
A complete procedure, including DAF scaling (if the ratio between the natural period and the peak period is higher than 60 %), of the drag-inertia method given in the ISO standard and SNAME 5-5A is shown in Appendix A.

4.4.1.2   Weibull fitting (Weibull method)

Weibull fitting is based on the assumption that for drag dominated marine structures, the cumulative distribution of the maxima of the structural response can be fitted to a Weibull class of distribution.

$$F_R\left(R,\alpha,\beta,\gamma\right) = 1 - \exp\left[-\left(\frac{R-\gamma}{\alpha}\right)^{\beta}\right] \tag{4.12}$$

where

α   - Weibull scale parameter
β   - Weibull slope parameter
γ   - Weibull threshold parameter

The extreme values for a specified exceedance probability (e.g., 1/N) can therefore be calculated as:

$$R = \gamma + \alpha\left[-\ln\left(1-F_R\right)\right]^{1/\beta} \tag{4.13}$$

Using a uniform level of exceedance probability 1/N, Eq. (4.13) leads to:

$$R_{MPME} = \gamma + \alpha\left[-\ln\left(1/N\right)\right]^{1/\beta} \tag{4.14}$$

The key issue for using this method is to calculate the parameters α, β and γ, which can be estimated from regression analysis, maximum likelihood estimation or static moment fitting. The ISO standard [5] recommends when using this method, to fit the distribution to a distribution of a three-hour probability level, only peaks corresponding to a probability of non-exceedance greater than 0.2 to be used in the curve fitting and use a least square regression analysis (nonlinear data fitting, Levenber-Marquardt algorithm) to determine the parameters α, β and γ [9] [20].

4.4.1.3 Gumbell fitting (Gumbel method)

This method is based on the assumption that the three-hour extreme values follow the Gumbel distribution:

$$F(x) = \exp\left[-\exp\left(\frac{1}{\kappa}(x - \psi)\right)\right] \quad (4.15)$$

Where

κ - Gumbel scaling parameter
ψ - Gumbel location parameter

As discussed, the MPME corresponds to a 63 % chance of exceedance in an extreme probability function (e.g. three-hour storm).

The X_{MPME} of the response can therefore be calculated as:

$$X_{MPME} = \psi - \kappa \ln\left\{-\ln\left[F(X_{MPME})\right]\right\} \approx \psi \quad (4.16)$$

The important issues with this method is to calculate the parameters ψ and κ based on the response obtained from the time domain simulations. The ISO standard [5] recommends that the maximum simulated value to be extracted for each of the ten three-hour response simulations, and the parameters ψ and κ to be calculated by maximum likehood estimation. As a simplified calculation procedure, the ψ parameter can be obtained by a moment fitting solution [9].
A similar procedure will generate the quasi-static MPME in order to obtain the DAF of the BS and OTM.

4.4.2 Winterstein/Jensen method (W/J method)

This method is based on that a non-Gaussian process can be expressed as a Hermite polynomial of zero mean, narrow band Gaussian process.

$$R(U) = C_0 + C_1 U + C_2 U^2 + C_3 U^3 \quad (4.17)$$

Since MPME of a Gaussian process U is theoretically known, the MPME of the non-Gaussian process can be found by determining the coefficients in Eq. (4.17).
Procedure and determination of coefficients for this method is referred to Lu et al. [9].

4.4.3 Random seed effects

Random seed represent the random phase angle of each wave components that are combined to create the random wave simulation. The random phase angles are uniformly distributed between 0 and 2π and constant with time. The random seed generator generates different data series according to random seed selection. Depending on the method used to predict the MPME responses and DAFs, the random seed effect could be significant.
Except for a Gumbel fitting method, which uses 10 simulations with a simulation time of 180mins, the random seed effect is diminished to the large number of simulations.

However, all the three other methods can predict the MPME responses and the resulting DAFs from one simulation.

Lu et al. [9] and Zhang, Cheng and Wu [20] have investigated the effects of random seeds with respect to the four methods, conducted on two rigs with multiple simulations and random seeds. Their findings agree for the D/I method and Weibull method but distinguish for the W/J method.

Both studies, find a little change of the mean and standard deviation with different random seed selection. This makes the random seed effects irrelevant for the D/I method, as this method only use these two parameters to calculate the MPME and DAFs.

Their independent investigations find the Weibull method sensitive to random seeds and conclude that five simulations (recommendations by the ISO standard) may not be enough to obtain reliable DAFs.

Lu et al. [9] finds that random seed effects is small when using the W/J method, but more significant using the Weibull method. Based on his findings, he concludes that among the four methods, the W/J is the most efficient.

Zhang, Cheng and Wu [20] also finds the Weibull method sensitive to the random seed effects, while in contrary, finds the W/J also sensitive to random seed effects. They [20] argue, that the skewness and kurtosis is fluctuating with random seeds and since the W/J method use the first four moments (mean, standard deviation, skewness and kurtosis), this method is also sensitive to varying random seeds.

Based on acceptance criteria's given the ISO standard [5], both of them [9] and [20] conclude that the Weibull should have longer simulation duration and more simulation runs, than required in the ISO standard [5], in order to obtain reliable results. They differ in the W/J method, because Zhang, Cheng and Wu [13] concludes that it requires longer simulations duration and more simulation runs, while Lu et al. [9] express this method as the most efficient.

They also agree that the Gumbel method is stable and reliable, but very time consuming, and that D/I method seems stable, consistent and insensitive to random seed effects, but weak in theory. The D/I method is also considered very time efficient since it uses only a single seastate and peak period combination.

A general rule should be that care must be taken to ensure that predicted results are not affected by the selection of random seeds.

4.4.4 Acceptance criteria given in ISO 19905-1 [5]:

Table 4-1 - Acceptance criteria given in ISO standard

	Drag-inertia Method	Fitting Weibull Method	Fitting Gumbel Method	Winterstein/Jensen Method
Number of simulations and simulation time	≥60 minutes; 4 runs with different control parameters (C_D, C_M)	60 minutes, ≥ 5 simulations	180 minutes, ≥10 Simulations	180 minutes, Kurtosis>5 1 simulation

5   JACK-UP ANALYSES STUDY

5.1   Introduction

In this study, two Site-Specific Assessment (SSAs) have been performed of a jack-up unit for all-year operations at the Johan Sverdrup development in the Southern North Sea, to address the Ultimate Limit State (ULS) condition.
The jack-up unit is a "similar" design as the MSC-CJ70 Class drilling unit. The design basis is based on data for the CJ70-X150-B design, assumptions and previous papers [9] [23] [24] [27].
This study has assessed the unit in its elevated mode under all-year survival conditions using Omni-directional 100-year wind and wave and 10-year current data extracted from the metocean report [30] given in Appendix E.
The Site-Specific Assessment has been carried out in accordance with the requirements of the ISO 19905-1 [5] with specific reference to the Norwegian Annex criteria.

Spudcan penetrations are assumed to be of approximately 3.0 – 3.5 m from tip of skirt for each leg. Foundation fixity parameters have been calculated and incorporated based on this basis.

Two cases have been analysed. In the first case, the centre of gravity (CofG) is located in the centroid of the legs, while in the second case it is assumed that the LCG is offset 4 % of the hull length from the legs centroid, i.e. LCG is 3.5 meters. The second case applies to jack-up units with an XY cantilever drilling system, because of in stormy survival condition the cantilever is taken to be extended such that there is effectively a significant hull weight LCG offset from the legs centroid [26] [27].

The SSAs has been carried out using the FE software SACS.

This study has assessed the overturning stability, preload capacity, foundation bearing capacity, leg sliding, leg strength and the leg holding system strength. Finally the unit's hull displacements have been addressed. No assessment of hull strength or fatigue has been made.

5.2   Description of unit

The jack-up unit is a "similar" design as MSC-CJ70 Class drilling unit, with 3 triangular 3-chorded X-braced truss legs, with internal span-breaker bracing and split-tubular chords which have opposed racks.

Figure 5-1 - Gusto's MSC CJ70-X150-B design
(http://www.gustomsc.com)

5.2.1   Principal dimensions

Principal dimensions are summarized in Table 5-1.

Table 5-1 - Principle dimensions

Hull Length (m)	88.8
Hull Width (m)	102.5
Hull Depth (m)	12.0
Longitudinal Leg Spacing (m)	60.6
Transverse Leg Spacing (m)	70.0
Leg Chord Spacing (m)	18.0
Leg Length (m)	206.7

5.2.2   Weights and Centres of Gravity

Hull weights and centres of gravity (CofG) used in this study are summarised in Table 5-2. The LCG and TCG are measured from the legs centroid with LCG +ve forward and TCG +ve to port side.

Table 5-2 - Hull and leg weights

Hull Lightship Weight (t)	23 500
Storm Survival Variables (t)	4 000
Total Hull Weight (t)	27 500
Centre of Gravity from Leg Centroid	
LCG (m)	0.0 and -3.5
TCG (m)	0.0 and 0.0
Single Leg, inc. Footing (t)	3 200

5.2.3   Barstool model

A simplified barstool model is used to represent the jack up unit. Legs are represented by equivalent beam elements with appropriate stiffness properties estimated by formulas provided in the ISO standard [5].
Equivalent leg hydrodynamic properties have been calculated in accordance with methodology described in the ISO standard [5] and Section 3.3.3.
The hull is represented by a simplified hull grillage of equivalent beam elements with appropriate stiffness properties derived confidential construction drawings.
The equivalent beam elements for the legs and hull are connected by a single element which itself has stiffness properties representative of the entire leg-hull interface structure. The vertical and rotational stiffness properties of the leg-hull connection has been assumed based on previous jack-up designs.

5.2.4   Preload capacity

The preload capacity at the level of the footing is assumed equal as for the MSJ-CJ70 design, 220.7 MN. This is the basis for maximum vertical bearing capacity, as the ISO standard states that the vertical load bearing capacity shall not exceed the preload capacity, although the calculations in a particular location can show that the vertical load capacity is higher.

The maximum preload capacity is therefore determined by the hull design in relation to lightship weight and variable deck load capacity including full ballast tanks i.e. maximum vertical load the unit can produce in the preload condition.

However, for each specific location, the capacity has to be calculated. If the soil conditions are very soft and the foundation bearing capacity is lower than the preload capacity, then this capacity will be the maximum allowable preload for that particular location.

5.3   Johan Sverdrup field data

The Johan Sverdrup field is located in Block 16/2 and 16/3 in the central North Sea, about 140 kilometres west of Stavanger, Norway.
A map showing the location is presented below.
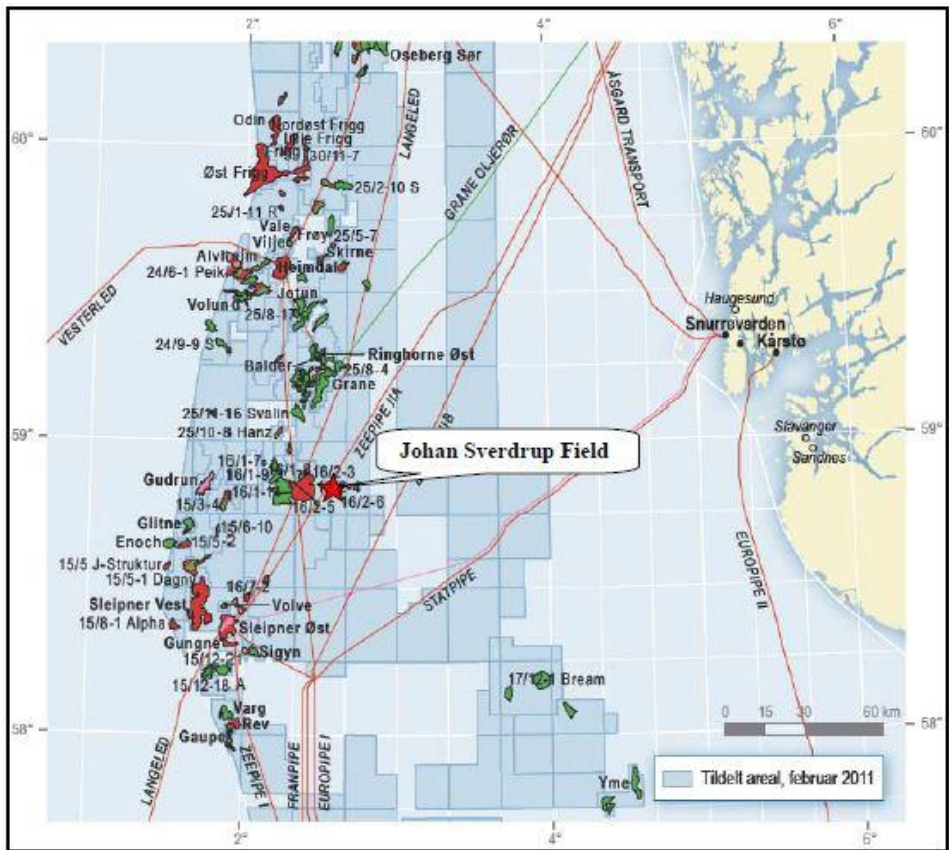
Figure 5-2 – Johan Sverdrup field located in Block 16/2 and 16/3, extracted from Johan Sverdrup field, metocean design basis [30]

5.3.1   Metocean conditions

The 100-year wind and wave and 10-year current extremes used in this assessment at the Johan Sverdrup field are based the metocean report [30] given in Appendix E.
The analysis has been carried out using the ISO standard [5] combination of Omni-directional 100 year wave and wind and 10 year current, factored by load factor of 1.25, extracted from the Norwegian Annex to the ISO standard.
Jack-up units are commonly used to drill over jacket platforms in North Sea. The airgap is therefore set to 35m, which is approximately equal to that required to drill over the unit, measured from MSL to keel.

The environmental data used in this SSA is summarised in Table 5-3 and Table 5-4.

Table 5-3 - 100-year environmental extreme parameters for the Johan Sverdrup location

Environmental conditions	
Water Depth (LAT) (m)	110.0
Tidal rise (MHWS) (m)	0.6
Storm Surge (m)	0.9
Airgap (m) (MSL to keel)	35.0

Table 5-4 - 100 year wind and wave and 10-year current – Omni-directional environmental extremes for the Johan Sverdrup field. (Incl. 90 % confidence bands for the peak- and associated period of H_{max})

Parameter	Omni-directional storm heading		
	Lower-bound, P5	Mid-bound, P50	Upper-bound, P95
Significant wave height, H_s (m)		14.5	
Peak period, T_p (s)	14.2	16.1	18.1
Max wave height, H_{max} (m)		27.1	
Associated period, T_{ass} (s)	12.8	14.5	16.3
Wind speed – 1 min mean at 10m (m/s)		42.5	
Current velocity (m/s) at depth 0 m (surface)		0.95	
20 m		0.83	
40 m		0.80	
60 m		0.79	
80 m		0.78	
108.5 m (3 m above seabed)		0.69	

5.3.2   Soil conditions

In this study, the soil condition is assumed to be a thin layer of silty clayey sand (<1.0-2.0m) followed by a large layer of homogenous stiff clay. This is a very general assumption for areas located in the central/southern part of the North Sea, but is made due to lack of geotechnical data.

Expected spudcan tip penetration are assumed to be of approximately 3.0 -3.5 m from tip of skirt for each leg, based on assumptions and geotechnical data from previous papers [1] [2] [8] [27] [31].

5.3.2.1   Foundation parameters

Initial foundation small strain stiffnesses and ultimate capacities have been estimated using formulas given in ISO 19905-1 [5] and in Section 3.6.1. For simplicity, stiffnesses and capacities are equal for all the three legs.

The resulting foundation parameters are tabulated in Table 5-5.

Table 5-5 - Foundation parameters

Foundation capacities and initial stiffnesses	
Vertical small strain stiffness, K_1 (MN/m)	5 300
Horizontal small strain stiffness, K_2 (MN/m)	1 100
Rotational small strain stiffness, K_3 (MNm/rad)	93 130
Ultimate vertical capacity, Q_v (MN)	220.7
Ultimate horizontal capacity, Q_h (MN)	45.0
Ultimate moment capacity, Q_m (MNm)	500.0

In the dynamic analysis, the linearized rotational small strain stiffness is calculated by, $K_{rot}= 80\% K_3$ (MNm/rad).

Usually a lower and upper bound of foundation stiffnesses and capacities are calculated and assessed. This is not performed in this study, due to lack of geotechnical data.
The effects of varying foundation stiffnesses and capacities are generally discussed in the next Chapter.

5.4 Site assessment analysis methodology

The assessment of the jack-up unit adopts the two-stage deterministic procedure described in ISO 19905-1 [5].
The first stage of this procedure is to perform a random wave time domain analysis to establish the dynamic response and determine the DAFs. An inertial loadset is calculated by these DAFs. During the second stage, a quasi-static deterministic extreme wave analysis is carried out which includes the inertia forces calculated during the first stage within the overall loadset.
The loadset within the first stage comprises a random wave train and current only, plus the inertia forces. The loadset within the second stage comprises a maximum extreme deterministic wave, current, wind and a series of point forces to represent the effective dynamic amplification as derived in the first stage.

A flow chart summarising the main areas covered in a SSA is given in Figure 5-3.
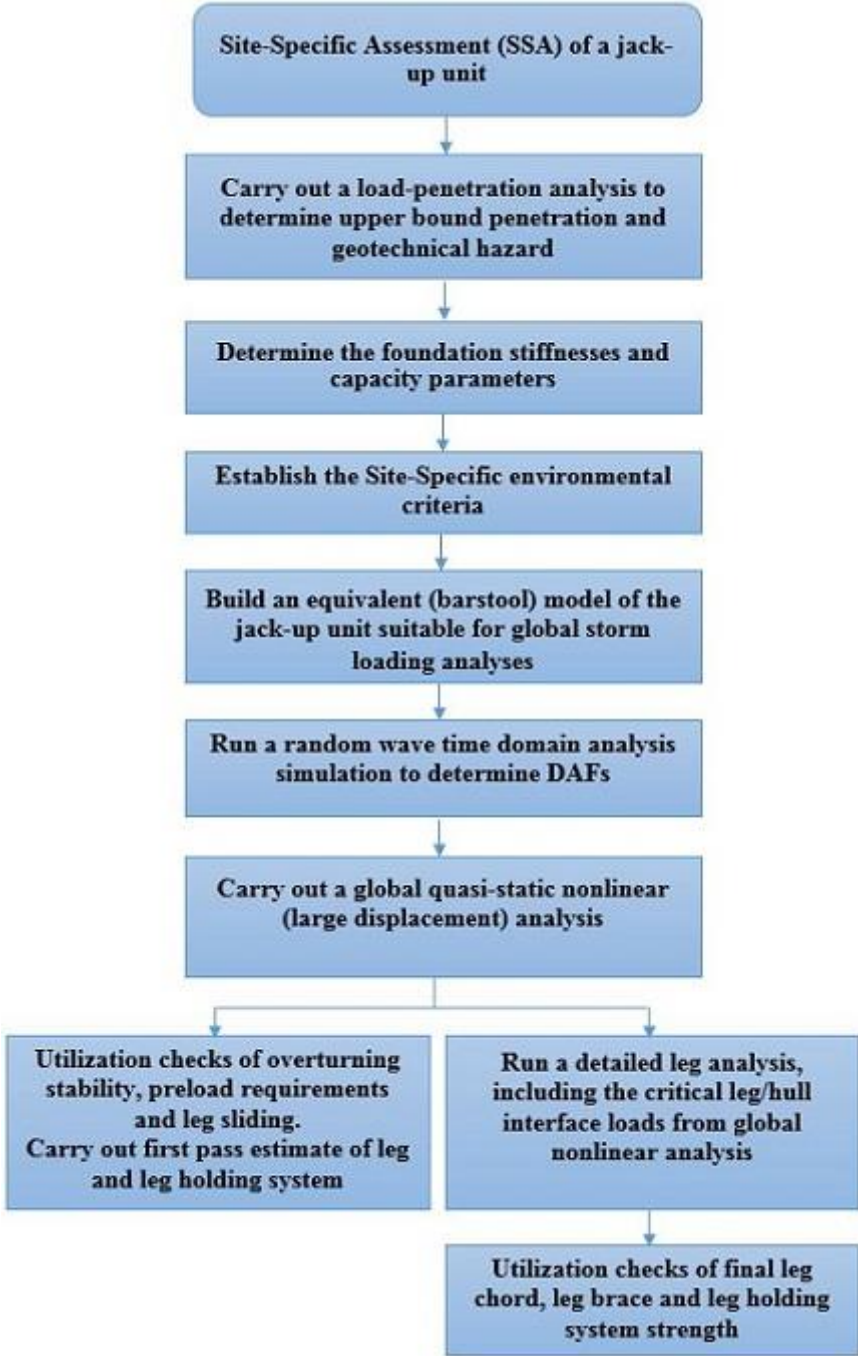
Figure 5-3 – Main areas covered in a Site-Specific Assessment

5.4.1   Details on dynamic analysis

The dynamic random wave analysis was carried out using a qualified wave surface history and the DAFs were calculated using the 'drag-inertia parameter' method. This method is explained in Section 4.4.1.1 and in Appendix B.
The qualified wave surface history was established by a random wave train of one-hour simulation time, generated using 400 Airy wave components, and then stepped through the in 0.5 second intervals. The analysis procedure is described in Section 4.3.2.

The analysis accounted for P-δ effects by including negative springs to reduce leg stiffness due to axial load.

The damping was specific as 7% of critical, as recommended in the ISO standard [5].

A JONSWAP spectrum, with a gamma factor of 3.3, was used to define the seastate energy. Added mass on the submerged part of the legs was accounted for and linear (Wheeler) stretching was used to define the current profile in the vicinity of the wave action.

5.4.2 Details on global quasi-static nonlinear analysis

The loading in the final quasi-static analysis comprised:

- Gravity loads applied partly at hull grillage, and partly by applying point loads at leg centres
- Wave-current loading using Stokes 5th order wave theory. The wave-current loading comprise a deterministic extreme wave plus current
- Wind loads applied at hull and legs
- Inertia loads applied as point forces to the hull grillage at the leg centres to represent the inertia base shear and overturning moment

An environmental load factor of 1.25 was applied in accordance with the ISO standard [5].

The final quasi-static extreme global response analysis was carried out using the nonlinear fixity (rotational stiffness reduction) procedure of the ISO standard [5].

Using this procedure, the level of rotational restraint (fixity) at the foundations is taken as a function of the vertical, horizontal and moment loads at each footing under all applicable loadings (see equation (3.28) and applicable loads given above).

Since the response (and therefore the footing loads) is a function of the foundation stiffness, an iterative procedure is required to determine the correct fixity.

This is achieved by using a nonlinear large displacement analysis in SACS. The procedure is given in the Section 5.4.4.

5.4.3 Large displacement analysis procedure

A large displacement analysis is performed for each necessary iteration in the nonlinear fixity analysis. The procedure of the large displacement analysis is as follows: Loads are applied in increments (10 load increments is used in this analysis). The structural stiffness is progressively updated to allow for the displaced shape, using a secant method. The response is the sum of all applied load increments.

The nonlinear large displacement analysis directly accounts for P-δ effects, as explained in Section 3.3.6.

5.4.4 Nonlinear fixity procedure in ISO 19905-1

The analysis procedure is as follows:

The initial small strain foundation stiffnesses is applied to the barstool model and the nonlinear large displacement analysis run.

Then, the value of the yield interaction formula is calculated using the resulting forces and moment on each footing. Depending the soil condition, the appropriate formulation is applied to calculate the failure ratio, r_f.

If r_f is in excess of unity, the force combination lies without the yield surface. If r_f is less than unity, that means that the force combination is within the yield surface and that the load combination is acceptable.

If, on the first iteration and with the small strain stiffness, the load combination is acceptable, the initial small strain stiffness is reduced by a factor f_r in stages. The analysis is re-run several times, until the change in the rotation stiffness at the footing is within a pre-set tolerance (2%). The maximum permitted change in the rotational stiffness throughout any one iteration is 1/50th of the small strain stiffness.

If, on the first iteration and with the small strain stiffness, the load combination is not acceptable, the initial small strain stiffness is arbitrary reduced in a graded fashion, depending on the value of r_f, until the value of r_f implies that the load combination is now within the yield surface. If the rotational stiffness has to be reduced to less than 1/100th of the small strain stiffness, this implies a bearing failure, and the stiffness is reduced to a very small stiffness, equivalent to a pinned condition. That footing is then left at that stiffness until all the other legs converge or indeed also reduce to a pinned condition [5] [29].

The vertical and horizontal foundation stiffness are maintained at their small strain value throughout the analysis.

5.5 Results

In the following section key results and utilisation checks will be presented.

The presented results are denoted by case 1 or case 2. These are defined as:

- **Case 1 - Centre of gravity (CofG) located at centroid of the legs**

- **Case 2 – LCG is located -3.5m from legs centroid**

5.5.1 Loading directions

The storm loading directions and leg numbering system used in the assessment are illustrated in Figure 5-4. The loading direction is such that 180° is bow-on, 270° port-on, etc. Leg number 1 refer to the bow leg, while leg number 2 and 3 refer to port- and starboard leg respectively.

In total seven storm direction have been analysed for the ULS condition: 0° (or 360°), 180°, 210°, 240°, 270°, 300°, 330°.
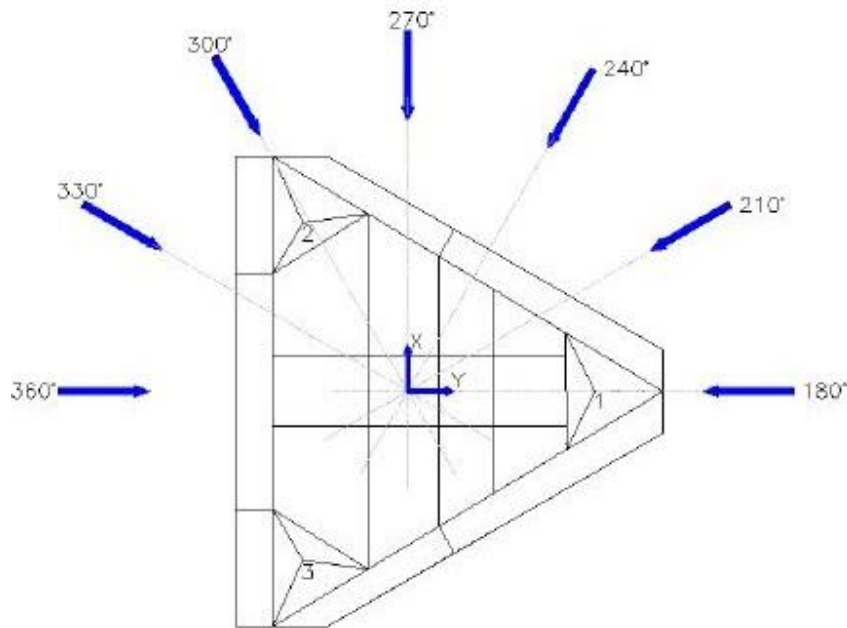
Figure 5-4 – Storm loading directions

5.5.2   Dynamic response

The dynamic response of the unit is presented in terms of natural periods and dynamic
amplification factors (DAFs) for a range of storm loading directions. In all cases the DAFs
were calculated for a range of peak periods (lower, mid and upper bound). DAFs are
calculated with respect to wave/current base shear (DAF_{BS}) and overturning moment
(DAF_{OTM}).

5.5.2.1   Natural periods

Modes 1, 2 and 3 correspond to sway, surge and yaw respectively. Natural periods are based
on the total hull weight condition given in Table 5-2, an airgap of 35m and the foundation
stiffnesses given in Table 5-5, but the rotational stiffness is reduced to 80 %.

Table 5-6 - Natural periods

Mode	$T_o(s)$	
	Case 1	Case 2
1	**9.03**	**9.09**
2	**8.98**	**8.99**
3	**7.01**	**7.08**
4	0.80	0.81
5	0.79	0.78
6	0.78	0.77
7	0.77	0.75
8	0.74	0.74
9	0.72	0.72
10	0.70	0.70

5.5.2.2 *Dynamic amplification factors (DAFs)*

The calculated DAFs are tabulated in Table 5-7 and Table 5-8.

Table 5-7 - Calculated DAFs, Case 1

Storm Heading (°)	Lower bound T_p		Mid bound T_p		Upper bound T_p	
	DAF_{BS}	DAF_{OTM}	DAF_{BS}	DAF_{OTM}	DAF_{BS}	DAF_{OTM}
0	1.15	1.44	1.12	1.38	1.11	1.38
180	1.22	1.74	1.16	1.60	1.13	1.50
210	1.23	1.70	1.17	1.55	1.14	1.47
240	1.22	1.65	1.18	1.56	1.13	1.46
270	1.26	1.65	1.19	1.50	1.15	1.43
300	1.18	1.52	1.14	1.45	1.11	1.39
330	1.12	1.52	1.14	1.40	1.12	1.40

Table 5-8 - Calculated DAFs, Case 2

Storm Heading (°)	Lower bound T_p		Mid bound T_p		Upper bound T_p	
	DAF_{BS}	DAF_{OTM}	DAF_{BS}	DAF_{OTM}	DAF_{BS}	DAF_{OTM}
0	1.16	1.47	1.12	1.39	1.11	1.37
180	1.21	1.74	1.17	1.61	1.13	1.50
210	1.24	1.74	1.18	1.58	1.14	1.49
240	1.22	1.68	1.18	1.56	1.13	1.46
270	1.26	1.65	1.18	1.47	1.14	1.41
300	1.20	1.54	1.14	1.45	1.11	1.38
330	1.21	1.57	1.15	1.43	1.13	1.41

5.5.2.3 *Environmental loads*

The environmental loads applied for this study is tabled in Table 5-9 and Table 5-10. The inertia base shear (BS) and overturning moment (OTM) are calculated by multiplying the wave/current force BS/OTM by ($DAF_{BS/OTM}$-1).
The total environmental loading is the sum of wave/current, wind and inertia contributions. The values include an environmental load factor of 1.25 as per ISO 19905-1 requirements.

Table 5-9 - Environmental loads, Case 1

Storm heading (°)	Wave/Current		Wind		Inertia		Total	
	BS (kN)	OTM (kNm)	BS (kN)	OTM (kNm)	BS (kN)	OTM (kNm)	BS (kN)	OTM (kNm)
0	17 782	1 718 647	8 458	1 469 897	2 743	758 212	28 981	3 946 757
180	16 470	1 605 069	8 456	1 469 770	3 591	1 180 051	28 517	4 254 891
210	15 576	1 464 748	8 470	1 471 721	3 623	1 018 793	27 669	3 955 262
240	17 622	1 702 542	8 460	1 470 139	3 831	1 102 300	29 913	4 274 981
270	15 510	1 457 775	8 471	1 471 805	4 000	951 402	27 981	3 880 982
300	16 320	1 588 894	8 458	1 469 976	2 941	827 091	27 719	3 885 961
330	15 622	1 469 392	8 469	1 471 638	3 121	764 361	27 212	3 705 391

Table 5-10 - Environmental loads, Case 2

Storm heading (°)	Wave/Current		Wind		Inertia		Total	
	BS (kN)	OTM (kNm)	BS (kN)	OTM (kNm)	BS (kN)	OTM (kNm)	BS (kN)	OTM (kNm)
0	17 781	1 718 647	8 457	1 469 897	2 833	804 590	29 073	3 993 134
180	16 470	1 605 068	8 455	1 469 770	3 485	1 191 748	28 411	4 266 586
210	15 576	1 464 748	8 470	1 471 721	3 762	1 089 056	27 808	4 025 526
240	17 621	1 702 542	8 459	1 470 139	3 885	1 161 174	29 967	4 333 855
270	15 509	1 457 774	8 470	1 471 805	4 000	951 417	27 981	3 880 996
300	16 319	1 588 893	8 457	1 469 976	3 210	857 379	27 987	3 916 249
330	15 621	1 469 391	8 469	1 471 638	3 324	830 345	27 415	3 771 375

5.5.2.4   *Still water reactions*

The vertical footing reactions for the still water condition are given in Table 5-11 . These are based on the total hull weight, a single buoyant leg plus the footing weight and a hull centre gravities given in Table 5-2.

Table 5-11 - Still water footing reactions

	Vertical footing reaction	
	1	2
Bow leg (kN)	118 762	100 498
Port leg (kN)	116 916	126 008
Starboard leg (kN)	116 916	126 008

5.5.3   Global results - Site-Specific Assessment

Results from the quasi-static nonlinear analyses are given in Table 5-15 to Table 5-20 and present the maximum footing reactions and loads in the legs at the rack-chock level. The lower bound peak period and the lower bound associated period of H_{max} gives the highest footing reactions, utilisations and response. The results presented are based on these lower bounds and on the following:

- Environmental load factor of 1.25
- Omnidirectional, 100-year, all year, wind and wave with the 10-year, all-year current.
- Total hull weight of 27 500 tonnes
- Inertia loads calculated by DAFs derived from the lower bound T_p
- Lower bound T_{ass}
- Kinematic factor of 0.86
- 35m airgap (MSL to keel)
- Foundation stiffnesses based on the values given in Table 5-5.
- Resistance factors given in Table 5-12

Table 5-12 - Resistance factors in accordance with the ISO standard [5]

Resistance factors	
Righting moment	1.05
Foundation bearing capacity	1.1
Leg sliding	1.56
Preload capacity	1.1
Chord capacity	1.1
Rack-chock capacity	1.15

5.5.3.1 Foundation evaluation

The foundation capacities are evaluated in two steps.

i) A preload check, requiring that the foundation reaction during preloading on any leg should be equal to, or greater than, the maximum vertical reaction arising from gravity loads and 100% of environmental loads. The preload defines the static foundation capacity under pure vertical loading immediately after installation.

ii) A foundation capacity and sliding checks. The checks are based on resultant loading on the footing under the design storm.

5.5.3.2 Maximum footing reactions and leg loads at rack-chock level

The maximum footing reactions and leg loads at rack-chock level occurs in a loading direction of 240°. The maximum base shear (BS) is situated on the port leg, while the maximum vertical load is at the starboard leg. This applies to both cases. The values are given in Table 5-13 and Table 5-14.

Table 5-13 - Maximum footing reactions and leg loads at rack-chock level, Case 1

Storm heading	Leg	Footing reaction			Leg load at Rack-chock level		
		BS (kN)	Vertical (kN)	Moment (kNm)	BS (kN)	Vertical (kN)	Moment (kNm)
240	Bow	10 694	89 071	484 133	3 097	-66 464	894 682
	Port	11 074	87 119	483 246	3 261	-64 512	940 919
	Starboard	8 142	176 353	341 851	7 088	-153 743	1 173 130

Table 5-14 - Maximum footing reactions and leg loads at rack-chock level, LCG is -3.5m from legs centroid (Case 2)

Storm heading	Leg	Footing reaction			Leg load at Rack-chock level		
		BS (kN)	Vertical (kN)	Moment (kNm)	BS (kN)	Vertical (kN)	Moment (kNm)
240	Bow	11 164	68 520	481 956	3 486	-45 904	940 064
	Port	11 176	94 975	482 829	3 457	-72 366	987 536
	Starboard	7 630	188 968	241 174	6 707	-166 361	1 216 102

5.5.3.3 Overturning stability

The critical load case was the 180° (bow-on) storm heading for both cases.

The righting moment includes a safety factor of 1.05 in accordance with the ISO standard [5].

Table 5-15 - Overturning stability check

Storm heading °	Case	Overturning Moment (kNm)	Righting Moment (kNm)	O/T UC
180	1	4.792E+06	7.707E+06	0.62
	2	4.921E+06	6.685E+06	0.74

5.5.3.4 Foundation bearing capacity

Foundation bearing capacity checks uses the vertical-horizontal (V-H) bearing capacity envelope presented in Figure 5-5 and Figure 5-6. The maximum bearing utilisations was on the starboard leg for a 240° storm direction.
In accordance with ISO standard, a resistance factor of 1.1 is applied to the bearing capacity curve.
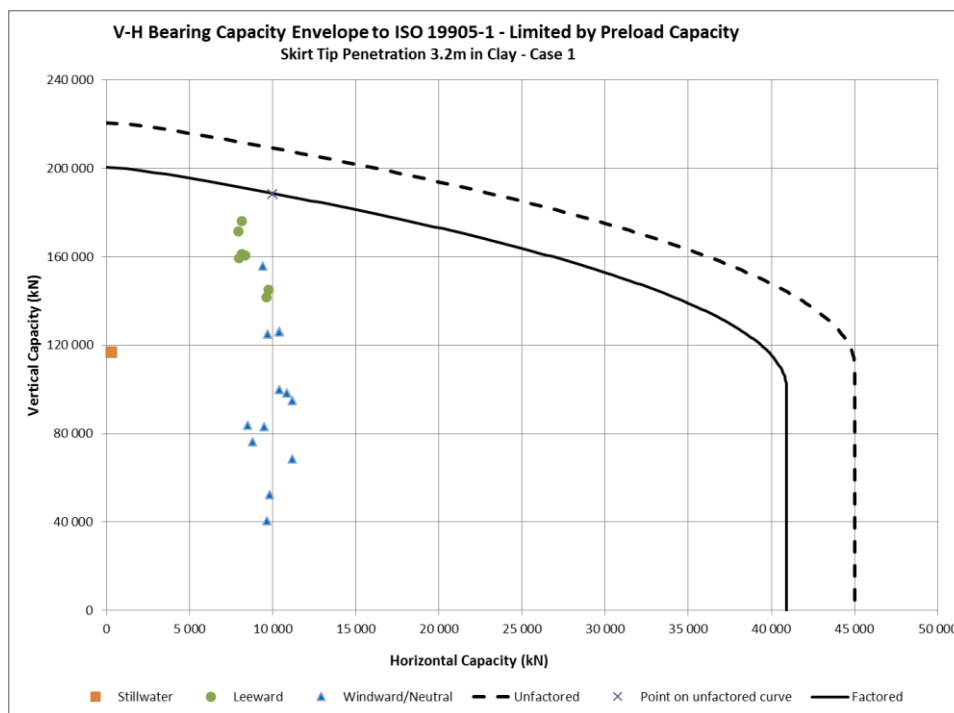
Figure 5-5 – V-H Bearing capacity envelope, Case 1
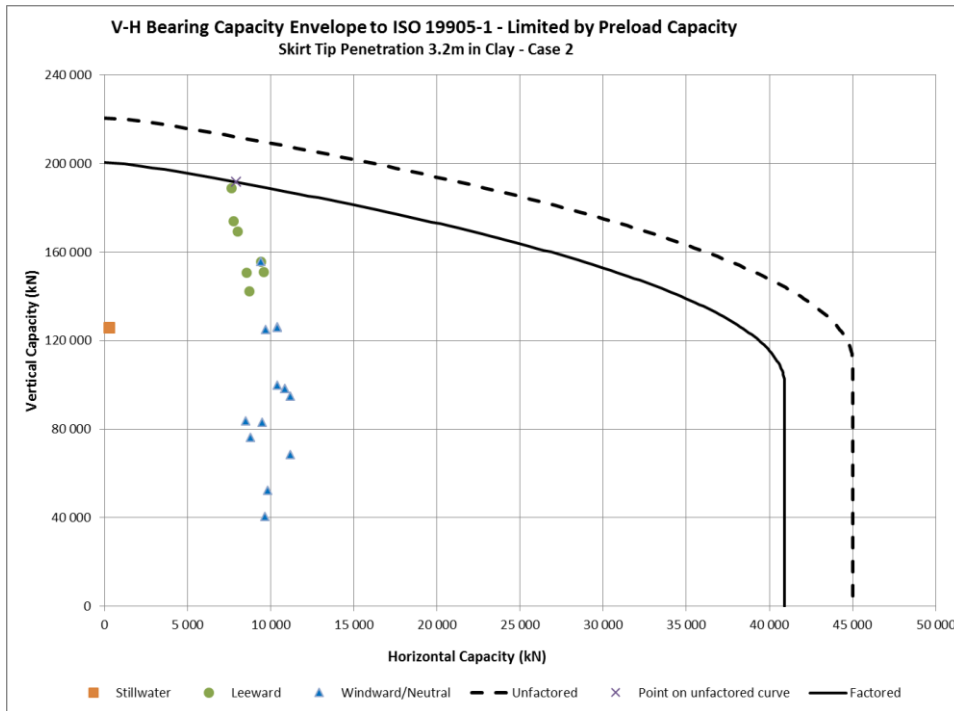
Figure 5-6 - V-H Bearing capacity envelope, Case 2

Table 5-16 - Bearing capacity check

	Case 1	Case 2
Measure of Bearing capacity UC		
Bow leg	0.77	0.48
Port leg	0.49	0.56
Starboard leg	0.89	0.96

5.5.3.5 Leg sliding

The leg sliding utilisation checks presented in Table 5-17 are based on a ratio of the horizontal footing reaction (base shear) to the factored horizontal foundation capacity. For both cases, the maximum horizontal footing reaction is situated in the port leg for a 240° storm direction.

The horizontal capacity includes a sliding resistance factor of 1.56.

Table 5-17 - Leg sliding check

	Case 1	Case 2
Leg sliding UC		
Bow leg	0.37	0.40
Port leg	0.38	0.43
Starboard leg	0.36	0.40

5.5.3.6 Preload requirement

The preload check was based on a factored preload capacity at the level of the footing of 200 640 kN. A resistance factor of 1.1 is included in the preload capacity.

The preload utilisation checks are for the most onerous leg of each storm direction. The critical preload was on the starboard leg for a 240° storm heading for both cases.

Table 5-18 - Preload capacity check

	Case 1	Case 2
Preload UC		
Bow leg	0.86	0.75
Port leg	0.72	0.77
Starboard leg	0.88	0.94

5.5.3.7 *First pass leg and holding system strength*

The leg and leg holding system strength is based on calculated leg loads and loads at the hull interface. The chord capacity of 161 400kN is calculated after the ISO standard [5], while the rack-chock capacity is an assumed value of 145 000kN.

An additional moment at the hull interface due to nominal leg inclination is included. After recommendations in the ISO standard, this is set to 0.5 % of the distance between footing and leg/hull interface.

The chord strength included a safety factor of 1.1, while a safety factor of 1.15 is included in the rack-chock capacity.

Maximum utilisations for the leg and leg holding system strength checks is on both the port and starboard leg for a 180° (bow-on) storm heading, for case 1 and 2.

Table 5-19 - First pass leg chord strength check

	Case 1	Case 2
Leg chord strength UC		
Bow leg	0.61	0.63
Port leg	0.77	0.82
Starboard leg	0.77	0.82

Table 5-20 - First pass rack-chock strength check

	Case 1	Case 2
Rack-chock strength UC		
Bow leg	0.78	0.71
Port leg	0.82	0.87
Starboard leg	0.82	0.87

5.5.3.8 *Jack-up hull displacements*

The maximum jack-up lateral hull displacements have been calculated for normal limit state conditions (SLS, ULS and ALS).

The critical loading case is at a 240° storm heading for both cases and in all conditions.

The maximum lateral hull displacements are tabulated in Table 5-21, and illustrated in Figure 5-7 and Figure 5-8.

Table 5-21 - Lateral hull displacement for limit state conditions

	Lateral hull displacement			
Load condition	Case 1		Case 2	
	Incl. load factor	Excl. load factor	Incl. load factor	Excl. load factor
SLS (m)	1.6	1.3	1.6	1.3
ULS (m)	2.0	1.6	2.2	1.7
ALS (m)	3.9	3.1	4.0	3.2
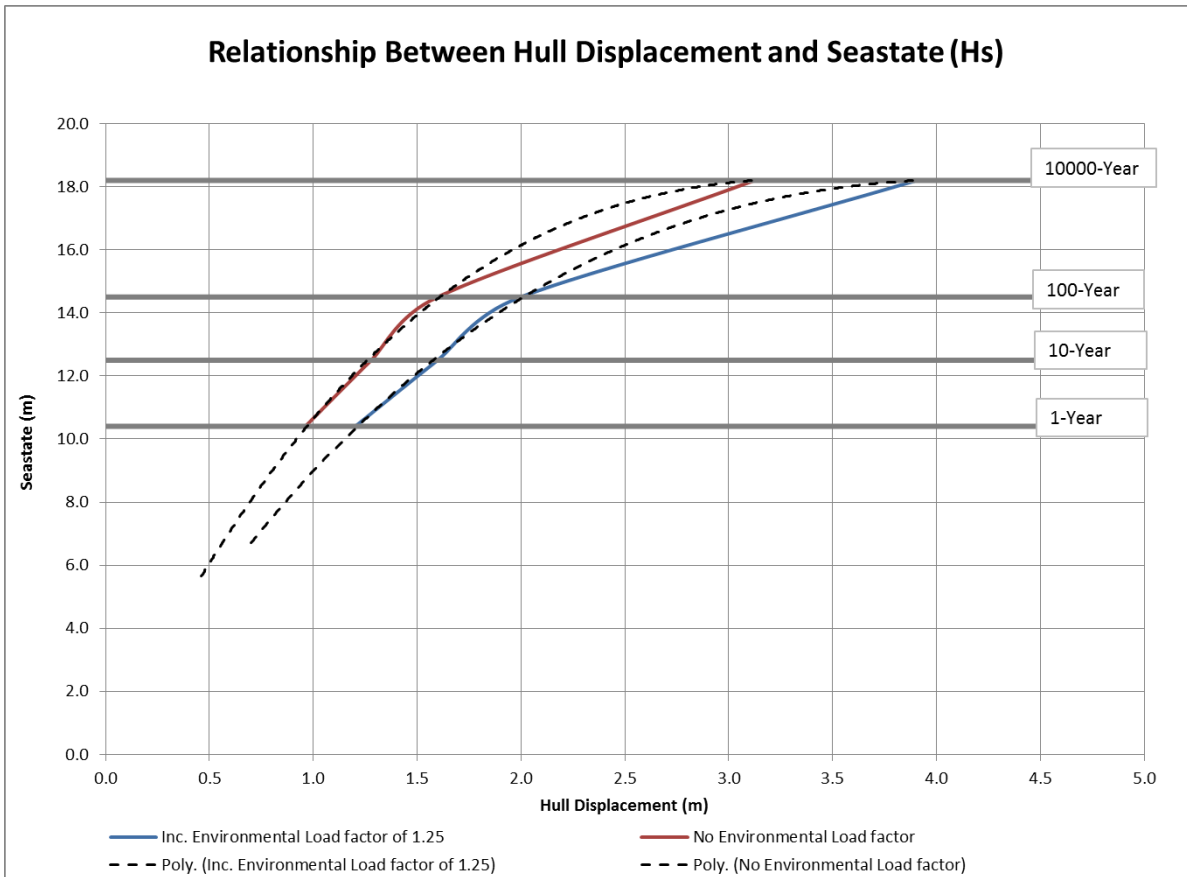
Figure 5-7 – Graphic illustration of lateral hull displacements in various Seastates, Case 1
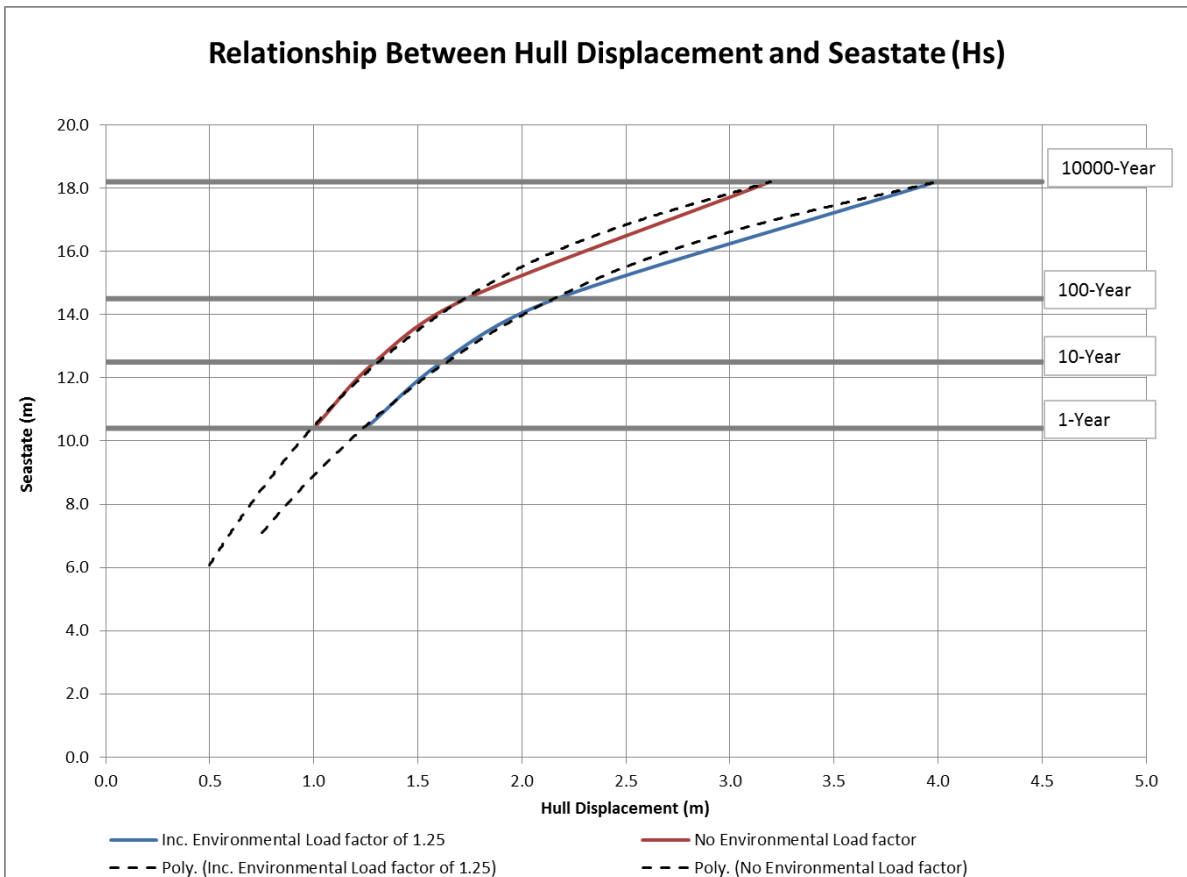
Figure 5-8 - Graphic illustration of lateral hull displacements in various Seastates, Case 2

5.6   Summary

The results from this assessment show that the jack-up unit satisfies the ISO standard requirements with respect to overturning stability, leg sliding, preload capacity, leg strength, leg holding system strength and foundation bearing capacity.
The foundation capacities were highest utilised with a bearing and preload capacity utilisations of 0.96 and 0.94 respectively. This was caused by a storm heading of 240° resulting in large vertical footing reactions (approximate 17 800tons for case 1 and 19 250tons for case 2) in the starboard leg, see Table 5-22 and Table 5-23.
The highest structural strength utilisations were below 90%, located at both the port and starboard leg at a storm heading of 180 deg.

A summary of the maximum footing reactions and leg loads at rack chock level for the two worst headings are given in Table 5-22 and Table 5-23. In addition, the maximum utilisations checks (UCs) are summarised in Table 5-24.

Table 5-22 - Maximum footing reactions and leg loads at rack-chock level for two storm headings, Case 1

Storm heading	Leg	Footing reaction			Leg load at Rack-chock level		
		BS (kN)	Vertical (kN)	Moment (kNm)	BS (kN)	Vertical (kN)	Moment (kNm)
180	Port & Starboard	9 726	145 152	437 979	2 264	-122 563	855 873
240	Starboard	8 142	176 353	341 851	7 088	-153 743	1 173 130

Table 5-23 - Maximum footing reactions and leg loads at rack-chock level for two storm headings, Case 1

Storm heading	Leg	Footing reaction			Leg load at Rack-chock level		
		BS (kN)	Vertical (kN)	Moment (kNm)	BS (kN)	Vertical (kN)	Moment (kNm)
180	Port	9 393	155 900	403 980	2 113	-133 313	881 884
240	Starboard	7 630	188 968	241 174	6 707	-166 361	1 216 102

Table 5-24 - Maximum utilisation checks and lateral hull displacements

Parameter	Case 1	Case 2
Overturning stability (UC)	0.62	0.74
Bearing capacity (UC) Starboard leg	0.89	0.96
Leg sliding (UC) Port leg	0.38	0.40
Preload capacity (UC)	0.88	0.94
Leg chord strength (UC)	0.77	0.82
Rack-chock strength (UC)	0.82	0.87
Lateral hull displacements (m)	2.0	2.3

6 PARAMETRIC SENSITIVITIES

6.1 Introduction

Inherent in all analyses are uncertainties related to assumptions made in the analyses, analysis procedures and assumptions and other parameters used such as weights and centre of gravities, hydrodynamic loads, dynamic responses, soil-structure interactions and operational aspects related to air gap etc. In this Chapter, the effect on the Site-Specific Assessments (SSAs) of the jack-up unit performed in Chapter 5 will be addressed based upon varying some of these parameters.

The jack-up unit is checked against sensitivities for parameters such as amount of damping, foundation stiffnesses, airgap, water depth, hull weight, drag coefficients, added mass and P-δ effects.

This parametric assessment has been based on all-year survival conditions using Omni-directional 100-year wind and wave and 10-year current data extracted from the metocean report [30] given in Appendix E.

This parametric study has assessed sensitivities in regard to the dynamic analysis (i.e. natural periods, DAFs and inertia forces), and the global quasi-static analysis (bearing capacity, leg sliding, leg strength and leg holding strength and lateral hull displacements).

6.2 Modelling procedures

In order to study sensitivities for the jack-up unit, the two cases studied in Chapter 5 have been defined as "base cases".
In this study, these two cases were analysed for each parameter. In the first case, the centre of gravity (CofG) is located in the centroid of the legs, while in the second base case it is assumed that the LCG is offset 4 % of the hull length from the legs centroid.

The following parametrical cases are checked for sensitivities:

- Excluding P-δ effects and added mass in the dynamic analysis
- Increased hull weight to 30 000tons
- Increased water depth to 130meters (LAT)
- Increased water depth to 145meters (LAT)
- Increased airgap to 60meters (MSL to keel)
- Increased airgap to 69meters (MSL to keel)
- No rotational foundation stiffness, i.e. a pin-supported condition
- 5 % of critical damping level
- Variation in drag coefficient
- Infinite rotational stiffness, i.e. fully fixed support condition

The case of an airgap of 69m refers to Mariner field development in the North Sea. In this field a jack-up unit, of MSCG CJ-70 design, is going to operate and drill over a jacket platform, see illustration in Figure 6-1.

At the Mariner field the water depth level, relative to MSL, is of 110.0m, approximately equal to the Johan Sverdrup field.

The Mariner field is located in Block 9/11 of the UK sector of the North Sea. Foundation parameters are different, but within the same range for the environmental extremes.

Figure 6-1 - illustration of Statoil Cat j (CJ70 design) at the Mariner field (http://www.statoil.com/en/newsandmedia/pressroom/pages/presskitmariner.aspx)

6.2.1   Leg lengths requirements

The required leg lengths for the parametric studies are given in Table 6-1:

Table 6-1 – Required leg lengths

	Water depth		Airgap		All other
	130m	145m	60m	69m	cases
Leg requirement up to keel (m)	166.5	176.5	171.5	180.5	146.5

6.3   Analysis procedure

The analysis methodology used in this parametric study is similar to the Site-Specific Assessment performed in the previous Chapter, which is covered in Section 5.4.

6.4 Results

In the following section parametrical sensitivity results will be presented along with the results from the two base cases.

The leg numbering system used in this study is similar to the assessment performed in Chapter 5.

Sensitivities are checked against 180° and 240° storm headings, combined with the lower bound peak period T_p and the associated period T_{ass}, given in Table 5-4, which are considered to give the most unfavourable outcomes.

Results are presented in terms of maximum utilisations and lateral hull displacements for both these storm headings. The maximum structural strength utilisations arise from a 180° loading direction, while the lateral hull displacements and maximum utilisations of the bearing, sliding and preload capacity checks comes from a 240° storm heading.

6.4.1.1 Sensitivity to natural periods

Foundation fixity and the required leg length are the two governing parameters determining natural periods.

The effect of increased hull lightship weight (LSW) and the variable deck loading to a total hull weight of 30 000t (approximate 8% of the base cases), gives a 4 % increase of the natural periods, while excluding P-δ effects gives a decrease of approximately 6% of the natural periods compared to the base cases.

The effect of excluding the added mass is negligible.

The natural periods are tabulated in Table 6-2 and Table 6-3.

Table 6-2 – Natural periods, Case 1

Natural periods for various parameters			
Parameter	Mode		
	Sway (s)	Surge (s)	Yaw (s)
Base Case 1	9.03	8.98	7.01
Excluding P-δ effects	8.49	8.46	6.66
Excluding added mass	8.96	8.92	6.95
30 000t Total hull weight	9.43	9.38	7.31
130m water depth (LAT)	10.21	10.16	7.83
145m water depth (LAT)	10.85	10.80	8.27
60m airgap	10.53	10.48	8.04
69m airgap	11.10	11.05	8.43
Pinned support condition	12.82	12.73	9.94
Fully fixed supported condition	6.43	6.40	5.13

Table 6-3 – Natural periods, Case 2

Natural periods for various parameters			
Parameter	Mode		
	Sway (s)	Surge (s)	Yaw (s)
Base Case 2	9.09	8.99	7.08
Excluding P-δ effects	8.54	8.46	6.73
Excluding added mass	9.02	8.92	7.00
30 000t Total hull weight	9.50	9.38	7.37
130m water depth (LAT)	10.28	10.16	7.90
145m water depth (LAT)	10.93	10.80	8.34
60m airgap	10.61	10.48	8.12
69m airgap	11.19	11.05	8.51
Pinned support condition	12.93	12.73	10.02
Fully fixed supported condition	6.55	6.47	5.22

In a Site-Specific Assessment (SSA), usually a lower and upper bound of foundation stiffnesses and capacities are calculated and assessed. This is because the effect of foundation fixity or rotational small strain stiffnesses have a large impact on the natural periods.
The natural periods calculated in a pinned support condition gives approximately twice the natural periods calculated in a fully fixed supported condition. This results in large differences of dynamic effects and on the final results.
The effect of a pin supported condition versus a fully fixed supported condition results can be shown in terms of the resulting DAFs.
In a fully fixed condition, the resulting DAF_{BS} and DAF_{OTM} are approximate 21-23 % and 25-29 % of the DAFs in a pinned condition. This result in an average increase of inertia loads by 445% and 366% larger base shear and overturning moment in a pinned- versus a fixed supported condition.

Table 6-4 – Rotational stiffness and natural periods

Rotational foundation stiffness (MNm/rad)	**Sway natural period $T_o(s)$**	
	Base case 1	Base case 2
Pinned	12.82	12.90
10000	11.73	11.81
50000	9.64	9.71
100000	8.60	8.67
500000	7.04	7.10
>5000000 Fully fixed	6.43	6.55

The relationship between natural periods and rotational foundation stiffness can be illustrated in Figure 6-2.
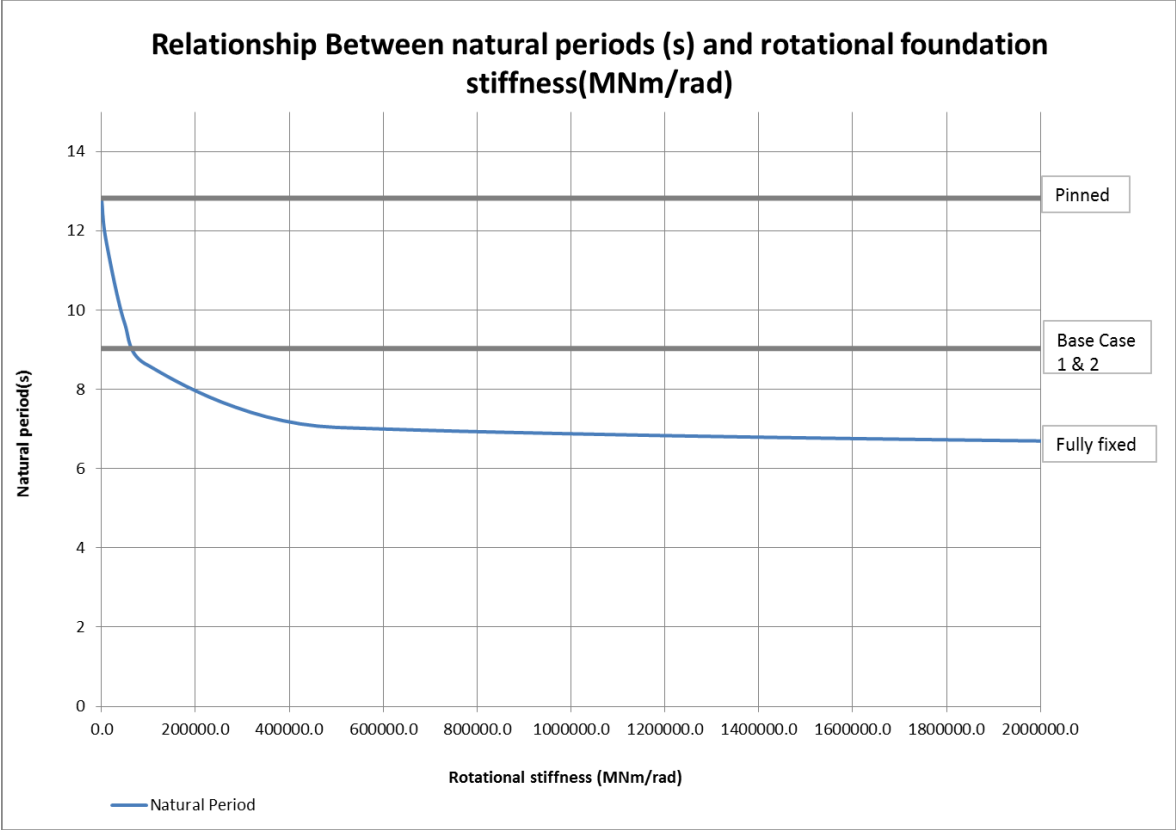
Figure 6-2 – Relationship between natural periods and rotational foundation stiffness

6.4.1.2   *Sensitivity to dynamic amplification factors (DAFs)*

Sensitivities related to dynamic amplification factors (DAFs) are close related to the natural periods, e.g. a pin supported condition yields the highest natural periods and the largest resulting DAF_{BS} and DAF_{OTM} values.

Comparing to the base cases, and to the pinned support condition, we observe higher DAF values for all parametric cases who have higher natural periods than the base cases.

The calculated DAFs are tabulated in Table 6-5 and Table 6-6.

Table 6-5- Calculated DAFs, Case 1

	Lower bound T_p			
Storm Heading (°)	180		240	
Various parameters	DAF_{BS}	DAF_{OTM}	DAF_{BS}	DAF_{OTM}
Base Case 1	1.22	1.74	1.22	1.65
Excluding P-δ effects	1.17	1.67	1.18	1.59
Excluding added mass	1.22	1.69	1.24	1.66
30 000t Total hull weight	1.25	1.86	1.28	1.81
130m water depth (LAT)	1.33	1.92	1.39	1.95
145m water depth (LAT)	1.42	2.02	1.45	2.16
60m airgap	1.32	2.12	1.35	2.10
69m airgap	1.37	2.32	1.37	2.26
Pinned support condition	1.61	3.04	1.68	2.96
Fully fixed supported condition	1.13	1.56	1.16	1.54
5% damping	1.24	1.82	1.30	1.89

Table 6-6 - Calculated DAFs, Case 2

	Lower bound T_p			
Storm Heading (°)	180		240	
Various parameters	DAF_{BS}	DAF_{OTM}	DAF_{BS}	DAF_{OTM}
Base Case 2	1.21	1.74	1.22	1.68
Excluding P-δ effects	1.18	1.70	1.17	1.61
Excluding added mass	1.23	1.71	1.23	1.64
30 000t Total hull weight	1.25	1.86	1.28	1.81
130m water depth (LAT)	1.33	1.91	1.39	1.96
145m water depth (LAT)	1.41	2.02	1.45	2.16
60m airgap	1.31	2.12	1.35	2.11
69m airgap	1.36	2.32	1.37	2.31
Pinned support condition	1.61	3.04	1.68	2.97
Fully fixed supported condition	1.14	1.60	1.15	1.50
5% damping	1.24	1.82	1.30	1.89

6.4.1.3 *Sensitivity to added mass and P-δ effects*

The effect of excluding added mass on the natural periods in the dynamic analysis is negligible, while the DAFs experience a small increase and a decrease compared to the base cases.
Excluding P-δ effects in the dynamic analysis yields a 5-6 % (0.5s) lower natural periods. This result in a small reduction of the DAFs compared to the base cases.

6.4.2   Global results

Results from the quasi-static nonlinear analyses are tabled from Table 6-7 to Table 6-16 and present the maximum utilisations and lateral hull displacements.

The global results are based on the following parameters:

- Increased total hull weight to 30 000tons
- Increased water depth to 130meters (LAT)
- Increased water depth to 145meters (LAT)
- Increased airgap to 60meters (MSL to keel)
- Increased airgap to 69meters (MSL to keel)
- No rotational foundation stiffness, i.e. a pinned condition
- 5 % of critical damping level
- Variation in drag coefficient

6.4.2.1   *Sensitivity to total hull weight of 30 000 tonnes*

The effect of increasing the LSW and variable load to a total hull weight of 30 000t show a larger footing reactions and higher loads within the structure, leading to a small increase of utilisations and hull displacements.

The increased utilisations may induce a foundation collapse (bearing and preload failure are utilised over 100%). This is a conservative approach, because the preload capacity should be increased equal to the amount of weight increase. This is not been considered.
The maximum utilisations and lateral hull displacements are tabulated in the Table 6-7.

Table 6-7 - Maximum utilisation checks and lateral hull displacements for increased hull weight (30 000t)

Maximum utilisations and lateral hull displacements		
	Case 1	Case 2
Overturning stability	0.60	0.72
Bearing capacity		
Starboard leg	1.00	1.04
Leg sliding		
Port leg	0.41	0.46
Preload capacity	0.96	1.03
Leg chord strength	0.79	0.84
Rack-chock strength	0.83	0.89
Lateral hull displacements (m)	2.3	2.5

6.4.2.2   *Sensitivity to water depth*

Sensitivity towards water depths were studied for two water depth levels. In the first parametric case, the water depth was increased from 110m to 130m (LAT) with an airgap of 35m, measured from MSL to keel.

In the second study, the water depth level was 145m (LAT), but with a lowered airgap to 30m (MSL to keel).

The results in Table 6-8 and Table 6-9 show that water depth is a very sensitive parameter. Comparing to the base cases, results show a high increase of utilisations and displacements. In particular for the structural utilisations, which were increased by approximately 30 % and 57% for a water depth of 130m and 145m respectively. Other utilisations were increased somewhere in between 10-30%.

This results in high and exceeding utilisations for both studies, suggesting that the jack-up unit is not suited for these water depth levels combined with such high (>30m) airgaps. Large lateral hull displacements of 5m also supports this recommendation.

The maximum utilisations and lateral hull displacement for these studies are tabled in Table 6-8 and Table 6-9.

Table 6-8- Maximum utilisation checks and lateral hull displacements for increased water depth (up to 130m)

Maximum utilisations and lateral hull displacements		
	Case 1	Case 2
Overturning stability	0.81	0.95
Bearing capacity Starboard leg	1.01	1.04
Leg sliding Port leg	0.44	0.49
Preload capacity	0.97	1.03
Leg chord strength	1.00	1.05
Rack-chock strength	1.06	1.11
Lateral hull displacements (m)	3.6	3.9

Table 6-9- Maximum utilisation checks and lateral hull displacements for increased water depth (up to 145m)

Maximum utilisations and lateral hull displacements		
	Case 1	Case 2
Overturning stability	0.99	1.04
Bearing capacity Starboard leg	1.07	1.10
Leg sliding Port leg	0.48	0.53
Preload capacity	1.07	1.12
Leg chord strength	1.22	1.28
Rack-chock strength	1.29	1.35
Lateral hull displacements (m)	5.0	5.1

6.4.2.3 *Sensitivity to airgap*

Sensitivity toward airgaps were studied for two large airgap levels. In the first case, the airgap was 60m and in the second case, the airgap was 69m. Both airgaps were measured from MSL to keel.

Results given in Table 6-10 and Table 6-11 indicate a similar tendency as for the water depth parameter, that the airgap, or generally, the leg length is a very sensitive parameter and is one of the governing parameter influencing the dynamic loading and final results.
The 60m airgap study show high utilisations and large lateral motions. Utilisations were increased by 5-25% compared to the original base cases.

Results from the 69m airgap study gave even higher utilisations and larger motions.
The structural utilisations produced the highest utilisations. They were increased by approximately 40 % compared to the base cases.
In addition to large lateral hull displacements, this implies that a 69m airgap at the Johan Sverdrup field is not recommended.

Table 6-10 - Maximum utilisation checks and lateral hull displacements for increased airgap to 60m

Maximum utilisations and lateral hull displacements		
	Case 1	Case 2
Overturning stability	0.80	0.95
Bearing capacity Starboard leg	0.99	1.03
Leg sliding Port leg	0.44	0.49
Preload capacity	0.95	1.01
Leg chord strength	0.98	1.03
Rack-chock strength	1.04	1.09
Lateral hull displacements (m)	3.6	3.8

Table 6-11 - Maximum utilisation checks and lateral hull displacements for increased airgap to 69m

Maximum utilisations and lateral hull displacements		
	Case 1	Case 2
Overturning stability	0.89	1.06
Bearing capacity Starboard leg	1.03	1.06
Leg sliding Port leg	0.46	0.52
Preload capacity	1.00	1.06
Leg chord strength	1.09	1.15
Rack-chock strength	1.15	1.21
Lateral hull displacements (m)	4.4	4.7

6.4.2.4   *Sensitivity to pin-supported condition*

Sensitivities for a pin-supported condition are given in Table 6-12. A pin-supported condition for a jack-up unit is considered as a very conservative approach. For this study, all utilisation checks (except for the leg sliding) were exceeded, indicating that the rotational foundation stiffness is a necessity to be included in our Site-Specific Assessment (SSA).

Table 6-12 - Maximum utilisation checks and lateral hull displacements for a pinned support condition

Maximum utilisations and lateral hull displacements		
	Case 1	Case 2
Bearing capacity Starboard leg	1.12	1.13
Leg sliding Port leg	0.50	0.54
Preload capacity	1.12	1.17
Leg chord strength	1.29	1.32
Rack-chock strength	1.37	1.40
Lateral hull displacements (m)	4.2	4.3

6.4.2.5 *Sensitivity to amount of damping*

Sensitivity to amount of damping was performed because PSA require a damping of 5% of critical, while ISO standard recommends a damping level of 7 %.
A reduced level of damping increase the DAFs and inertia loads, leading to higher utilisations. The maximum vertical footing reaction was increased by approximate 13%, resulting in a 5-10% increase in the foundation capacity utilisations. The structural utilisations also experienced a small increase by approximately 2%.
Maximum utilisations and lateral hull displacement for the reduced damping study is given in Table 6-13.

Table 6-13 - Maximum utilisation checks and lateral hull displacements for 5% damping

Maximum utilisations and lateral hull displacements		
	Case 1	Case 2
Overturning stability	0.63	0.76
Bearing capacity Starboard leg	0.98	1.01
Leg sliding Port leg	0.41	0.46
Preload capacity	0.93	0.99
Leg chord strength	0.79	0.84
Rack-chock strength	0.84	0.89
Lateral hull displacements (m)	2.3	2.5

6.4.2.6 *Sensitivity to drag factors*

Sensitivities to increased drag factors were performed because there are uncertainties in predicting the accuracy of these factors for large chords dimensions combined with a rack, which applies in deep water truss-type jack-up units.

Results show approximately a 0.7% increase per percent increase of the drag coefficient, in the total environmental loading. The results are tabulated in Table 6-14.

Table 6-14 – Effect of increased drag factors on the environmental loading, Case 2

Parameter	Wave and current loading		Total	
	BS (kN)	OTM (kNm)	BS (kN)	OTM (kNm)
Base case	17 621	1 702 542	29 967	4 333 855
C_D 10%	19 303	1 866 451	32 165	4 634 456
C_D 20%	20 988	2 031 040	34 369	4 936 442
C_D 30%	22 666	2 194 595	36 561	5 236 183

6.4.2.7 *Effect of the natural periods and DAFs*

The natural periods are considered the governing factor determining the outcome of assessing a jack-up unit. Their contribution are significant because they determine the magnitude of applicable dynamic loading and calculated DAFs.

A small increase of natural periods results in rapidly increasing dynamic loading and a possibly large impact of the assessment.
If we solely compare the dynamic drag loading from the waves and currents in the 145m water depth case and base cases, the base shear and overturning moment are increased by 4% and 38%, respectively. If we include the dynamic amplifications (DAFs) we get a total increase of approximately 17% (520tons) in base shear and around 50% (222 000t-m, 2180MNm) in overturning moment, illustrating the extreme effect of the DAFs and natural periods by only a small increase in natural periods of less than 2s (1.84s in sway).

By comparing the base cases to the increased airgap cases and the pinned support condition, we see a corresponding effect as for increasing the water depth.
The main difference is that the induced wave-current loading remain unchanged when we increase the airgap or reduce the rotational stiffness.

The extreme effects of the DAFs are greatly illustrated for the pinned support condition, where the overturning moment is amplified twice the magnitude of the overturning moment induced by wave-current loading. See Table 6-15.

The effects of the natural periods and DAFs to the environmental loading are tabulated in Table 6-15.

Table 6-15 – Effects of the natural periods and DAFs to the total environmental loading

Parameter	Natural period (sway) (s)	DAF BS	DAF OTM	Wave/current loading BS (kN)	Wave/current loading OTM (kNm)	Inertia BS (kN)	Inertia OTM (kNm)	Total BS (kN)	Total OTM (kNm)
Base case	9.09	1.22	1.68	17 621	1 702 542	3 886	1 161 174	29 967	4 333 855
145m water depth	10.93	1.45	2.16	18 337	2 328 566	8 252	2 701 136	35 048	6 516 630
69m Airgap	11.19	1.33	2.10	17 621	1 702 542	5 762	1 878 836	32 237	5 284 430
Pin-suppor	12.93	1.68	2.97	17 621	1 702 542	11 983	3 354 008	38 064	6 526 690

In accordance with Table 6-5 and Table 6-6, we see that the pin-supported condition case, the 69m large airgap case and the 145m water depth case are the most dynamically sensitive parameters.

These cases have been analysed by excluding the dynamic effects (DAFs) in order to illustrate the influence of the dynamic effects on these parameters.

Results show considerably lower utilisations and displacements, illustrating the extreme dynamic sensitiveness on jack-up units in deep water.
The maximum vertical footing reaction governing the foundation utilisations, located in the starboard leg for a 240° loading direction, was reduced by approximately 17-19% for all analyses. This reduction resulted in that both the bearing and preload capacity checks were within requirements for all three cases.
Structural strength utilisations were reduced up to 36%, while the lateral displacements achieved a reduction of 36-45% respectively.

The maximum utilisations and lateral hull displacements for these analyses are tabulated in Table 6-16. Only the results from the second case is presented, i.e. LCG equal -3.5m.

Table 6-16 - Maximum utilisations and lateral hull displacements when inertia loads are excluded, Case 2

Maximum utilisations and lateral hull displacements			
	145m water depth	69m Airgap	Pin-supported
Bearing capacity Starboard leg	0.96	0.95	0.99
Leg sliding Port leg	0.37	0.39	0.33
Preload capacity	0.91	0.88	0.96
Leg chord strength	0.84	0.78	0.96
Rack-chock strength	0.89	0.83	0.99
Lateral hull displacements (m)	2.7	2.9	2.7

6.5 Summary

The parametric study provide valuable information about the sensitivities applicable to purpose-built jack-up units in harsh environmental conditions in relation to deep water.

We observe high and exceeding utilisations combined with large lateral hull displacements in the majority of the parametrical studies. Indicating that the jack-up unit is sensitive towards several parameters.

The maximum foundation capacity utilisation exceeded the allowable capacity by 17%, while the lowest foundation capacity utilisations were close up to a 100% utilisation. The risk of the foundation collapsing is high based on the parameters.

The structural strength utilisations and overturning stability show large variation in utilisations. For example, the maximum structural utilisation was estimated to 140% of the allowable strength capacity, while the lowest utilisation was measured to 79%, showing the variation in utilisations increase from only 2 % and up to 60% comparing to the base cases.

The effect of the natural periods and DAFs where investigated in Section 6.4.2.7.

By increasing the water depth or airgap, or reducing the spudcans rotational stiffness, the jack-unit becomes considerably more susceptible for higher dynamic non-Gaussian responses as the natural periods increases and move towards the peak of the wave energy spectrum, resulting in larger dynamic effects (DAFs). Increased dynamic amplification of the responses, results in more dominant nonlinear effects and therefore stronger non-Gaussian distribution of the extreme responses.

These extreme dynamic effects have been quantified for the most dynamic sensitive parameters, showing dynamic amplifications of up to twice the amount of which was induced by the wave-current loading (for overturning moment). The effects of the DAFs on the total environmental loading are quantified for the most sensitive parameters in Table 6-15. The results illustrate the extreme effect the DAFs can have on the total environmental loading. The effect is so large that a small increase in natural periods can alter the outcome of an assessment. In this view of context, uncertain parameters, such as amount of foundation fixity, must be assessed accurately due their sensitiveness for the natural periods.

The maximum utilisations and lateral hull displacements for all studies are summarised in Table 6-17 and Table 6-18.

Table 6-17 – Maximum utilisations and lateral hull displacements, Case 1

Parameter	Base Case	30 000t Weight	Water depth		Airgap		Pinned	5 % damping
			130m	145m	60m	69m		
Overturning stability (UC)	0.62	0.60	0.81	0.99	0.80	0.89	-	0.63
Bearing capacity (UC) Starboard leg	0.89	1.00	1.01	1.07	0.99	1.03	1.12	0.98
Leg sliding (UC) Port leg	0.38	0.41	0.44	0.48	0.44	0.46	0.50	0.41
Preload capacity (UC)	0.88	0.96	0.97	1.07	0.95	1.00	1.12	0.93
Leg chord strength (UC)	0.77	0.79	1.00	1.22	0.98	1.09	1.29	0.79
Rack-chock strength (UC)	0.82	0.83	1.06	1.29	1.04	1.15	1.37	0.84
Lateral hull displacements (m)	2.0	2.3	3.6	5.0	3.6	4.4	4.2	2.3

Table 6-18 - Maximum utilisations and lateral hull displacements, Case 2

Parameter	Base case	30 000t Weight	Water depth		Airgap		Pinned	5 % damping
			130m	145m	60m	69m		
Overturning stability (UC)	0.74	0.72	0.95	1.04	0.95	1.06	-	0.76
Bearing capacity (UC) Starboard leg	0.96	1.04	1.04	1.10	1.03	1.06	1.13	1.01
Leg sliding (UC) Port leg	0.40	0.46	0.49	0.53	0.49	0.52	0.54	0.46
Preload capacity (UC)	0.94	1.03	1.03	1.12	1.01	1.06	1.17	0.99
Leg chord strength (UC)	0.82	0.84	1.05	1.28	1.03	1.15	1.32	0.84
Rack-chock strength (UC)	0.87	0.89	1.11	1.35	1.09	1.21	1.40	0.89
Lateral hull displacements (m)	2.3	2.5	3.9	5.1	3.8	4.7	4.3	2.5

7 CONCLUSIONS AND RECOMMENDATIONS

The main objectives of this work have been to study purpose-built jack-up units for extreme environmental conditions in the North Sea and to assess and quantify the responses due to the variation of the parameters important for such units.

Two Site-Specific Assessments (SSAs) have been performed of a jack-up unit for all-year operations at the Johan Sverdrup field. This unit is a "similar" design as to MSC CJ-70 Class drilling unit. This unit is a "tailor-made" design for operations in harsh environment on the Norwegian Continental Shelf (NCS).

Traditional analysis methods and procedures for assessing jack-up units are reviewed. A two-stage deterministic procedure is described and has been used to perform the analyses. This analysis procedure is recommended by the ISO standard and together with the requirements in the Norwegian Annex the procedure has been used as the basis for the analyses undertaken.

Various parametric studies have been performed for the jack-up unit and their sensitiveness to the responses have been quantified. The parameters considered are variations in water depth levels, the nonlinear soil-structure interaction, damping levels, airgaps and structural modifications.

Results from the Site-Specific Assessments for the Johan Sverdrup field show that the purpose-built jack-up unit (MSC CJ-70 Class design) satisfies ISO standard requirements in all respects (Overturning stability, foundation capacities and structural strength). However, the results show that the foundation capacities are almost fully utilised (0.96), indicating two possible conclusions:

  i)   That the applied foundation parameters are underestimated or
  ii)   Marginal limit is left to prevent foundation collapse.

Results from the parametric studies show a marginal safety level against risk of foundation collapse for almost all the parameters.
The vertical foundation capacity is dictated by the maximum preload capacity of the unit, if the soil is strong enough. Although the soil capacity may be higher, the maximum vertical foundation capacity is equal to the maximum preload capacity in accordance with the regulatory requirements. Since for most parameters the storm loading exceeds the preload capacity, this results in utilisations of foundation exceeding the capacities.

Results from the majority of the parametric studies show that the "tailor-made" jack-up unit analysed must be strengthened in order to satisfy the ISO standard requirements. In accordance with the brochure from Gusto MSc, the unit should be good for operating in water depths up to 150 meters. This may be the case for operations outside the NCS, as the regulatory requirements here are more stringent and the weather conditions are harsher than other places in the world.

The unit is in particular sensitive to larger water depth, variation of the stiffness terms representing the soil conditions, reduction in the damping level, increased airgap and increase in drag coefficients. The accuracy in determining these parameters are of outmost importance

for the analyses of this type of units. Other parameters such as increase in lightship weight and increase in added mass of the legs are less significant to the results.

Analysis of most of the significant parameters shows that we introduce larger dynamic amplification of the responses, more dominant nonlinear effects and therefore stronger non-Gaussian distribution of the extreme responses. The methods applied for determining the responses are therefore more uncertain with regards to the assumptions and simplifications of the nonlinear effects. In order to obtain acceptable statistical parameters for the analyses, the time for the analyses increased considerably. Current rules, guidelines, methods and analyses procedures have been developed for jack-ups in shallow water depths (less than 100 meters) and less severe weather conditions.

Based on the findings, a significant effect of increasing the natural periods (by less than 2 seconds) towards the maximum wave energy in extreme weather conditions (when the water depth increases from 110 meters to 145 meters) has been quantified to increase the total environmental loading by 17% on the overall base shear and by 50% on the overturning moment. The effect of the nonlinear response increases also quite considerable and is reflected in the overall increase in the utilisation of the chord. This increases by nearly 60%. The lateral displacement is increasing from 2 meters to 5 meters, which is 250% increase. This will have an impact on the operational weather conditions the unit can operate in for those cases where she will operate with a drilling machine through a conductor on a permanent installation.

Variation of the airgap has also been investigated due to the fact that the unit may operate above drilling modules on permanent installations. The airgap may vary from a base case of 30 meters and up to 69 meters (as required on the Statoil operated Mariner field). The bearing capacity increases from 0.89 and up to 1.03 giving an increase of nearly 16% and the leg chord strength utilisation is increasing from 0.77 to 1.09 corresponding to an increase of more than 40%, which will require strengthening of the chords. The lateral displacement will increase from 2.0 meters and up to 4.4 meter. This will also give a reduction in operational uptime of the unit.

Based on the parametric study we can draw conclusions for the so-called "tailor-made" jack-up units (CJ70) whether it is realistic to go into deeper water than 110 meters in relation to the volatile and hazardous weather in the North Sea without jeopardising the required safety level. Several of the parameters will also reduce the uptime operation of the unit as it is operating through conductors on permanent installations.

The design will have to be enhanced to be able to survive in deeper water. CJ80 is the latest class of jack-up units capable of operating in somewhat deeper water. However, based upon the dimensions of these units and the high yield strength utilised in the legs, exceeding 150 meter water depth seems unrealistic with current technology in harsh environment. As the unit is lateral sensitive in deeper water, it is highly likely that the operability will be effected by the lateral displacement of the unit carrying out workover operations.

7.1 Recommendations for future work

Current rules and procedures for carrying out jack-up analyses for site assessment are based upon linearization processes of the nonlinear effects due to the nonlinear hydrodynamic loading, dynamic responses and large displacements. The procedures are developed based

upon moderate responses in water depths below 100 meters. Each of the assumptions should be addressed individually in future studies to establish their validity.

The experience with the analyses carried out clearly indicated that the increased water depths resulted in increased number of simulations to achieve satisfactory standard deviations of the extreme responses. The processes became more non-Gaussian dominated. The drag inertia method seems to have reached its limit and should be compared with other analysis methods.

Other software packages should also be used to validate the results and methods used with the SACS software package.

The study indicate that the natural period of existing high standard robust jack-up units have natural periods of the first modes in the region of about 10 seconds in water depth greater than 100 meters meaning that they are close to the peak periods of the large extreme wave heights giving large responses. The study has shown that the jack-up units are susceptible to variation in the definition of the soil conditions, damping ratios, and the drag coefficients. Sensitivity analyses should be carried out of the most dominant parameters and the level of uncertainty inherit in the values. The results should be further validated against model testing and full scale measurements.

Analyses of varies soil conditions should be carried out to verify the recommended values defined in the ISO standard and perhaps refine the values to include a larger variation of soil conditions. Such high cyclic loading on the foundations may also cause changes to the soil stiffness characteristics over time and should be further explored as we know that the fixation of the spud cans is an important parameter for the dynamic response.

Attention should also be drawn to the fatigue analyses assessment as well as operability of the unit due to the large lateral displacement of the unit. The large first order natural periods of the unit will give rise to high dynamic responses and therefore high cyclic loading as the energy of the seastates are coincident with the first order natural periods. This will also give high lateral movements at lower seastates giving rise to reduction in the operability of the unit when operating through the conductors on a permanent installation.

Finally, there may be other nonlinear effects that are not considered to take place that may have an effect on the responses. The first order modes have increased considerable for these units operating in deeper waters. Similar for the natural periods of the corresponding second modes, that have grown to just below < 1 second. This means that springing effects may increase the first order motions and the fatigue damage of the legs due to the resonance and low damping characteristics for the second order natural periods being coincident with the nonlinear high frequency wave energy. Another nonlinear effect that can take place is ringing phenomena. Ringing is excitation of a transient structural deflection due to nonlinear third-harmonic incident wave fields. This may occur as the dimensions of the legs have increased considerably compared to standard sizes and resonance may occur due to the nonlinear force component arising at higher order of the wave steepness and the low damping level at higher order natural modes. None of these effects have been reported so far, but moving into deeper water they may play a role.

8   REFERENCE LIST

1. Cassidy, M. J. (1999). Non-linear analysis of jack-up structures subjected to random waves. Doctoral dissertation. University of Oxford, England
2. Thompson, R. S. G. (1996). Development of non-linear numerical models appropriate for the analysis of jack-up units. Doctoral dissertation. University of Oxford, England.
3. Hoyle, M. J. R., Stiff, J.J., Hunt, R. J. (2012) Background to the ISO 19905-Series and an overview of the new ISO 19905-1 for the Site-Specific Assessment of Mobile Jack-up Units.
   Paper number: OTC- 23047, Offshore Technology Conference, Houston, USA
4. Baerheim, M., (1993), Structural effects of foundation fixity on a large jack-up. Proceedings of the Fourth International Conference on the Jack-up platform Design, Construction and Operation. Edited by L.F Boswell and C. D'Mello, City University, London, England
5. ISO-19905-1 (2012). Petroleum and natural gas industries – Site-specific assessment of mobile offshore units, with the Norwegian Annex. Part 1: Jack-ups.
   The British Standards Institution (BSI), England
6. SNAME Technical & Research Bulletin 5-5A (2008), Recommended Practice For Site Specific Assessment of Mobile Jack-Up Units. Rev. 3.
   The Society of Naval Architects and Marine Engineers. Houston, USA
7. SNAME Technical & Research Bulletin 5-5A (2008), Commentaries To Recommended Practice For Site Specific Assessment of Mobile Jack-Up Units. Rev. 3.
   The Society of Naval Architects and Marine Engineers. Houston, USA
8. Templeton, J. S. (2007), Spud can fixity in clay, findings from additional work in a study for IADC.
   Proceedings of the Eleventh International Conference on the Jack-up platform Design, Construction and Operation. Edited by L.F Boswell, B. McKinley and C. D'Mello, City University, London, England
9. Karunakaran, D. (1993), Nonlinear dynamic response and reliability analysis of drag-dominated offshore platforms, Doctoral dissertation. Norwegian University of Science and Technology, Norway.
10. Greeves, E.J., Jukui, B. H., Sliggers, P. G. F., (1993), Evaluating jack-up dynamic response using frequency domain methods and the inertial load set technique.
    Proceedings of the Fourth International Conference on the Jack-up platform Design, Construction and Operation. Edited by L.F Boswell and C. D'Mello, City University, London, England
11. Karunakaran, D., Spidsoe, N., Gudmestad, O. T., (1993) Non-linear dynamic behaviour of jack-up Platform.
    Proceedings of the Fourth International Conference on the Jack-up platform Design, Construction and Operation. Edited by L.F Boswell and C. D'Mello, City University, London, England
12. Azarhoushang, A. (2010), Dynamic response of fixed offshore platforms to environmental loads, Doctoral dissertation.
    Curtin University of Technology, Faculty of Science and Engineering, Department of Civil Engineering, Australia

13. Lancelot, M. (1993), A study of the nonlinearities, dynamics, and reliability of a drag-dominated marine structure. Doctoral dissertation
    Stanford University, USA
14. Skjelbreia, L., Hendrickson, J., (1961), Fifth order gravity wave theory
    Proceedings of the seventh Coastal Engineering Conference, The Hague, Netherlands. Volume 1, pp 184-196
15. SACS Manual (2012), version 7, revision 1.
    Bentley System INC, USA
16. ABS – Guidance notes on dynamic analysis procedure for self-elevating units (2014)
    American Bureau of Shipping, New York, USA
17. Borgman, L.E. (1967), Random hydrodynamic forces on objects.
    Annals of mathematical statistics, Volume 38, Issue (1), pp 37-51
18. Kvitrud, A., (2006), Response of jackups in stormy conditions
    Link: http://home.online.no/~akvitrud/2006%20Response%20of%20jackups.doc
19. Lu, Y. J., Chen, Y. N, Tan, P. L., Bai, Y., (2002), Prediction of most probable extreme values for jackup dynamic analysis
    Marine Structures 15 p 15-34
    Elsevier Science LTD, USA
20. Zhang, X. Y., Cheng, Z. P., Wu, J. F. (2010), Dynamic response of jack-up units – reevaluation of SNAME 5-5A Four methods
    Proceedings of the Twentieth (2010) International Offshore and Polar Engineering Conference, Beijing, China.
21. ABS (2014), Guidance on dynamic analysis procedure for self-elevating units
    American Bureau of Shipping, Houston, USA.
22. Barltrop, N. D. P., Adams, A. J. (1991), Dynamics of fixed marine structures, third edition.Butterworth-Heinemann Ltd, Oxford, England.
23. Carrington, T., Hodges, B., Aldridge, T., Osborne, J., Mirrey, J., (2003), Jack-up advanced foundation analysis by automatic re-meshing (large strain) FEA methods.
    Proceedings of the Ninth International Conference on the Jack-up platform Design, Construction and Operation.
    September 23th and 24th 2003. City University, London, England
24. Hayward, M., Hoyle, M., J., R., Smith, N., P., (2003), Determining acceptable rack phase difference for jack-up legs
    Proceedings of the Ninth International Conference on the Jack-up platform Design, Construction and Operation.
    September 23th and 24th 2003. City University, London, England
25. Morandi, A., C. (2003), Impact of changes to T&R 5-5A on jack-up system reliability
    Proceedings of the Ninth International Conference on the Jack-up platform Design, Construction and Operation.
    September 23th and 24th 2003. City University, London, England
26. Blankestijn, E., P., Mommaas, C., J., de Bruijn., R., (2003), The MSC XY-cantilever system
    Proceedings of the Ninth International Conference on the Jack-up platform Design, Construction and Operation.
    September 23th and 24th 2003. City University, London, England

27. ABSG Consulting Inc (2013), Summary report, phase 2 benchmarking of draft, International Standard ISO 19905-1, "Site-Specific Assessment of Mobile Jack-Up units"
Proceedings of the 14th International Conference on the Jack-up platform Design, Construction and Operation.
2013. City University, London, England

28. Jack, R., L., Hoyle, M., J., R., Smith., N., P., Hunt, R., J., (2013), Jack-up accident statistics – A further update
Proceedings of the 14th International Conference on the Jack-up platform Design, Construction and Operation.
2013. City University, London, England

29. Berberic, S., (2013), SACS Toolbox 3 user manual, rev 0 (in-house), Provided for Global Maritime.
London, England

30. Statoil, Johan Sverdrup Field Metocean Design basis. Metocean RE2012-001, Rev No. 1.

31. Cassidy, M., J., Hoyle, M., J., R., Houlsby, G., T., Marcom, M., R., (2002), Determining appropriate stiffness levels for spudcan foundations using jack-up case record.
Proceeding of OMAE, 21th International Conference on Offshore Mechanics and Artic Engineering. June 23-28/ 2002, Oslo, Norway

32. Zhang, Y., Bienen B., Cassidy, M., J., (2013), On the VHM capacity of a buried spudcan in soft clay as it relates to the new ISO 19905-1 guidelines
Proceedings of the 14th International Conference on the Jack-up platform Design, Construction and Operation.
2013. City University, London, England

33. MSL Engineering Limited (2004), Guidelines for jack-up rigs with particular reference to foundation integrity
MSL Engineering Limited, Egham, Surrey, England

34. Morandi (2004), "Jack-ups capabilities", In-house power point presentation for Global Maritime.
Houston, USA

35. Guidelines For Offshore Structural Reliability – DNV Application to Jackup Structures, DNV Technical Report no. 95-0072
Link: http://research.dnv.com/skj/Offguide/Jack-up-appl.pdf

36. Bathe, K. J. (1996). Finite element procedures, second edition.
Prentice-Hall, Inc. Upper Saddle River, New Jersey, USA.

37. Cook., R. D., Malkus, D. S. , Plesha, M. E., Witt, R. J., (2002) Concepts and applications of finite element analysis, fourth edition.

38. Zienkiewicz, O., C., Taylor, R., L., (2005), The finite element method for solid and structural mechanics, sixth edition
Elsevier Butterworth-Heinemann, Oxford, England.

39. Bell, K., (2013), An engineering approach to finite element analysis of linear structural mechanics problems, first edition

Akademika Publishing. Trondheim. Norway

40. Bell, K., (2011) Static calculations of frame structures (translated from Norwegian: Matrisestatikk : Statiske beregninger av rammekonstruksjoner), second edition. Tapir akademisk forlag, Trondheim. Norway

41. De Borst, R., Crisfield, M., A., Remmers, J., J., C., Verhoosel, V., (2012), Non-linear finite element analysis of solids and structures, second edition. John Wiley and Sons Ltd. Baffins Lane, West Sussex, England

42. Langen, I., Sigbjörnsson, R., (1979) Dynamic analysis of structures (translated from Norwegian: Dynamisk analyse av konstruksjoner). Tapir, Trondheim, Norway.

43. Continuum Mechanics, direct link: http://www.continuummechanics.org/cm/introduction.html

44. Yaw, L., L., (2009) Nonlinear Static - Explicit and Implicit Analysis Example Walla Walla University, Washington, USA. Link: http://people.wallawalla.edu/~louie.yaw/nonlinear/ExIm_analysis.pdf

45. Crisfield, M., A., (2000), Non-linear finite element analysis of solids and structures, volume 1 John Wiley and Sons Ltd. Baffins Lane, West Sussex, England

46. Belytschko, T., Liu, W., K., Moran, B. (2001), Nonlinear finite elements for continua and structures, first edition. John Wiley and Sons Ltd. Baffins Lane, West Sussex, England

APPENDIX A

Notes on the Finite Element Method (FEM)

Symbols

A   System matrix
C   Damping matrix
EI   Flexural rigidity
f   Vector of body forces
F   Vector of external nodal forces
H   Work of external loads
I   Identity matrix
K   Stiffness matrix
M   Mass matrix
M   Bending moment
N   Shape functions
p   Distributed loading
Q_k Orthogonal matrix
R   Vector of external nodal forces at time t
R_k Upper triangular matrix
T   Tri-diagonal transformation matrix
u   Structural displacement vector
u̇   Structural velocity vector
ü   Structural acceleration vector
u_m Mode shape vector
U   Strain energy
V   Shear force
w   Lateral deflection

Greek letters

α_1 and α_2 Damping constant depending on damping level
γ and β Parameters
$\delta\varepsilon$ Vector of virtual strains
δu Vector of virtual displacements
ε Normal strain
ζ_1 and ζ_2 Damping ratios associated with the natural frequencies
λ Eigenvalues
Π Potential energy
σ Normal stress
Φ Vector of surface tractions
ω_0 Natural frequency
ω_1 and ω_2 Natural frequencies for the two lowest modes

Table of Content

A.1 STRUCTURAL FORMULATION FOR LINEAR AND NONLINEAR STATIC AND DYNAMIC PROBLEMS

A.1.1 General

A jack-up platform is usually simulated through a Finite Element Analysis (FEA) using an FE software, such Structural Analysis Computer Software (SACS), which is used in this case. In the following Chapter a literature review of the structural formulation for linear and nonlinear relation to static and dynamic problems is presented.

A.1.2 Finite Element Method (FEM)

The finite element method (FEM) is a numerical technique for finding approximate solutions to partial differential equations (PDE) that arise in physical problems.
The idealization of a physical problem to a mathematical model requires certain assumptions that together lead to PDEs governing the mathematical model.
A mathematical model is discretized into a 'discrete model' consisting of an assembly of finite elements, also called a mesh that is further split up into beam, plate and volume elements. A mesh is programmed to contain information of material, structural properties and boundary conditions.
Small individual finite elements can be visualized as small pieces of a structure and is represented by an interpolating function, which is a function for approximating the displacements within the element. The response of each element is expressed in terms of a number of degrees of freedom (DOF), characterized as the value of the interpolating function at a set of nodal points. DOFs are parameters needed to describe the geometry of the discrete model.
An approximated solution to the physical problem is obtained through the mathematical model determined by a finite element analysis (FEA) [36] [37].
A FEA solves the mathematical model expressed by PDEs through various techniques. These techniques involves different formulations of the PDEs. A so-called weak formulation is normally preferred in FEM.
A weak formulation is an integral form mathematically equivalent to the governing PDE, while a strong formulation is the PDE plus boundary conditions.
Three distinct procedures are pursued for obtaining the approximation in such integral forms, and used to formulate FEM problems [38] [39].
The first procedure is the methods of weighted residuals. Examples of such methods are the Galerkin method, Collocation method and Least Squares Method.
The second procedure is a variational- or the Rayleigh-Ritz method. The variational method is based on the determination of variational functionals for which stationary is sought. In structural mechanics, this method is based on potential energy consideration, i.e. principle of minimum (stationary) potential energy (PMPE), and variational calculus, which applies to the Rayleigh-Ritz method. The potential energy equation can be expressed [39] [40].

$$\prod = U + H \qquad (A.1.1)$$

where

U	- strain energy
H	- work of external loads

85

A third approach makes use of virtual work and the principle of virtual displacement (PVD) directly, without going through any mathematical manipulations and just by the actual principle.

A.1.3   Linear analysis in structural problems

A.1.3.1   Beam theory

Linear theory is based linear elastic material behavior, in addition to assuming that the displacements are so small, that with sufficient accuracy, it can base both equilibrium and kinematic compatibility on the original, undeformed geometry.
Beam elements are structural components that may carry loads in three-dimensions including axial forces, shear forces in two orthogonal directions and moments around three directions. Two mathematical beam models exists and both are commonly used in calculation of structural mechanical problems. A beam model based on elementary Euler-Bernoulli theory and a beam model based on Timoshenko's theory.
Both models are used to formulate finite beam elements in the FEM. Finite elements using the Euler-Bernoulli theory leads to so-called C^1 (Hermitian) beam elements, while using Timoshenko's beam theory, finite elements are known as C^0 beam elements, which includes a first order correction for transverse shear effects. Hence, the Euler-Bernoulli beam theory neglects the effect of transverse shear deformations and only accounts for bending moment deformation on the internal energy [39]. The tranverse shear is highly depending upon the magnitude of the beam height/shear area and the applied load. For normal beams, the effect on the deflection is marginal (less than 15%).

A.1.3.2   Euler-Bernoulli differential equation

The Euler-Bernoulli beam theory is based on linear assumptions, prismatic cross-section, and deformations in accordance with the strong form of Navier's hypothesis, i.e. *"plane cross-sections normal to the longitudinal beam axis remains plane and normal to the longitudinal beam axis after deformation"* [40].

The Euler-Bernoulli differential equation is extracted using the following sets of equations.

1) Static equilibrium

$$\frac{dV}{dx}=p \qquad \text{(A.1.2)}$$

$$\frac{dM}{dx}=V \qquad \text{(A.1.3)}$$

2) Kinematic relationships (strain-displacement relations)

$$\varepsilon=\frac{du}{dx}=-y\frac{d^2w}{dx^2} \qquad \text{(A.1.4)}$$

3) Constitutive relation (Hooke's law)

$$\sigma=E\varepsilon \qquad \text{(A.1.5)}$$

By combining the equations and the Euler-Bernoulli differential equation can be expressed.

$$EI\frac{d^4w}{dx^4}=p \tag{A.1.6}$$

where

V	- shear force
M	- bending moment
EI	- flexural rigidity
w	- lateral deflection
u	- axial deflection
p	- distributed loading
ε	- normal strain
σ	- normal stress

In contrary to the Euler-Bernoulli theory, Timoshenkos beam theory assumes that the cross-sections remain plane, but do not remain normal to the deformed beam axis. Other assumptions are similar in both models.
The choice of beam model depends the problem. Both models are typically combined with axial or torsion theories.

A.1.3.3   Governing equations in the FEM for a linear structural analysis

The standard formulation of a finite element solution in a linear structural analysis is using the displacement method. The general formulation of this method is based on the use of the PVD, which is equivalent to the use of Galerkin method and the MPME/Rayleigh-Ritz method.
The PVD for a structural element is an expression of equilibrium, compatibility and a constitutive law (stress-strain relationship), and can be stated in the form [37].

$$\int\delta\varepsilon^T\sigma dV=\int\delta u^T f dV+\int\delta u^T\Phi dS \tag{A.1.7}$$

where

$\delta\varepsilon$	- vector of virtual strains
δu	- vector of virtual displacements
f	- vector of body forces
Φ	- vector of surface tractions

The displacement method have a set of algebraic equations describing the linear structural behavior in static equilibrium between the systems internal (left side) and external applied forces (right side of the equation (A.1.7). External forces are body forces, point forces and surface tractions, while the internal forces correspond to element stresses. The internal forces in the system are produced by unknown nodal displacements multiplied with a stiffness matrix.
A stiffness matrix yields the primary characteristics of a finite element. For a structural finite element, the stiffness matrix contains the geometric and material behavior information that indicates the resistance of the element to deformation when subjected to loading.
An element stiffness matrix is generated via the interpolating functions for the element displacements. A stiffness matrix is always quadratic (n x n), where n is determined by number of DOFs.

In a structural model, composed of many finite elements and nodal DOFs, a global stiffness matrix is constructed by connecting or assembling the collection of stiffness matrices for all elements. This matrix determines the overall stiffness of the structural model.

The set of equilibrium equations applicable to the structural model, equal to the number of DOFs, may require advanced solution techniques, in order to obtain a solution. The Gauss elimination method and LU decomposition technique are mainly used for solving such sets of linear static equilibrium equations [36].

Imagine a jack-up model, which is pieced together of possibly hundreds three-dimensional beam elements and thousands of nodal DOFs, yields over thousands of equilibrium equations to be solved.

$$Ku=F \tag{A.1.8}$$

where

K	- stiffness matrix
F	- vector of external nodal forces
u	- structural displacement vector

A.1.3.4   Finite element formulation

Finite elements are represented by an interpolation functions, or shape functions, expressed by polynomial or hyperbolic-trigonometric functions describing the element displacements. Polynomial shape functions representing beam elements of second order are C^0 elements, while Herimitian (C^1) elements are polynomials of cubic order.

Shape functions may be expressed in terms of isoparametric coordinates, because of their advantage to map more complex shapes and compatible geometries [37] [41].

In accordance with Borst [41], a continuous displacement field of a single spatial three-dimensional beam element, represented in isoparametric coordinates, can be given as:

$$u=\sum_{i=1}^{12} N_i \left(\xi,\eta,\zeta\right) u_i \tag{A.1.9}$$

Where

N	- shape functions
u	- vector of nodal displacements

Where the displacements at nodes of the element are considered as the fundamental unknowns and where each of the 12 shape functions are describing one nodal DOF.

A.1.3.5   Convergence requirements

Shape functions must fulfil three requirements in order ensure convergence of the FEM. These requirements are interelement compatibility condition (continuity), completeness condition and interpolation condition.

A.1.3.5.1   Continuity

The displacement field must be continuous within the element.
Displacements and its derivative up to the order N-1 must be continuous along the boundary
between neighbouring elements. N is the highest derivate in the energy functional and
dictated from the requirement the strain-displacement relation between two elements. This
condition is a premise in order to establish the total energy or the total virtual work as a sum
of contribution for each element.

A.1.3.5.2   Completeness

The displacements must be capable of representing the rigid body motions correctly, that is, a
pure rigid body motion must not contain or produce strain/curvature or stresses in the element.
The shape function must be able to give a condition of constant strain/curvature in the
element.

A.1.3.5.3   Interpolation condition

N_i must yield when $v_i=1$ and $v_j=0$ when $j \neq i$.
$N_i=0$ along all edges/surfaces that do not contain a dof i.
$\sum N_i=1$

This first condition apply to all elements, while the second applies to only two and three
dimensional C^0 elements and the third applies to all C^0 elements.

A.1.3.6   Outline procedure using the displacement method in FEM

1) Discretization. Divide the structure into a mesh of finite elements. Elements are
   connected at nodal DOFs.
2) Element analysis. Obtain the stiffness matrix and load vector for each element,
   determined through the interpolation functions for each element.
3) System analysis. Establish the structures global stiffness matrix and load vector from
   all the elements.
4) Solve the set of equilibrium equations (A.1.8).

A.1.4   Nonlinear analysis in structural problems

The basic problem in a general linear and nonlinear analysis is similar, equilibrium between
internal and external forces must be satisfied [38]. However, in a nonlinear analysis the force-
displacement relationship requires continual updating in order to maintain equilibrium.
Numerical equilibrium is typically maintained by solving nonlinear equations with an
incremental-iterative approach, where the solution at each step being obtained from the
solution at the previous step [36] [41].

A state of equilibrium between externally applied loads and internal forces in a nonlinear
static analysis, derived through the basic principle of PVD using continuum mechanics, can
be expressed [36], at time t:

$$^t R - {}^t F = 0 \qquad\qquad (A.1.10)$$

Where

R   - vector of external nodal forces at time t
F   - vector of nodal forces corresponding to element stresses at time t

In static processes, where time plays no role, time however is typical a parameter employed to apply external load in increments, or in loading steps.

A.1.4.1   Nonlinear applications

Applications leading to nonlinear structural response arise from three contributions.

- Material nonlinearity, where material properties are functions of the state of stress or strain. Typical examples are material behaving elastoplastic or plastic, resulting in a nonlinear stress-strain relationship and a nonlinear constitutive law.
- Geometric nonlinearity, where large displacements effects causing geometrical nonlinearities on the structure. This may result in nonlinear strain-displacement relationship and large deformation kinematics.
- Nonlinear boundary conditions. Surface contact between two or more bodies.
- Nonlinear loading, e.g. the drag term in the Morisons wave equation.

Typical nonlinear analyses can be classified according to Bathe [36] in Table A-1.

Table A-1 Typical classifications of nonlinear analysis, extracted from Bathe [36]

Type of analysis	Description	Typical formulation used	Stress and strain measures used
Materially-nonlinear only	Infinitesimal displacements and strains; stress train relation is non-linear	Materially-nonlinear-only (MNO)	Engineering strain and stress
Large displacements, large rotations but small strains	Displacements and rotations of fibers are large; but fiber extensions and angle changes between fibers are small; stress strain relationship may be linear or non-linear	Total Lagrange (TL) Updated Lagrange (UL)	Second Piola-Kirchoff stress, Green-Lagrange strain Cauchy stress, Almansi strain
Large displacements, large rotations and large strains	Displacements and rotations of fibers are large; fiber extensions and angle changes between fibers may also be large; stress strain relationship may be linear or non-linear	Total Lagrange (TL) Updated Lagrange (UL)	Second Piola-Kirchoff stress, Green-Lagrange strain Cauchy stress, Logarithmic strain

A.1.4.2   Formulation of continuum mechanics

Three different approaches are being pursued in incremental nonlinear FEA.
These approaches are based on using a consistent continuum mechanics based approach, employed in order to develop the governing finite element equations.
Continuum mechanics is a physical and modern discipline that describes the deformations and strains in objects and relate them to the resulting stress, using linear algebra.
Continuum mechanics provides a toolbox of methods needed to accomplish all calculations of a structural analysis [43].
The alternative continuum mechanics expressions can be listed below.

- Total Lagrangian (TL) formulation
- Updated Lagrangian (UL) formulation
- Eulerian formulation

The only difference between a TL and UL formulation is that in a TL formulation, all calculations at each stage of the incremental loading history, are always referred to the original (undeformed) geometry, while in a UL formulation, all calculations are referred to a current (deformed) configuration.
Both the TL and UL formulations can include kinematic nonlinear effects due to large displacements, large rotations and large strains, but with different efficiency.
For large displacements and rotations with small strains, a TL formulation is more efficient.
For small strains the UL formulation imposes a Cauchy stress tensor and an Almansi strain tensor, which makes the UL formulation numerically less efficient.
However, for large strains combined with large displacements and rotations, the UL formulated is generally recommended, due to its greater numerical efficiency, because of an initial displacement effect in the TL formulation that leads to a more complex strain-displacement transformation.
The only advantage of using one formulation rather than the other lies in its greater numerical efficiency [36].
An Eulerian formulation is usually employed in analysing of fluid mechanical problems and is therefore not discussed.

A.1.4.2.1   *Formulations of nonlinear structural problems*

The governing continuum mechanics equations for nonlinear structural problems, using a displacement-based finite element solution, can be regarded as an extension of the basic PVD equation given in (A.1.7), whereof the possibility that the body considered undergoes large displacements and rotations, large strains and that the stress-strain relationship is nonlinear.
The basic idea of the nonlinear finite element formulation is to linearize the weak form of the equation of the problem and solve these equations for the finite elements discretized domain.
A TL formulation is used in this thesis, in conjunction with stress and strain measured with second Piola-Kirchoff stress and Green-Lagrangian strain measurements.
A TL incremental analysis approach can express equilibrium of the body at time t+Δt using the PVD. This principle requires that:

$$\int_{^0V} \delta^{t+\Delta t}\varepsilon^{T}{}^{t+\Delta t}\sigma^{0}dV = {}^{t+\Delta t}R \qquad\qquad (A.1.11)$$

A.1.4.3   Three dimensional nonlinear beam elements

Three dimensional nonlinear beam elements are described using the same assumptions employed in a linear analysis, but with displacements and rotations being arbitrary large. Element strain may be assumed to be small or large, depending on the analysis. For most geometrically nonlinear analysis of beam type structures, small strain combined with arbitrary large displacements and rotations are appropriate assumptions.
Using the general continuum mechanics equations for nonlinear analysis, the calculation of the beam element matrices for nonlinear analysis represents a direct extension of the formulation linear formulation.

A.1.4.4   Solution schemes for incremental nonlinear static analysis

A solution scheme for a nonlinear problem can be obtained using both implicit and explicit methods. The chosen method should be determined based on good convergence characteristics and employed efficient in regard to the given problem.
A solution scheme is obtained from a procedure of linearization the virtual work equation (A.1.11). The method of procedure depends on the element formulation and stress/strain measures. The reader is referred to Bathe [36] for detailed linearization forms from the most relevant approaches.

In an implicit analysis approach, the method includes an incremental procedure at the end of each increment and updates the stiffness matrix based on geometry changes and material changes. A new tangent stiffness matrix is calculated corresponding to the last calculated displacement, and the next load increment is applied to the structure. After each increment, Newton-Raphson iterations are used to enforce equilibrium before moving to the next step. Internal forces and external forces will not be in equilibrium unless the stiffness is linear for the given step. Hence, in order to achieve equilibrium, corrections must be made to the displacement. This is accomplished by using Newton-Raphson iterations to minimize the residual between the internal and externally applied loads [44]. Displacements are determined as the sum of all the individual incremental displacements.
An explicit procedure follows the same procedure as the implicit, but without enforcing the equilibrium between the internal and external loads.

The basic equations to be solved in nonlinear analysis are, at time t+Δt:

$$^{t+\Delta t}R - ^{t+\Delta t}F = 0 \tag{A.1.12}$$

Where the $^{t+\Delta t}F$ force vector is the unknown and iteration is needed to find it.

A.1.4.4.1   *Newton-Raphson Schemes*

Some form of the Newton-Raphson is the most frequently used iteration schemes for solving nonlinear finite element equations. The standard or full Newton-Raphson method, is referred to as an implicit method. The full Newton-Raphson method is per definition a root-finding algorithm for a nonlinear equation. The Newton-Raphson iteration may be derived by using a Taylor series expansion. The simple derivation is not provided in this thesis, but is shown in [10] [46].

The relations in the following two formulas constitute the full Newton-Raphson solution of equation (A.1.12). Equation (A.1.13) is a set of simultaneous linear equations which can be solved for $\Delta U^{(i)}$ and adding it to the previous estimate in the equation (A.1.14), to get out a new estimate for the new nodal point displacement.

$$^{t+\Delta t}K^{(i-1)}\Delta U^{(i)} = {}^{t+\Delta t}R - {}^{t}F^{(i-1)} \tag{A.1.13}$$

$$^{t+\Delta t}U^{(i)} = {}^{t+\Delta t}U^{(i-1)} + \Delta U^{(i)} \tag{A.1.14}$$

where

$^{t+\Delta t}K^{(i-1)}$	- tangent stiffness matrix at t+Δt, corresponding to iteration i-1
$U^{(i)}$	- vector of nodal displacement, corresponding to iteration i
$\Delta U^{(i)}$	- vector of nodal displacement increments, corresponding to iteration i

i=1,2,3…

The full Newton-Raphson method is calculating and factorising the tangent stiffness for each iteration, because it always starts with a Taylor series about the point i-1. This is considered costly and can be reduced, by adopting 'modified' iteration schemes, such as an initial stress method and a modified Newton-Raphson iteration method.
A modified Newton-Raphson method have a constant tangent stiffness matrix through all the incremental steps, sat up at the beginning of the iterative process. Comparing to the full Newton-Raphson procedure, it require more iterations but iterates faster.

A second 'class' of methods has been developed as alternatives to Newton-Raphson's methods, called quasi-Newton or Secant Newton methods. The strategy in these methods are approximating the tangential stiffness matrix using a secant approach.
Common quasi-Newton methods are the BFGS method and Crisfield methods [45].

A.1.5 Dynamic equation of motion

Dynamic equilibrium problems using a FEM formulation are typically formulated via energy consideration methods (Hamilton's principle or Rayleigh-Ritz method) or by virtual work (PVD)]42].

A.1.5.1 Hamilton's principle

Hamilton's principle states that the development in time for mechanical system is the integral of the difference between the kinetic and potential energy is stationary. This is analog with the principle of minimum potential energy (MPME) in a static analysis. Dynamic problems can be solved using Hamilton's principle in conjunction using procedures of variational operations. Mathematically, Hamilton's principle can be expressed [42] as

$$\delta \int_{t_1}^{t_2} L dt = 0 \tag{A.1.15}$$

Where

L   - Lagrange functional, defined as difference between the kinetic and potential energy

$$L = T - \Pi \qquad \text{(A.1.16)}$$

A.1.5.2   Rayleigh-Ritz method

This method, shortly explained in Section A.1.2, is used to derive the dynamic equilibrium equation. Similarly in the Hamilton's principle, using variational calculus operations and other energy considerations, we can obtain formulations of dynamic problems using FEM. A Rayleigh-Ritz analysis is used for finding approximate solutions to natural frequencies and corresponding mode shapes in a structure.

A.1.5.3   D'Alembert's principle

Using D'Alembert's principle on general form (PVD combined with D'Alembert's principle), is dynamic analogue to the PVD on a static system. We obtain, using a similar procedure for a static analysis, by requiring work done by externally applied loads to be equal to the sum of work absorbed by the inertial, dissipative and internally forces for any virtual displacement, the dynamic equilibrium equation, or the so-called dynamic equation of motion for an element.
The principle states [42] that *"a system of rigid bodies is in dynamic equilibrium when the virtual work of the sum of the applied forces and the inertial forces is zero for any virtual displacement of the system"*.

The dynamic equation of motion is given below.

$$M\ddot{u} + C\dot{u} + Ku = F_t \qquad \text{(A.1.17)}$$

where

M   - mass matrix
C   - damping matrix
K   - stiffness matrix
F_t - vector of external nodal forces
u   - structural displacement vector
$\dot{u}$ - structural velocity vector
$\ddot{u}$ - structural acceleration vector

A.1.5.4   Dynamic characteristics

Dynamic characterizations, mode shapes and natural frequencies, depends upon the restoring force (stiffness) and the resistance to change of motion (inertia).
Natural frequencies are computed in absence of damping and nodal forces. If we assume harmonic oscillations, we can express the dynamic stiffness matrix, also called the natural frequency equation on a general form.

$$\left(K - \omega_0^2 M\right)u_m = 0 \qquad \text{(A.1.18)}$$

Where

ω_0 - natural frequency

u_m - mode shape vector

This equation represents n simultaneous homogenous equations. There are n solutions each representing a natural frequency and mode shape.

There are corresponding modes of free vibrations and natural frequencies as the number of DOFs. For a jack-up platform modeled with thousands of DOFs, only the three lowest natural frequencies are of interest, two lateral (sway and surge) and one torsional (yaw).

Multiple solution techniques are available, and some methods produce all natural frequencies, while other permit a limited number of natural frequencies to be determined.

Equation (A.1.18) is generally written in standard eigenvalue form.

$$\left(-\lambda + AI\right)u_m = 0 \qquad\qquad (A.1.19)$$

Where

A   - system matrix

λ - eigenvalue ($= \omega_0^2$, one per degree of freedom or mode)

I   - identity matrix

A.1.5.5   Solution procedure for obtaining eigenvalues

A variety of solution techniques for solving eigenproblems are available. The choice of method depends upon the size of the structure (number of DOFs) and results (number of needed eigenvalues and eigenvectors and requirement to accuracy).

For small and medium structural models, transformation methods are considered the most effective method. For larger structural models, vector iteration methods or subspace iteration methods can be recommended.

Solution procedures are based on iteration techniques derived from algorithms based on similarity transformation matrices, orthogonalitzation, matrices deflation or introduction of shift properties.

Bathe [36] have listed available solution procedures into categories.

- Vector iteration methods
  Inverse iteration
  Forward iteration
  Rayleigh quotient iteration
  Matrix deflation and Gram-Schmidt orthogonalization
- Transformation methods
  The Jacobi or generalized Jacobi method
  The Householder-QR-Inverse iteration solution
- Polynomial iterations and Sturm sequence techniques
  Explicit or implicit polynomial iteration
- The Lanczos iteration method
- The subspace iteration method

The scope of this thesis is limited to a thorough review of the Householder-QR algorithm, because this method is used to calculate the natural frequencies and mode shapes for the jack-up studied.

A.1.5.6   Householder QR/QL Inverse iteration solution

The optimum strategy for finding eigenvalues and eigenvectors is, first, to reduce the matrix to a simple form, and then begin an iterative procedure [36] [37].
The Householder QR/QL (HQRI) is considered the most efficient technique for finding eigenvalues and eigenvectors of a symmetric matrix. The symmetric matrix is reduced to a simple tri-diagonal form, followed by the QR or QL algorithm that can diagonalize a tri-diagonal matrix within a finite number of steps without eigenvectors. If eigenvectors are required then the number of operations grows.

In accordance with Bathe [36], The name HQRI solution method stands for the following three solution steps:

1. Householder transformations are employed to reduce the matrix to a tri-diagonal form.
2. QR iteration yields all eigenvalues.
3. Using inverse iteration the required eigenvectors of the tri-diagonal matrix are calculated. These vectors are transformed to obtain the eigenvectors.

A.1.5.6.1   *The Householder reduction form*

The Householder reduction is a finite procedure, where the symmetric matrix is reduced to a tri-diagonal form by n-2 orthogonal transformations. The orthogonal transformation ensure symmetry and a tri-diagonal form, while the n-2 means that there are only n-2 off diagonal elements, see below.

$$T = \begin{pmatrix} a_1 & b_1 & & & & \\ b_1 & a_2 & b_2 & & & \\ & b_2 & a_3 & b_3 & & \\ & & b_3 & . & & \\ & & & & . & \\ & & & & & . \end{pmatrix} \qquad (A.1.20)$$

Where

T   - tri-diagonal transformation matrix of 'A', given in equation (A.1.19).

A.1.5.6.2   *The QR iteration*

The QR iteration is applied to the tri-diagonal matrix obtained by the Householder transformation. The basic idea of the QR iteration is to perform a QR decomposition, writing the matrix as a product of an orthogonal matrix and an upper triangular matrix and multiply the factors in the reverse order, and iterate. A QR decomposition and QR algorithm can be written as [36]:

$$T_k = Q_k R_k \tag{A.1.21}$$

Where

Q$_k$ - orthogonal matrix
R$_k$ - upper triangular matrix

$$T_{k+1} = R_k Q_k = Q_k^{-1} T_k Q_k \tag{A.1.22}$$

The T$_k$ matrices will converge to a triangular matrix, with eigenvalues on the diagonal. When the eigenvalues are found with sufficient accuracy, we calculate the eigenvectors to the tri-diagonal matrix T by inverse iteration with shifts equal to the corresponding eigenvalues. More information can be found in [38].

A.1.5.7   Methods to reduce the number of DOFs

Several methods are used to reduce the number of DOFs in order to reduce the time consumption and only produce relevant results for dynamic problems, such as eigenvalues. In this study a Guyan reduction is used for the dynamic analysis, also called a static condensation for a static analysis.

A.1.5.7.1   *Guyan reduction or static condensation*

This method is based on a master-slave technique, by diving the number of DOFs into two groups, master and slave freedoms, where the slave freedoms depends or are *condensed* to the master freedoms. In matrix notation the overall matrices in a structural model may be partitioned into master (m), slave (s) and cross coupling terms (ms or sm). This can be formulated as below (the damping term is excluded).

$$\begin{bmatrix} M_m & M_{ms} \\ M_{sm} & M_s \end{bmatrix} \begin{Bmatrix} \ddot{u}_m \\ \ddot{u}_s \end{Bmatrix} + \begin{bmatrix} K_m & K_{ms} \\ K_{sm} & K_s \end{bmatrix} \begin{Bmatrix} u_m \\ u_s \end{Bmatrix} = \begin{Bmatrix} F_m \\ F_s \end{Bmatrix} \tag{A.1.23}$$

If, by definition, no external forces are applied directly to the slave DOFs, we can express formulas for reduced stiffness matrix and mass matrix as:

$$\begin{bmatrix} K_m' \end{bmatrix} = \left(K_m - K_{ms} \frac{K_{sm}}{K_s} \right) \tag{A.1.24}$$

$$\begin{bmatrix} M_m' \end{bmatrix} = \begin{bmatrix} 1 & -K_{ms} K_s^{-1} \end{bmatrix} \begin{bmatrix} M_m & M_{ms} \\ M_{sm} & M_s \end{bmatrix} \begin{bmatrix} 1 \\ -K_s^{-1} K_{sm} \end{bmatrix} \tag{A.1.25}$$

Where

$K_m^{'}$ - reduced stiffness matrix

$M_m^{'}$ - reduced mass matrix

Master DOFs are generally chosen where displacements are expected to have largest amplitudes and most contribution to the kinetic energy.
The advantage of Guyan is that it is easy to implement and computationally efficient.

A.1.5.8   Damping

Structural damping is the caused by several damping mechanism. Mathematical damping models have therefore been established. These can be listed as:

- Linear and nonlinear viscous damping (velocity related damping)
- Structural damping (displacement dependent damping)
- Coulombs damping (constant damping).

The most common method to model structural damping is to model the damping as proportional damping using a Rayleigh model, specified by the modal damping of the lowest natural modes of the structure. In a jack-up structure, the lowest modes refers to surge and sway.

The damping matrix using a proportional damping in a Rayleigh model can be expressed as follows [9] [42]:

$$C = \alpha_1 M + \alpha_2 K \tag{A.1.26}$$

Where

α_1 and α_2 - damping constant depending on damping level

The proportionality factors that characterize the damping are estimated by defining the damping ratio for the two lowest natural modes.
These factors may be given according to Langen and Sigbjornsson [42]:

$$\alpha_1 = 2 \frac{\omega_1 \omega_2}{\omega_2^2 - \omega_1^2} \left(\zeta_1 \omega_2 - \zeta_2 \omega_1 \right) \tag{A.1.27}$$

$$\alpha_1 = 2 \frac{\omega_1 \omega_2}{\omega_2^2 - \omega_1^2} \left(\frac{\zeta_2}{\omega_1} - \frac{\zeta_1}{\omega_2} \right) \tag{A.1.28}$$

Where

ω_1 and ω_2 - natural frequencies for the two lowest modes
ζ_1 and ζ_2 - damping ratios associated with the natural frequencies

A.1.5.9   Time domain response analysis

Time domain solutions are useful for nonlinear structural response and non-sinusoidal loading.
As described introductorily, nonlinear structural response applies to fixed offshore structure due to their nonlinear effects.
Nonlinear structural response is obtained by solving the dynamic equation of motion (A.1.17) usually in time domain, using a time history solution method.
For fixed offshore structures, time domain response analysis may be based on two different principles [9] [42].

- Integrated (explicit) analysis
- Stepwise (implicit) analysis

The explicit and implicit analyses are a bit different in regard to a dynamic context versus a static. Incremental steps are followed in a nonlinear static analysis, while time is followed in a dynamic analysis. In regard to a dynamic analysis, no Newton-Raphson iteration is required in an explicit or implicit analysis, unless we deal with a problem which is nonlinear in nature, e.g. geometrical or material nonlinear application, described in Section A.1.4.1.
In the following the two dynamic approaches will be described.

The integrated or explicit analysis implies that the dynamic equation of motion (A.1.17) is solved iteratively by time-step integration updating the position for calculation of hydrodynamic forces and the system properties at each time step according to the instantaneous position of structure. Mathematically expressed, obtaining a value at t+Δt by considering equilibrium at time t. This method is conditionally stable, which means it diverges from the correct answer unless the time step is very small.
The central difference method and the Runge-Kutta method are examples of methods using an explicit procedure [37].

The stepwise or implicit analysis is based on obtaining a value at t+Δt by considering equilibrium at time t+Δt. i.e. solving the dynamic equation of motion (A.1.17) at time t+Δt based on itself and using the solution obtained at time t.
This procedure is applicable for structures with small and moderate motions.
There exists a variety of implicit methods. The most famous one is the Newmark β method.

The main difference between the explicit and implicit is in the stability of the method, required time step and inversing the stiffness matrix. As the explicit method is conditionally stable, while in the implicit method it is unconditionally stable, which means that it can enable larger time step. The stiffness matrix must be inverted in an implicit method, but not in an explicit approach. Overall, the explicit methods are not usually recommended unless the steps are very small.

A.1.5.10   Time integration procedure

The Newmark-β method can be performed as a numerical procedure for both a linear and nonlinear time domain analysis. In this study, the dynamic equation of motion (A.1.17) is solved in time domain using a stepwise method, Newmark β method, with a time step interval of 0.5 s. This analysis method is considered sufficient, since linear springs are representing the nonlinear effects of the soil-structure interaction and the leg-hull connection, so the only

nonlinearity comes from the environmental loads, i.e. drag force and integration of forces to the instantaneous wave surface. These load nonlinearities are isolated in the external load vector F_t located on the right hand side of equation (A.1.17) and the solution can efficiently be carried out without any need for updating the system matrices. A linear numerical procedure of the time domain analysis is therefore considered sufficient.

A.1.5.10.1   *Newmark-ß method*

Newmarks general integration equations are a result of a Taylor series expansion where the residual term is approximated by squaring equations. The units γ and β are free parameters determined from stability and accuracy requirements. The equations are given in accordance with [42]:

$$\dot{u}_{t+1} = \dot{u}_t + \left(1-\gamma\right)h\ddot{u}_t + \gamma h\ddot{u}_{t+1}$$

(A.1.29)

$$u_{t+1} = u_t + h\dot{u}_t + \left(\frac{1}{2} - \beta\right)h^2\ddot{u}_t + \beta h^2\ddot{u}_{t+1}$$

(A.1.30)

The method is implicit stable if $\gamma \geq \frac{1}{2}$ and $\beta \geq \frac{1}{4}(\gamma + \frac{1}{2})^2$. For smaller β values, the method is only considered conditionally stable.
The choice of γ determines if the method has forced damping, i.e. decreasing amplitude for free undamped oscillations.
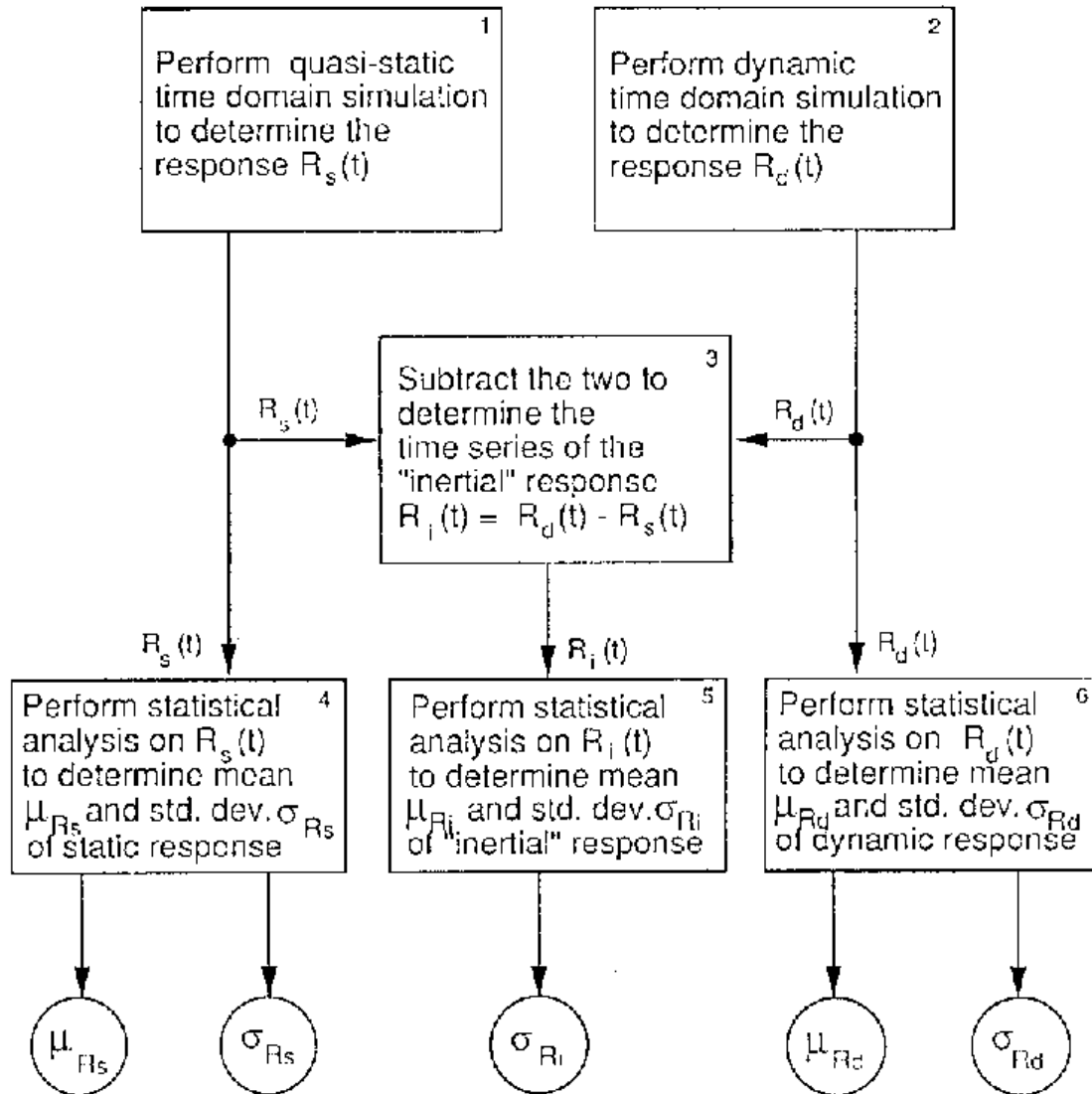The choice of β values yields other Newmark family methods, such as the central difference theorem ($\beta = 0$), Fox-Goodwins method ($\beta = 1/12$), linear acceleration ($\beta = 1/6$) and constant mean acceleration (trapezoid method) ($\beta = \frac{1}{4}$).

APPENDIX B

Notes on the Drag-Inertia DAF Method

Extracted from SNAME Technical & Research Bulletin 5-5A [6]

1 — Perform quasi-static time domain simulation to determine the response $R_s(t)$

2 — Perform dynamic time domain simulation to determine the response $R_d(t)$

$R_s(t)$ → **3** — Subtract the two to determine the time series of the "inertial" response $R_i(t) = R_d(t) - R_s(t)$ ← $R_d(t)$

$R_s(t)$ ↓ $R_i(t)$ ↓ $R_d(t)$ ↓

4 — Perform statistical analysis on $R_s(t)$ to determine mean μ_{Rs} and std. dev. σ_{Rs} of static response

5 — Perform statistical analysis on $R_i(t)$ to determine mean μ_{Ri} and std. dev. σ_{Ri} of "inertial" response

6 — Perform statistical analysis on $R_d(t)$ to determine mean μ_{Rd} and std. dev. σ_{Rd} of dynamic response

μ_{Rs} σ_{Rs} σ_{Ri} μ_{Rd} σ_{Rd}
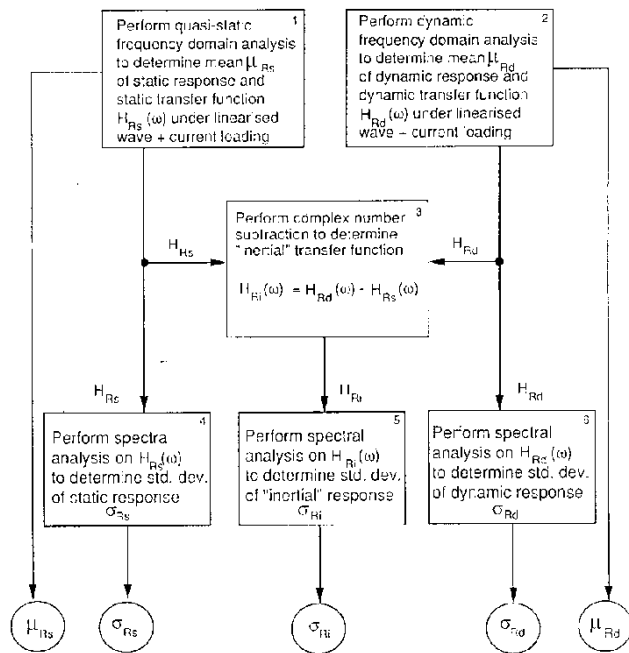
Specific notes with Figure C7.B.2

General

The procedure for estimating the extreme response due to hydrodynamic loading shown in Figure C7.B.4 requires knowledge of the mean and the standard deviation of the quasi-static and dynamic responses, and the standard deviation of the "inertial" response. A time domain procedure may be used to determine these.

Re blocks 4, 5, 6:   The mean of the "inertial" response is not used in the procedure. In most cases the mean of the static response will be (approximately) equal to the mean of the dynamic response. Therefore, the mean of the "inertial" response will be (approximately) zero. This may serve as a check on the simulations performed.

However, under certain conditions the means may truly be different. this can most clearly be seen when relative velocities (i.e. the wave induced water particle velocity minus the structure's velocity) are used to perform the dynamic simulation.

Figure C7.B.2 Time domain procedure for determining mean and standard deviation

Specific notes with Figure C7.B.3

General

The procedure for estimating the extreme response due to hydrodynamic loading shown in Figure C7.B.4 requires knowledge of the mean and the standard deviation of the quasi-static and the dynamic responses, and the standard deviation of the "inertial" response. A frequency domain procedure may be used to determine these. In order to reflect the interactions between the current velocity, the absolute wave induced water particle velocity and the structure's velocity (if a relative velocity formulation is adopted) and to linearize the associated drag loading adequately it is necessary to adopt a statistical or least squares linearization procedure as first formulated by Borgman (see Ref. below). Other forms of linearization in frequency domain analysis cannot handle these interactions.

For the least square linearization procedure, there only is a mean response in case of a non-zero current. The magnitude of the mean depends on the value of the current velocity and on the standard deviation of the wave induced (horizontal) water particle velocity, both taken at the same elevation z, and subsequently integrated over the full water depth. The wave induced water particle velocity may be the absolute or the relative velocity, depending on which of these is more appropriate for the case considered.

The transfer functions $H_{Rs}(\omega)$ and $H_{Rd}(\omega)$ between the response and the water surface elevation are similarly dependent on both the wave induced (horizontal) absolute or relative velocities and the current velocities at various elevations.

The means m_{Rs} and m_{Rd} and the transfer functions $H_{Rs}(\omega)$ and $H_{Rd}(\omega)$, are therefore a function of the seastate and the current sued in the environmental definition.

Re block 3:   The transfer function representing the difference between the dynamic and the quasi-static response is only notionally associated with "mass inertial" forces (not to be confused with inertial wave loading). The difference may additionally be due to damping forces and any effect causing (frequency dependent) phase differences between $H_{Rd}(\omega)$ and $H_{Rs}(\omega)$. (e.g. associated with multi degree of freedom system responses).

Re blocks 4, 5, 6:   The spectral analyses operate on the transfer functions $H_{Rx}(\omega)$, which by definition represent the time varying part of the response minus the mean, i.e. $R_x(t)-\mu_{Rx}$.
A similar note on the mean values of the various responses as given with Figure C7.B.2 should be made here. The mean value of the "inertial" response cannot be determined in a frequency domain analysis and is not required either. However, the fact remains that in most cases the mean of the static response will be (approximately) equal to the mean of the dynamic response. This should again serve as a useful check o the analyses performed.
From the above general note it can be seen that both means will only be non-zero if there is a current present. When relative velocities are used in the analysis of the dynamic problem the interaction between the current and the relative velocity may be different for the dynamic and the static case, resulting in realistically different mean values.

Reference:
L.E. Borgman
"Ocean wave simulation for engineering design"
Civil Engineering in the Oceans, ASCE conference, San Francisco, September 1967

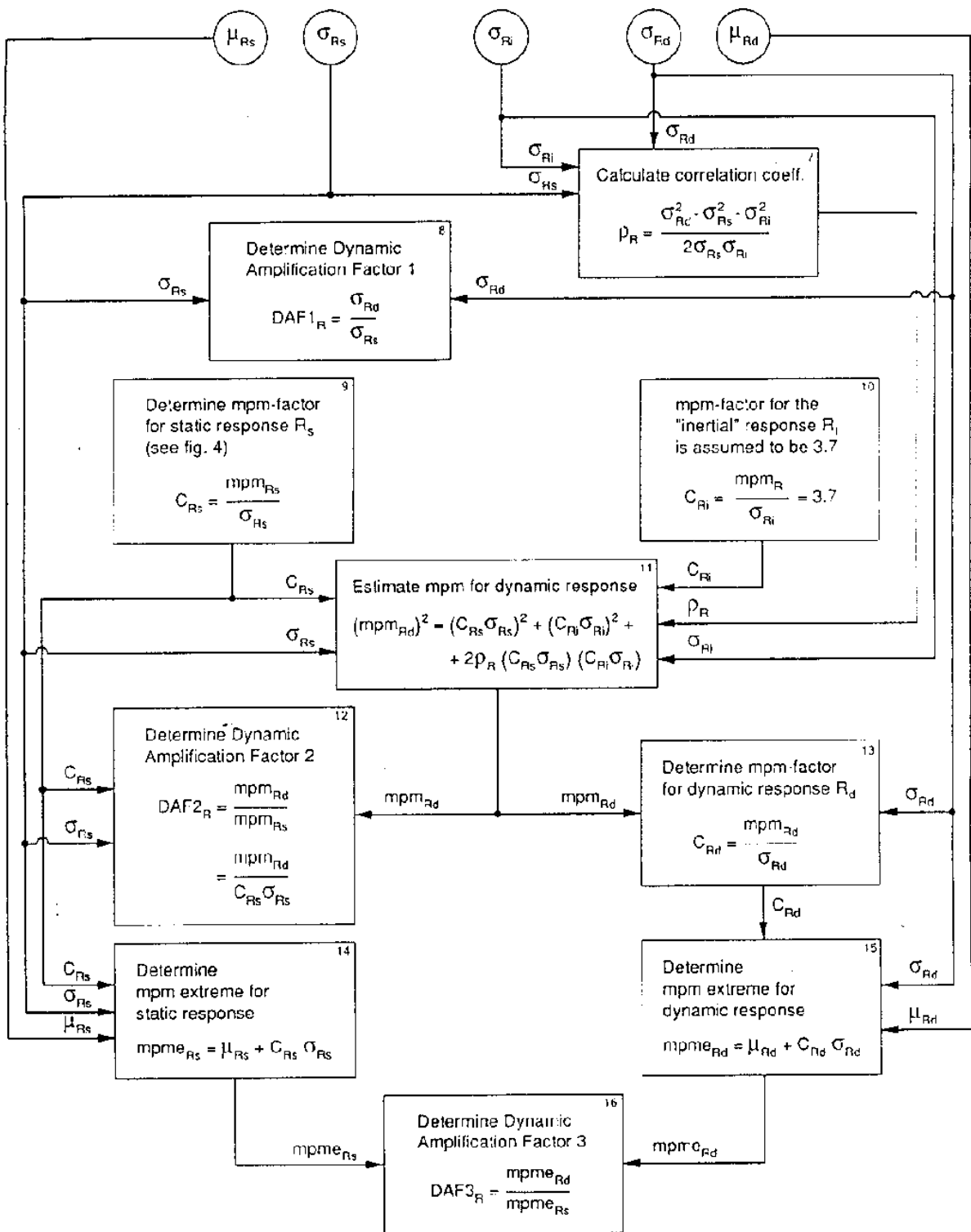Figure C7.B.3 Frequency domain procedure for determining mean and standard deviation

Figure C7.B.4 Procedure for estimating the extreme response

105

Specific notes with Figure C7.B.4

Re block 7: The correlation coefficient ρ_R is theoretically a value between -1 and +1. For virtually all applications to offshore structures problems it is expected that:

$$\delta^2_{Rd} > \delta^2_{Rs} + \delta^2_{Ri} \qquad \text{so that } 0 < \rho_R < 1.$$

For $r_R = 0$, zero correlation, the quasi-static and "inertial" responses do not influence one another and will be well separated in the frequency domain. This is generally only to be expected for relatively low natural periods which fall in the (very) high frequency tail of the wave spectrum and where $H_{Rs}(\omega)$ is also very low. Under these circumstances the variance (or mean square) of the full dynamic response is equal to the sum of the variances of the quasi-static response and the "inertial" response:

$$\delta^2_{Rd} = \delta^2_{Rs} + \delta^2_{Ri}$$

Geometrically, this means a direct addition of non-overlapping areas of the two parts of the response spectrum.

For $r_R = 1$, full correlation, the quasi-static and "inertial" responses are fully dependent on one another. The two parts of the response spectrum overlap strongly and will not really be distinguishable. This will increasingly be the case for high natural periods, considerably closer to the peak of the wave spectrum and therefore associated with a region of significant wave energy, and where $H_{Rs}(\omega)$ is also having appreciable values. Under these circumstances the standard deviation (instead of the variance) of the full dynamic response is equal to the sum of the standard deviations of the quasi-static response and the "inertial" response:

$$\delta_{Rd} = \delta_{Rs} + \delta_{Ri}$$

Re blocks 8, 12, 16: Several definitions of the dynamic amplification factor DAF are in use. The purest and most meaningful definition is believed to be DAF1, the ratio of the standard deviations of the dynamic and static responses (block 8), i.e. after eliminating the means which are not affected by dynamic magnification. If the static and the dynamic processes are both gaussian, or to an equal degree non-gaussian, then DAF2 = DAF1; however, this will not be the case in general. The ratio DAF3 of the most probably maximum extremes, including the means, is a practical overall measure of the increase in response due to dynamics.

Re block 9: The mpm-factor for an arbitrary non-gaussian response is not known. As an engineering postulate it is assumed that this is equal to the mpm-factor for Morison type wave loading on a cylindrical element of unit length. The factor for a nominal number of 1000 peaks (corresponding approximately with a 3 hr storm duration) then varies between the extremes of 3.7 (for inertial wave loading only and hence a gaussian process) and 8.0 (for drag waver loading only and consequently a strongly non-gaussian process). It can be determined on the basis of a drag-inertia parameter or the kurtosis of the response, as shown in Figure C7.B.5 with its associated notes.

Note that the factor 8.0 is different from the previously used factor of 8.6. This is due to the fact that in this report the most probably maximum is consistently used as a predictor for the maximum of a random process. The previous factor 8.6 referred to the expected maximum instead of the most probably maximum.

Re block 10: The mpm-factor for the "inertial" part of the response is associated with the dynamic behavior and predominantly of a purely narrow banded resonant nature. Experience has shown (and theory supports this) that such lightly damped dynamic processes tend towards gaussianity so that a mpm-factor of 3.7 is a reasonable and confident assumption for engineering purposes.

Re block 11: The relationship between the mpm-values is entirely analogous with the relationship between the standard deviations from which the correlation coefficient is determined. However, while it is theoretically proven equation for the standard deviations, it is an engineering postulate for the mpm-values.

Re blocks 14, 15: It should be recalled that the procedure depicted in Figures C7.B.2 to C7.B.6 is aimed at estimating the extreme short-term response due to hydrodynamic loading only (see General Note 1). Therefore, the effect of wind should be excluded from the most probably maximum extreme static and dynamic responses in block 14 and 15, respectively. Wind is assumed to produce a static load and a static response, and not to influence the dynamic behavior. To determine the ultimate response the mean response due to wind should be determined separately and added to $mpme_{Rs}$ and $mpme_{Rd}$.
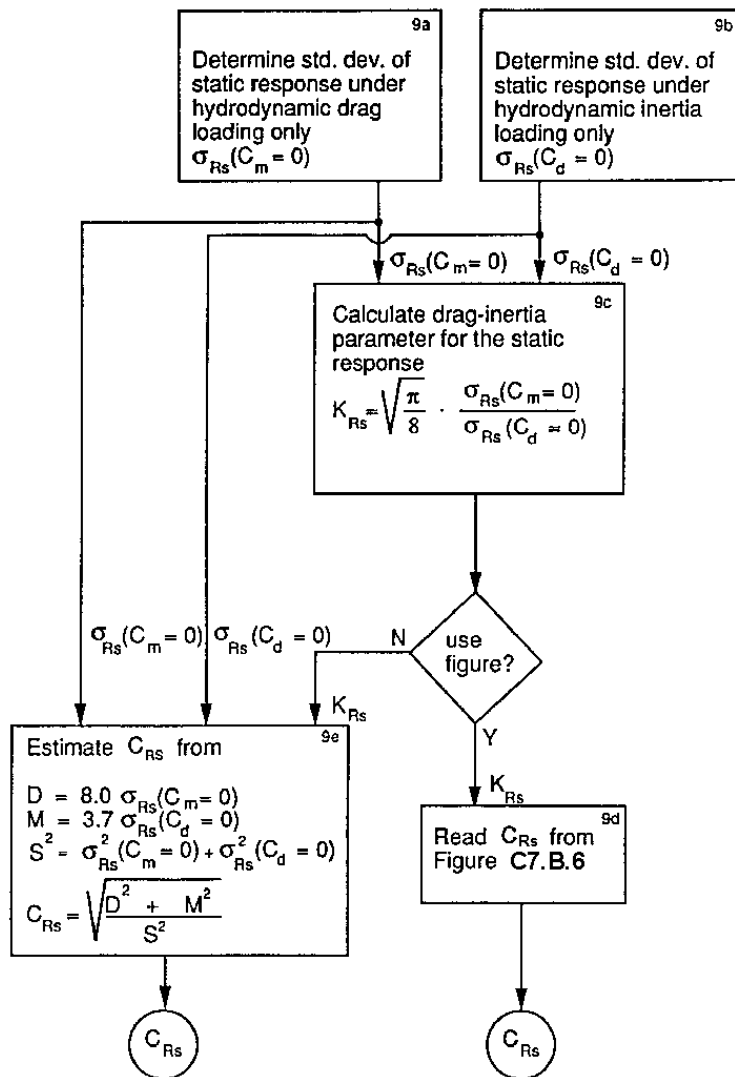
Notes to Figure C7.B.4

Figure C7.B.5 Procedure for determining the mpm-factor of the static response

107

Specific notes with Figure C7.B.5

Re blocks 9a and 9b: These standard deviations may be obtained from separate time domain simulations in the same manner as shown in Figure C7.B.2 (blocks 1 and 4) or, alternatively, from separate frequency domain analyses as shown in Figure C7.B.3 (blocks 1 and 4). The mean values are not required and neither is it necessary to subtract dynamic and static response time series or transfer functions, respectively.

Re block 9c: The drag-inertia parameter is defined as the ratio of the magnitude of the drag force to the magnitude of the inertia force due to waves. All relationships given below are valid for the case of zero current, which is used as the basis for the whole procedure in view of the engineering approximations involved. For an element of a circular cylinder of diameter D and unit length, subjected to a periodic wave, the drag-inertia parameter then becomes:

$$K = (\frac{1}{2} \rho\, C_d\, D\, v^2) / (\frac{1}{4} C_m\, \rho\, \pi\, D^2\, a)$$

$$= \frac{2 C_d v^2}{\pi C_m D a} \tag{1}$$

Where v and a are the velocity and the acceleration normal to the element, respectively. As both v and a depend on the wave parameters (wave height, wave period, waterdepth) and the elevation at which the element is located, it is obvious that K is also a function of depth, waterdepth, wave height and wave period. therefore, the theoretical definition of K is only meaningful for Morison wave loading per unit length of the element.

The definition of K can be generalized to random instead of periodic wave conditions by replacing the deterministic normal velocity v by the standard deviation of the random normal velocity σ_v and replacing the deterministic normal acceleration a by the standard deviation of the random normal acceleration σ_a. Equation (1) then becomes:

$$K = \frac{2 C_d \sigma_v^2}{\pi C_m D \sigma_a} \tag{2}$$

Using a statistical or least squares linearization procedure in the frequency domain, as developed by Borgman (see notes with Figure C7.B.3), it can be shown that for the wave force on an element of a single member the standard deviations of the two parts of the wave force are as follows:

$\sigma_R(C_m = 0) = \sqrt{8 / x}.\ 1/2\ \rho\ C_d\ D.\sigma v^2$

$\sigma_R(C_d = 0) = \rho\ C_m.1/4\ \pi\ D^2.\sigma_a$

These relationships can be used to determine σ_v^2 and σ_a, which can then be substituted into equation 2 to result in:

$$K = \sqrt{\frac{\pi}{8}}.\frac{\sigma_R (C_m = 0)}{\sigma_R (C_d = 0)} \tag{3}$$

With R being the wave force per unit length in a random sea.

Equation (3) may subsequently be generalized to apply to any other local or global response R selected for interest. It will be clear that such a generalization is purely an engineering postulate and not founded on theoretical reasoning. It is an attempt to incorporate the important but unknown non-gaussian effects on the maximum response through the assumed similarity with the wave loading process for which the non-gaussian statistics are known.

Yet another way to determine the drag-inertia parameter K for a generalized response R is by using the kurtosis of R. The kurtosis is defined through the expected values of the second and fourth order moments of the time simulations of R, i.e.:

$$\kappa = E \{R^4\} / [E \{R^2\}]^2 \tag{4}$$

For Morison wave loading per unit length of member the relationship between K and the kurtosis k is (see Ref. 2 below):

$$\kappa = \frac{105 K^4 + 18 K^2 + 3}{(3 K^2 + 1)^2} \tag{5a}$$

or in the inverse form:

Notes to Figure C7.B.5

$$K = \left[\frac{(\kappa - 3) + \left\{ \frac{26(\kappa - 3)}{3} \right\}^{1/2}}{(35 - 3\kappa)} \right]^{1/2} \tag{5b}$$

While K varies between 0 (inertia loading only) and infinity (drag loading only) κ ranges from 3 to 35/3. It may now be assumed that the same relationship holds for an arbitrary response variable R. Therefore, if the kurtosis of R is know the corresponding drag-inertia parameter K can be determined. If this is done, separate time domain simulations for the standard deviations in blocks 9a and 9b are not required but the route through block 93 cannot be followed. One enters the diagram in block 9c and must read C_{Rs} from Figure C7.B.6 as per block 9d.

Both the kurtosis and the drag-inertia parameter may be subject to appreciable statistical variability and their determination may require time domain simulations of substantial length; see Ref. 2 below.

Re blocks 9d and 9e: Figure C7.B.6 (referred to in block 9d) is equivalent to the figure that was derived by Brouwers and Verbeek and presented in Ref. 1 below as well as in Figure A1 of the SIPM - Practice (EP 89-0550). However, this latter figure presented the ratio of the expected value of the extreme to the standard deviation for a 1000 peaks, rather than the mpm-factor C_R which is the ratio of the most probable maximum value of the response to the standard deviation, which is used in this report. Therefore, Figure C7.B.6 has been recalculated in accordance with Ref. 3 and now truly presents the mpm-factor C_R. It should be noted that the figure is valid for a narrow band process, the corresponding ratios for a broad band process being somewhat smaller. Therefore, C_R is a slightly conservative estimate for the mpm-factor. This is in accordance with the general principles underlying a simplified engineering method and is well within the accuracy of the overall procedure.

An alternative and practical method to estimate K is to apply the engineering assumption for estimating the most probably maximum value of the dynamic response, as used in block 11 of Figure C7.B.4, to separate responses due to hydrodynamic drag loading only and inertia loading only, replacing R_S from block 9 and R_i from block 10, respectively. These two hydrodynamic loading components are fully uncorrelated and so are the responses caused by them; hence the correlation coefficient r = 0. Further, the mpm-factor for a totally drag dominated Morison force is 8.0 and for a totally inertia dominated Morison force it is 3.7. With these substitutions the equation in block 11 of Figure C7.B.4 becomes:
$mpm_R^2 = \{8.0\ \sigma_R\ (C_m = 0)\}^2 + \{3.7\ \sigma_R\ (C_d = 0)\}^2$

For zero correlation the standard deviation of the overall response is obtained from the equation:
$\sigma_R^2 = \{\sigma_R\ (C_m = 0)\}^2 + \{\sigma_R\ (C_d = 0)\}^2$
(see note with block 7 of Figure C7.B.4).
These are the equations presented in block 9e. The comments made with regard to conservatism included in the route through block 9d remain equally valid here.
Its determination in block 9c could therefore, strictly speaking be avoided. The input of K_{Rs} into block 93 of Figure C7.B.5 is symbolic, representing the implicit use through $\sigma_{Rs}\ (C_m = 0)$ and $\sigma_{Rs}\ (C_d = 0)$, resulting directly from blocks 9a and 9b. In practical applications it is recommended that both routes through block 9d and 93 are followed as a check on the calculations.

Reference 1:
J.J.H. Brouwers and P.H.J. Verbeek
"Expected fatigue damage and expected extreme response for Morison-type wave loading"
Applied Ocean Research, Vol. 5, No. 3, 1983, pp. 129-133

Reference 2:
P.M. Hagemeijer
"Estimation of drag/inertia parameters using time-domain simulations and the prediction of the extreme response"
Applied Ocean Research, Vol. 12, No. 3, 1990, pp. 134-140.

Reference 3:
J.J.M. Baar
Extreme values of Morison-type processes"
Report EP 90-33365, October 1990.
To be published shortly in Applied Ocean Research

Notes to Figure C7.B.5 (cont.)
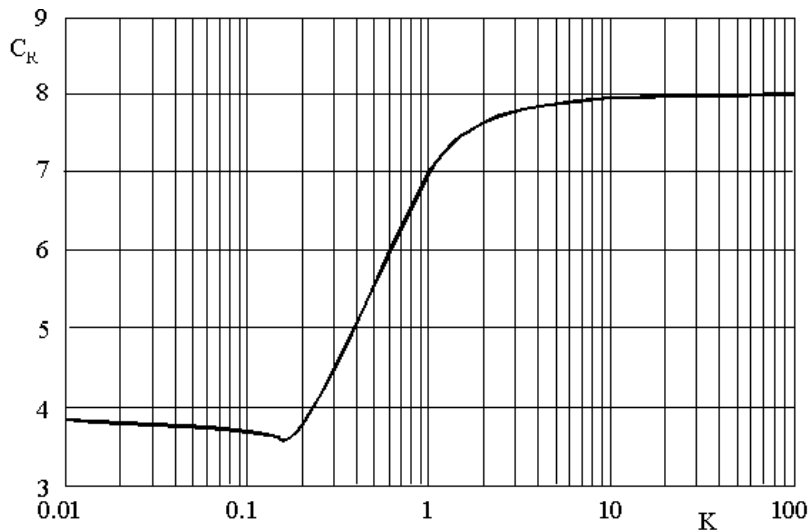
The equation for the curve is Ref. 3, Specific notes with Fig. C7.B.5

$$C_R = \begin{matrix} 3.72 / \sqrt{A} \\ (6.91 + D) / C \end{matrix} \quad if \begin{matrix} C_R < B \\ C_R < B \end{matrix} \quad \begin{matrix} (K < 0.135) \\ (K < 0.135) \end{matrix}$$

Where A, B, C and D are functions of k as follows:

A $=$ $3K^2 + 1$

B $=$ $1 / \left[(2K)\sqrt{(3K^2 + 1)} \right]$

C $=$ $\left[\sqrt{(3K^2 + 1)} \right] / (2K)$

D $=$ $1/(8K^2)$

Figure C7.B.6 Ratio C_R of most probable maximum to standard deviation as a function of drag-inertia parameter K for N = 1000 peaks

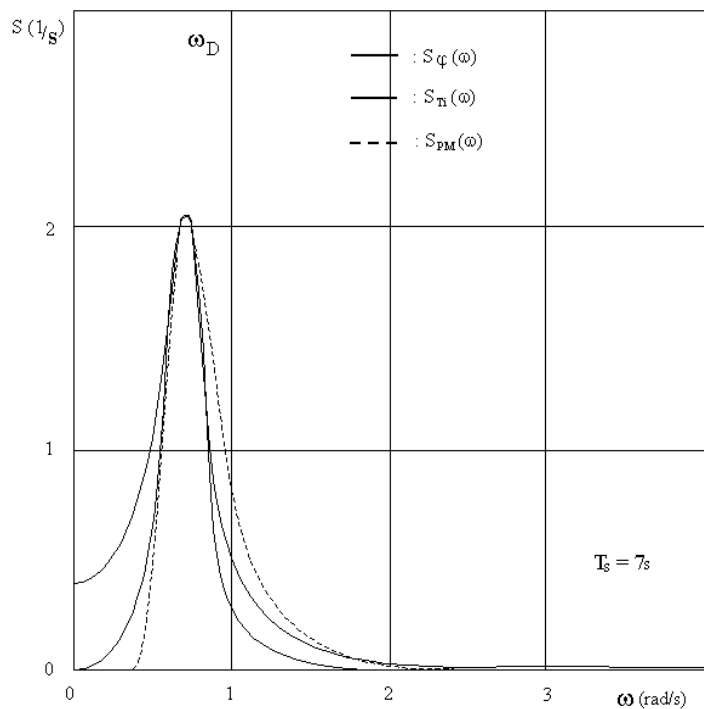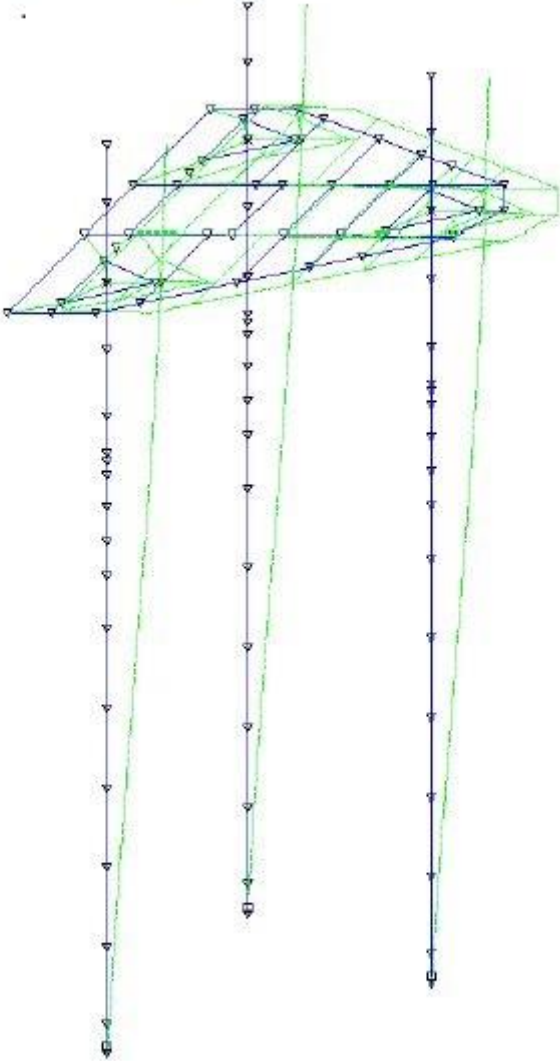Figure C7.B.7 Comparison between the normalized spectra $S_\eta(\omega)$, $S_\phi(\omega)$ and $S_{PM}(\omega)$
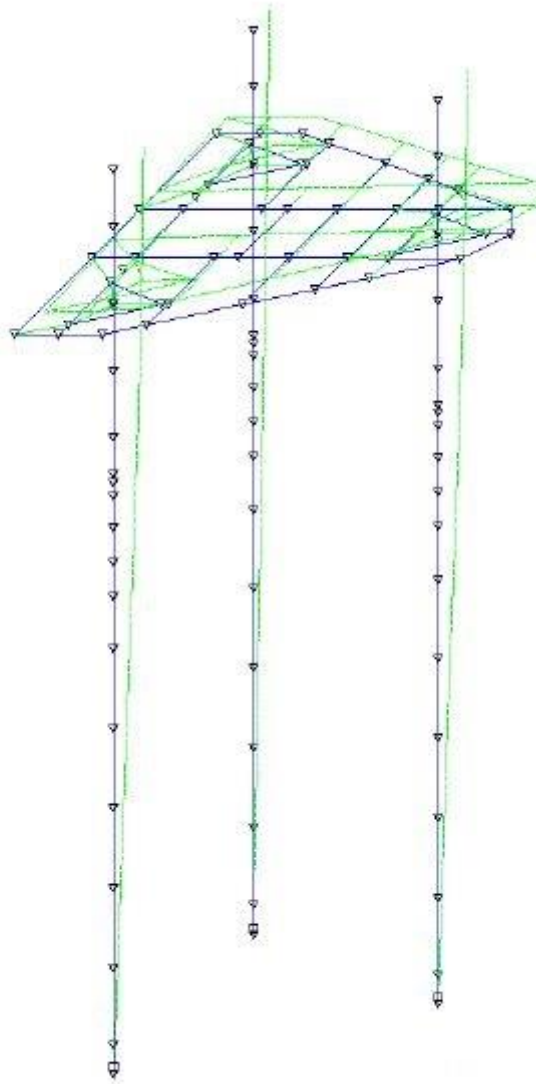
110

APPENDIX C

Mode Shapes

The three first mode shapes presented below are extracted from Case 2, in the Site-Specific Assessment at the Johan Sverdrup field. These mode shapes are representative for all studies and analyses.

MODE 1 FREQ. 0.110 HZ. PERIOD 9.094 SECS

Mode 1 Sway

Mode 2 Surge

114

MODE 3 FREQ 0.141 HZ PERIOD 7.079 SECS
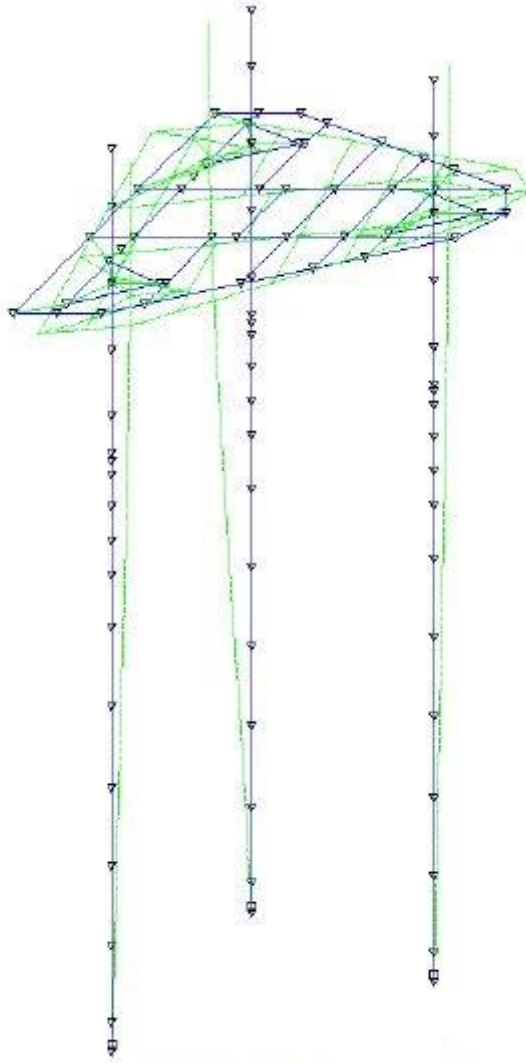
Mode 3 Yaw

APPENDIX D

Surface profile

Wave spectrum

Overturning moment

Base shear

A sample case obtained from the dynamic analysis of a surface profile, wave spectrum, overturning moment and base shear is presented.

The sample case is extracted from a storm heading of 240° in the Site-Specific Assessment at the Johan Sverdrup field.

WAVE SPECTRUM - M **2/HZ

SPECTRUM TYPE - JS
SIGN. HGT. 14.5 M
DOM. PER. 14.2 SEC
GAMMA PARA. 3.30
C VALUE 1.525

BASE SHEAR (KN)
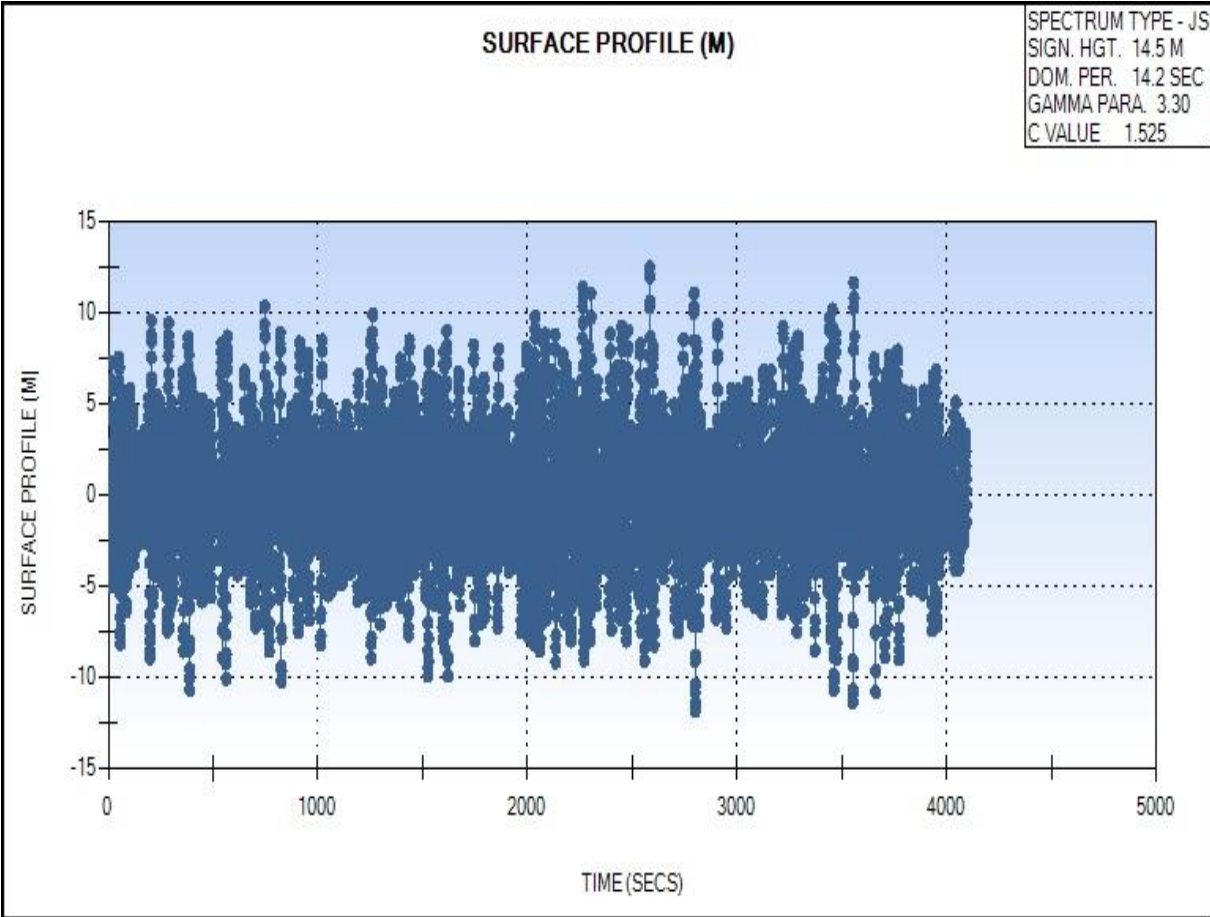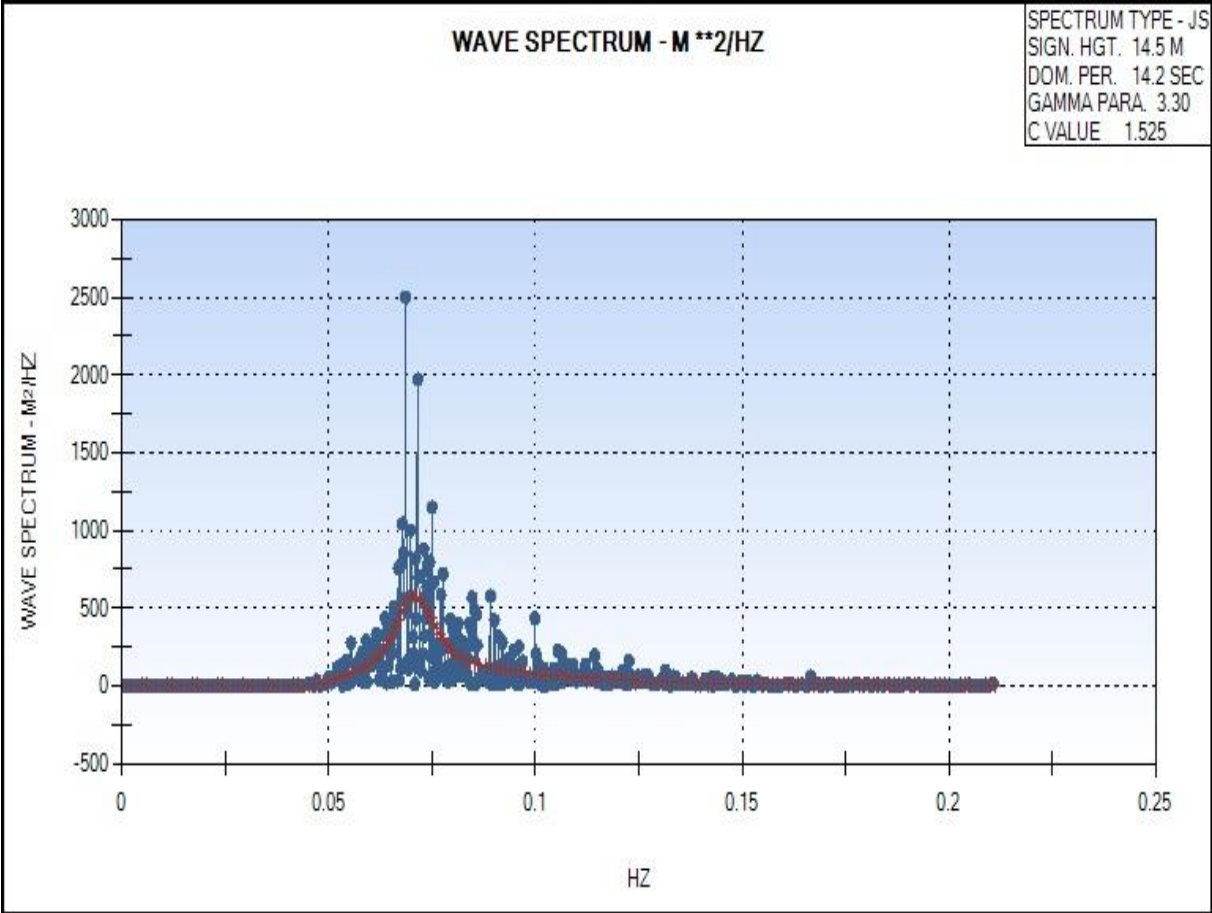
APPENDIX E

Metocean Report for Johan Sverdrup

Johan Sverdrup Field
Metocean Design Basis

Doc. no.
RE2012-001

Date
2012-01-30

Rev. no.
1

21 of 88

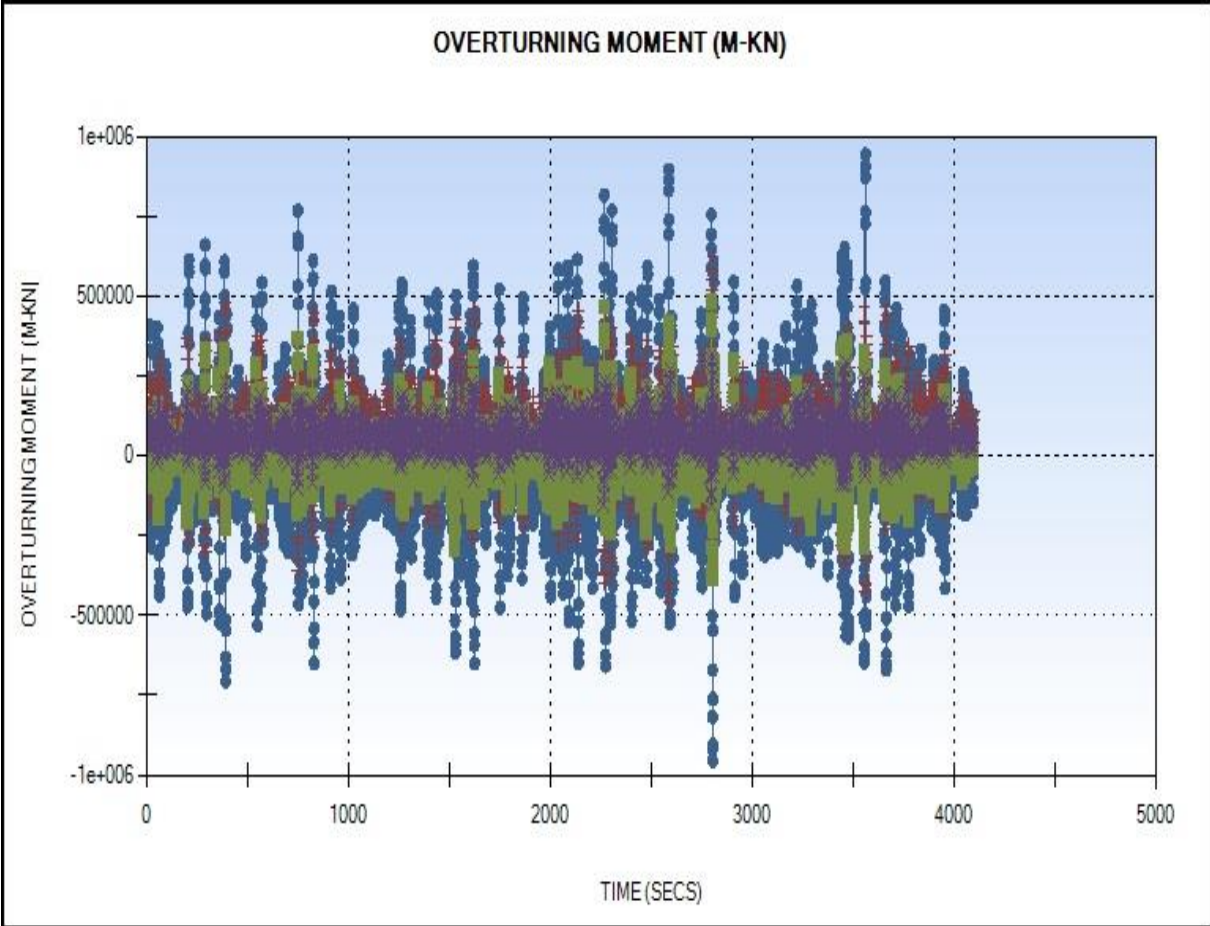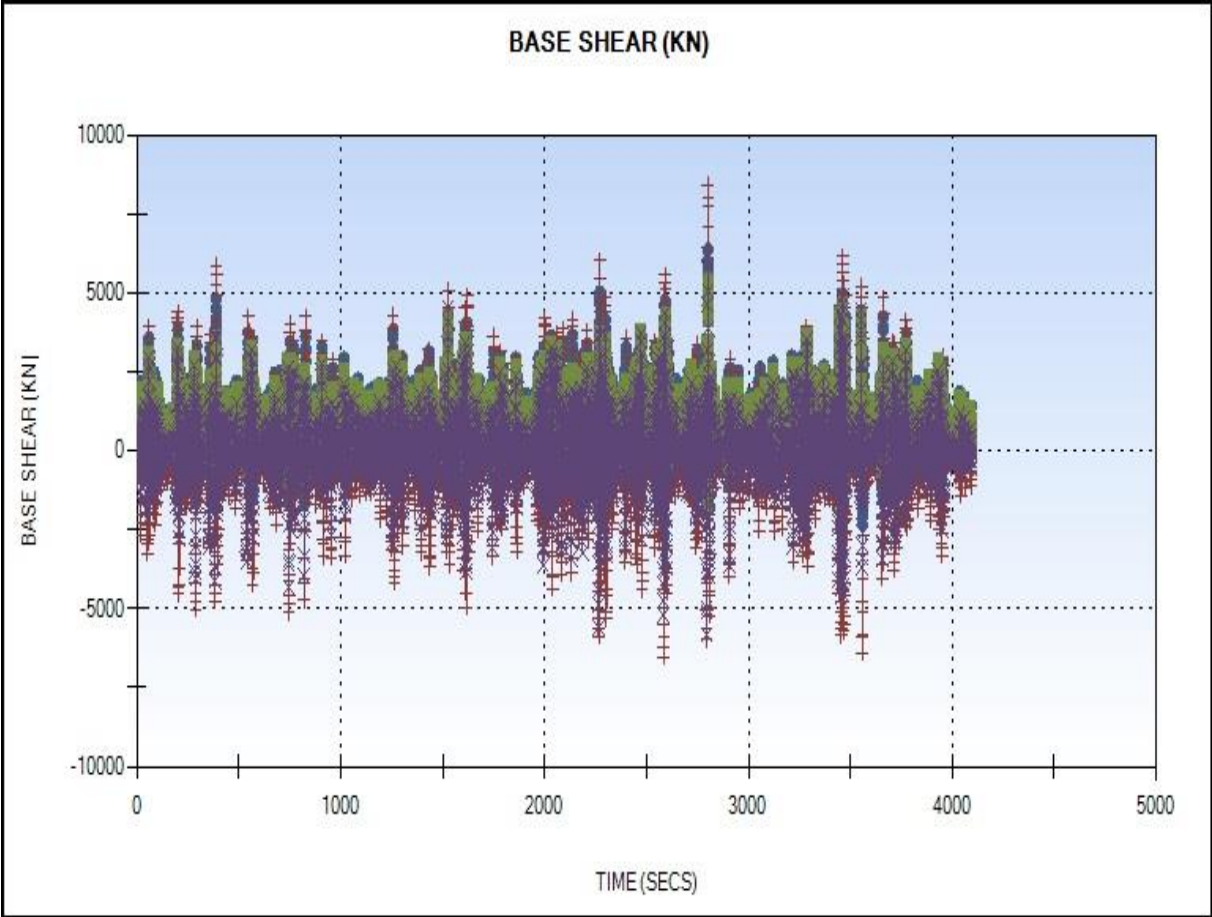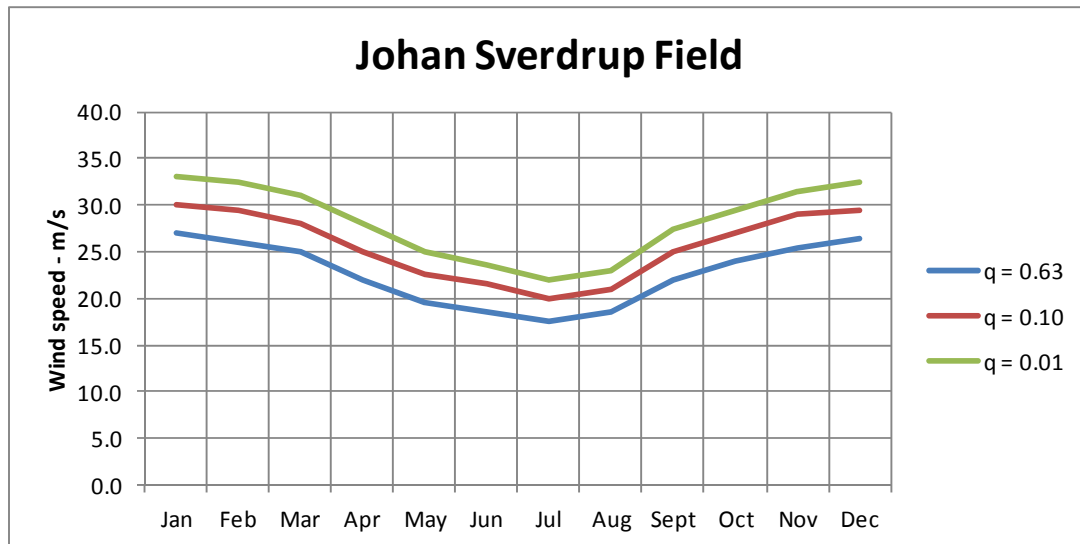**Figure 2.11**   Monthly variation of 1-hour average wind speed of annual probability of exceedance of 0.63, 10^{-1} and 10^{-2} 10 m above sea level at the Johan Sverdrup Field.

Table 2.10   Monthly and annual Weibull parameters and corresponding extreme values[*] for 1-hour average wind speed 10 m above sea level at the Johan Sverdrup Field. Duration of event is 1 hour.

Month	Annual prob.	Weibull parameters			Annual probability of exceedance			
		Shape	**Scale**	**Location**	**0.63**	**10^{-1}**	**10^{-2}**	**10^{-4}**
	%	**-**	**m/s**	**m/s**	**m/s**	**m/s**	**m/s**	**m/s**
Jan	8.33	2.687	13.92	-1.26	27.0	30.0	33.0	
Feb	8.33	2.500	12.68	-1.01	26.0	29.5	32.5	
Mar	8.33	2.456	11.76	-0.44	25.0	28.0	31.0	
Apr	8.33	2.188	9.22	-0.04	22.0	25.0	28.0	
May	8.33	2.223	8.47	-0.23	19.5	22.5	25.0	
Jun	8.33	2.262	8.21	-0.32	18.5	21.5	23.5	
Jul	8.33	2.340	8.01	-0.31	17.5	20.0	22.0	
Aug	8.33	2.359	8.50	-0.51	18.5	21.0	23.0	
Sept	8.33	2.342	9.96	-0.21	22.0	25.0	27.5	
Oct	8.33	2.523	11.41	-0.34	24.0	27.0	29.5	
Nov	8.33	2.580	12.68	-0.80	25.5	29.0	31.5	
Dec	8.33	2.621	13.29	-1.00	26.5	29.5	32.5	
Year	**100.00**	**2.138**	**9.96**	**0.10**	**28.0**	**31.0**	**34.0**	**39.0**

* Since no adjustment is made of the predicted extremes to match the marginal extremes, they may all be smaller than the all-year extreme value.

Table 3.8	Omni-directional extreme significant wave heights and corresponding spectral peak periods; mean values and 90 % confidence bands.

Annual probability of exceedance	Significant wave height H_S – (m)	Spectral peak period T_p – (s)		
		P5	Mean	P95
0.63	10.4	11.9	13.8	15.8
10^{-1}	12.5	13.1	14.9	16.9
10^{-2}	14.5	14.2	16.1	18.1
10^{-4}	18.2	16.1	18.1	20.3

The most consistent estimate for the q - annual probability load/response is obtained by performing a full long term analysis. Details regarding long-term response analysis are found in e.g. [28]. For a very complex response problem a full long term analysis will typically be out of reach. For such cases one can estimate the q - annual probability response using the environmental contour method. This method is also described into some detail in [28]. The major steps of the method are stated in NORSOK Standard N-003 Section 6.2.2.2 [5]. They are:

i.　At first the q-probability contour lines must be established for e.g. significant wave height and spectral peak period. The q - probability contour line provides all pairs of H_s and T_p corresponding to an annual probability of being "exceeded" by q.

ii.　For a given response problem one has to find the most unfavourable sea state along the q - probability contour line.

iii.　For the worst sea state along the contour the distribution function for the 3-hour maximum response is established.

iv.　Finally, the q-probability value of the selected response quantity is estimated by the value of the 3-hour extreme value distribution that is exceeded by probability 1-α. For q = 10^{-2}, NORSOK Standard N-003 Section 6.2.2.3 [5] recommends α = 0.85 – 0.90.

It must be remembered that the environmental contour method is an approximate method. The free parameter of the method is α. There are some few examples showing that the best estimate would be obtained for an α-value lower than 0.85 and there are examples that the "correct" value of α is larger than 0.9. The "true" value of α can only be found if it is calibrated to the result of a long term analysis.

Figure 3.7 and Table 3.11 show q – probability contour lines of H_s – T_p for q = 0.63, 10^{-1}, 10^{-2} and 10^{-4} for omni-directional waves.

Johan Sverdrup Field
Metocean Design Basis

Doc. no.
  RE2012-001

Date   Rev. no.   53 of 88
2012-01-30   **1**

Table 3.13   **Design wave heights for selected annual exceedance probabilities. Crest heights based on Stokes 5th order theory (for load calculations) and Forristall's theory (for air gap calculations) are given.**

Annual exceedance probability	Wave height (m)	Crest height (m)		Wave period (s)		
		Stokes V	**Forristall**	**P5**	**Mean**	**P95**
0.63	20.1	11.5	12.4	10.7	12.4	14.2
10^{-1}	23.6	13.5	14.7	11.8	13.4	15.2
10^{-2}	27.1	15.7	17.1	12.8	14.5	16.3
10^{-4}	34.5	20.5	22.0	14.5	16.3	18.3

Table 3.14   **Design wave height[*] versus direction. Annual probability of exceedance is 10^{-2}.**

Direction (º)	Wave height (m)	Wave period (s)		
		P5	**Mean**	**P95**
345 - 15	24.4	12.1	13.7	15.5
15 - 45	11.2	8.1	10.1	12.4
45 - 75	11.0	8.0	10.1	12.4
75 - 105	12.3	8.5	10.4	12.6
105 - 135	22.7	11.6	13.3	15.0
135 - 165	19.7	10.8	12.4	14.3
165 - 195	19.7	10.8	12.4	14.3
195 - 225	20.2	10.9	12.6	14.4
225 - 255	21.0	11.2	12.8	14.6
255 - 285	24.8	12.2	13.8	15.6
285 - 315	24.8	12.2	13.8	15.6
315 - 345	25.5	12.3	14.0	15.8
0 - 360	**27.1**	**12.8**	**14.5**	**16.3**

* Since no adjustment is made in order to have the worst directional extreme value matching the omni-directional extreme value, one will see that typically all directional extremes are smaller than the omni-directional extreme value. If directional wave height extremes shall be used for calculating response extremes for a wave governed structures, the extremes provided above are to be properly corrected, see Chapter 1.3.5.
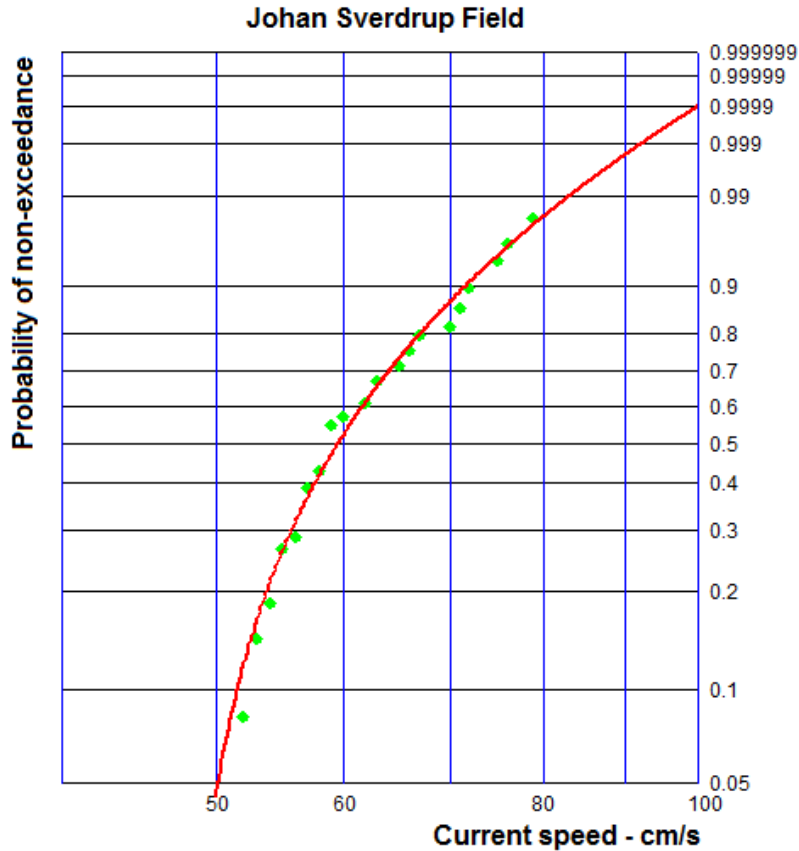
Johan Sverdrup Field
Metocean Design Basis

Doc. no.
  RE2012-001

Date
2012-01-30

Rev. no.
1

73 of 88

Figure 4.6   Observed (green dots) and fitted (red line) distributions of current speed maxima above 50 cm/s at 24 m depth at the Johan Sverdrup Field-

Table 4.15 shows omni-directional extremes for current speed 0, 24, 44, 64, 84 and 104 m depth at the Grane Field.

Table 4.15   Extreme values for omni-directional distributions of current speed at the Grane Field. Duration of extreme event is 10 minutes.

Depth	Sector probability	Annual probability of exceedance			
		0.63	10^{-1}	10^{-2}	10^{-4}
m	%	cm/s	cm/s	cm/s	cm/s
0	100.00	95	106	115	-
24	100.00	83	92	100	-
44	100.00	78	89	99	-
64	100.00	75	88	99	-
84	100.00	73	87	99	-
104	100.00	62	77	91	-